Regional Managed Aquifer Recharge and Runoff Analyses in Santa Cruz and northern Monterey Counties, California

A. T. Fisher[1,*], S. Lozano[2,†], S. Beganskas[1], E. Teo[1], K. Young[1,3], W. Weir[1], R. Harmon[1,4]

[1] Earth and Planetary Sciences Department, University of California, Santa Cruz, 95064, USA

[2] Resource Conservation District of Santa Cruz County, Capitola, CA 95010

[3] Current affiliation: United States Coast Guard

[4] Current affiliation: Colorado School of Mines

[*]Corresponding author: afisher@ucsc.edu

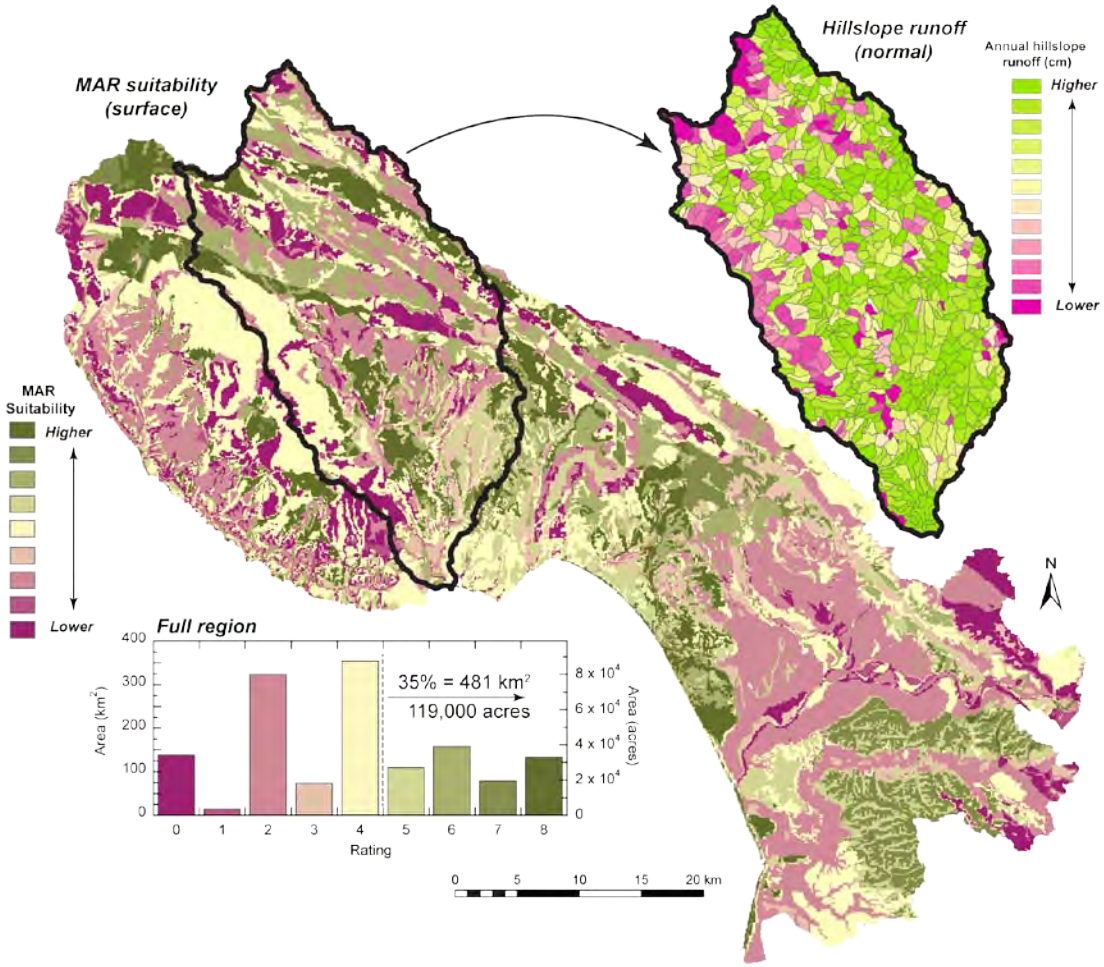

Prepared for:

The California State Coastal Conservancy

Project 13-118

Acknowledgements

This project could not have been completed without collaboration and advice from many people and organizations. The authors sincerely appreciate cooperation and encourage from numerous individuals including leadership, staff and contractors from these agencies: Scotts Valley Water District (P. Harmon, M. Maley), San Lorenzo Valley Water District (B. Lee, N. Johnson), City of Santa Cruz (R. Menard, H. Lackenbach), Soquel Creek Water District (R. Duncan, T. Dufour, C. Tana, N. Byler), Central Water District (R. Bracamonte), Pajaro Valley Water Management Agency (M. Bannister, B. Lockwood), County of Santa Cruz (J. Ricker), the Association of Monterey Bay Area Governments (J. Adelaars, G. Schmidt), M. Cloud, and members of the Community Water Dialog of the Pajaro Valley. We are also grateful for support from other personnel from the Resource Conservation District - Santa Cruz County (C. Coburn, K. Camara, S. Gillett - original project lead). Computing and GIS support was provided by E. Boring, A. Tores, R. McClenahan, M. Simoni, and B. Nickel.

Funding for this project was provided by: a Climate Ready grant from the California State Coastal Conservancy (Project 13-118, program managers T. Gandesbery and T. Chapman), the University of California Water Security and Sustainability Research Initiative (UCOP award #449214-RB-69085), and graduate student fellowships/scholarships from the U. S. National Science Foundation (S. Beganskas), the U. S. Coast Guard (K. Young), and the Cota Robles Graduate Fellowship Program (E. Teo).

Executive Summary

Overview

Groundwater resources in California are increasingly stressed by rising demand, a changing climate, and shifting land use. Basins on California's central coast are particularly vulnerable because groundwater supplies ~85% of regional freshwater needs (including municipal and extensive agricultural demands), but these regions lack large-scale infrastructure for multi-year surface storage, do not import water from other parts of the state, and are home to sensitive habitats that depend on the supply and quality of groundwater resources.

This study used spatial analysis and modeling to develop practical screening tools to find suitable locations in Santa Cruz and northern Monterey Counties (adjacent to Monterey Bay) where there may be good opportunities to improve groundwater resources using distributed stormwater collection linked to managed aquifer recharge (DSC-MAR). New data sets and methods developed through this project are now available and can be applied by water managers, environmental stewards, and other public and private stakeholders.

The DSC-MAR strategy targets relatively small drainage areas (generally 100-1000 acres) from which stormwater runoff can be collected to infiltrate ≥100 acre-feet of water per year. Infiltration can be accomplished in surface basins, typically having an area of 1-5 acres, or potentially through flooding of agricultural fields or flood plains, use of drywells, or other strategies. Implementing even a modest number of MAR basins can make a significant contribution to reduce aquifer overdraft and maintain long-term water supply reliability on the central coast.

The study is the first comprehensive, regional effort to: (1) quantify and map suitability for DSC-MAR and (2) evaluate the supply of stormwater runoff in support of MAR. The first part of

this project focused on quantifying and mapping spatial variations in suitability for infiltration and storage of excess surface water, using a geographic information system (GIS). Numerous datasets were acquired, processed, patched and combined to identify locations where there is alignment of properties that are most favorable for DSC-MAR. The assessment included surface and subsurface GIS coverages. Surface coverages (available for the full study region) provided an initial screening for MAR suitability and included parameters such as elevation, soil properties linked to infiltration, and bedrock geology (determining “presence or absence” of an underlying aquifer). Subsurface coverages (available only for certain areas within the project region) allowed for a more detailed assessment of opportunities to infiltrate and store stormwater runoff, and included hydrogeologic parameters such as the geometry (lateral extent, thickness) of aquifer and confining layers, transmissive and storage properties, the thickness of soil and rock layers above the shallowest aquifer, and recent changes in groundwater levels.

The second part of this project focused on modeling basin runoff response, including spatial variations under a range of climate scenarios (dry, normal, wet), with models driven by historical precipitation data. We used an open source, process-based numerical model (Precipitation Runoff Modeling System – PRMS) to assess potential opportunities for stormwater collection, based on soil properties, vegetation cover, and other hydrologic properties within and among small hydrologic units (25-250 acres) throughout two drainage basins. Once the climate scenarios were developed and simulations were completed, we analyzed model-generated outputs with an emphasis on relations between precipitation and hillslope runoff, before this runoff reaches "blue line" streams.

Stormwater runoff from hillslopes is not the only supply of water that could potentially be used for MAR, but we chose to focus on this supply because it can be accessed in many basins as

part of broader efforts to control runoff, limit the export of sediment, and enhance environmental conditions as part of mitigation for climate change and urbanization. Our goal in the present study is to help identify locations where stormwater runoff from hillslopes could generate DSC-MAR benefits on the order of 100 to 1000 ac-ft/yr, a scale of beneift that is intermediate between what is commonly known as low impact development (LID, ~1-10 ac-ft/yr) and highly engineered regional MAR systems ($\geq 10^4$ ac-ft/yr). PRMS has not been used for this specific purpose in the past, so this study also provides new understanding of data and technical requirements and limitations for this approach.

GIS analyses were completed for the full project region, comprising four distinct topographic drainage areas: Northern Santa Cruz County (NSCC), San Lorenzo River Basin (SLRB), Mid-Santa Cruz County (MSCC), and lower Pajaro Valley Drainage Basin (PVDB). Additional subsurface and composite analyses were completed for the Santa Margarita Groundwater Basin (SMGB, located the SLRB, Soquel Aptos Groundwater Basin (SAGB, within MSCC), and the Pajaro Valley Groundwater Basin (PBGB, within the PVDB). Runoff analyses have been completed for the SLRB and PVDB. Simulations of runoff within the MSCC region, which was outside the scope of this project, are in progress and should be completed in early 2017.

Suitability for Managed Aquifer Recharge

Of the full 1387 km^2 project area, 35% (481 km^2, 119,000 acres) is rated as suitable to highly suitable for MAR, based on analysis of surface data (soil properties and bedrock geology). These areas are distributed throughout the study region, sometimes in large swaths, but often as small patches of favorable conditions. Conditions differ considerably within individual parts of the study region. The fraction of landscape that is suitable for MAR is considerably lower when

screened for areas having a surface slope <10°. Much of the study region is mountainous and steep. The prevalence of steep slopes is especially apparent in the SLRB, where only 22% of the area has a surface slope <10°. In contrast, within the PVDB, a much larger alluvial basin, 58% of the ground has a slope <10°. Only a few acres many be needed to accomplished infiltration objectives associated with individual DSC-MAR projects, and there are many local areas having moderate to high MAR suitability based on surface data in all three of the main topographic basins. These areas are most extensive in the PVDB, especially along the coast, on either side of the Elkhorn Slough drainage, south of the Pajaro River, and in the northern part of the basin (Corralitos, Freedom). But there are also numerous 1-4 acre areas of elevated MAR suitability distributed across the SLRB and MSCC.

Subsurface and composite (surface + subsurface) maps cover smaller areas within each topographic basin, because key subsurface data is available only where detailed analyses have been completed, generally in association with development of a groundwater model. In SMGB, moderate to elevated composite MAR suitability values are mapped across ~40% of the basin. Less suitable areas are limited mainly by soil properties and bedrock geology. In other words, given generally good aquifer (subsurface) conditions in the SMGB, the surface factors are most important in distinguishing between more and less suitable DSC-MAR locations.

In the SAGB, subsurface suitability was calculated for a small region near the coast, but a composite analysis was completed two ways: with three factors (soils, bedrock geology, and transmissivity), and with six factors (where more data was available). The composite analysis with six factors tends to screen out small areas that were previously identified from surface analyses as being suitable for MAR, whereas the composite analysis with three factors shows a broader regional pattern. Much of the basin is moderately to highly suitable for MAR, with the

primary exceptions being areas underlain by Purisima subunits having poor aquifer properties. The eastern side of the basin tends to be more suitable for MAR, but there are zones of high suitability scattered throughout.

In the PVGB, subsurface suitability for MAR deviates significantly from that assessed based only on surface datasets, particularly in the central and eastern parts of the basin. In these areas, lower suitability based on surface data was assessed mainly on the basis of soils associated with the Pajaro River floodplain, Watsonville Sloughs, and other aquatic systems. However, these factors are offset to some extent by highly suitable aquifer conditions at depth in many locations. As a result, in the composite analysis of MAR suitability for the PVGB, there are moderately to highly suitable areas distributed throughout the basin, especially along the northern coast and south of the Pajaro River, but also adjacent to the hills bounding the eastern side of the basin.

Patterns of Stormwater Runoff

Variations in monthly and annual precipitation for dry, normal and wet climate scenarios illustrate important characteristics of the SLRB and PVDB. There is more precipitation overall in the SLRB than in the PVDB, illustrating a north-to-south gradient across the study region. Under all climate scenarios in both basins, the majority of precipitation falls during a wet season, November to April. Within both basins, there are occasional wet months even during the dry scenarios, often resulting from a single major precipitation event. But in addition to having more rain per month, the normal and wet climate scenarios tend to have greater persistence in rainy months. Typical precipitation more than doubles from dry to wet conditions in both the SLRB and the PVDB, but values are considerably lower overall in the PVDB. As a result, there are relatively few months that exceed a basin-wide average precipitation of ~6 in/month of rain in

the PVDB (equivalent to ~50 ac-ft/100 ac), even under wet conditions, whereas this threshold is met in the SLRB much more frequently, even under normal conditions.

The spatial distribution of precipitation is consistent for each basin under different climate scenarios. In the SLRB, there is much greater precipitation along the western and eastern boundaries of the basin, with much lower values near the coast and at the northwestern edge of the basin. The spatial trends are somewhat simpler in the PVDB, with a strong north-to-south gradient and higher precipitation in areas of higher elevation. In both basins, these patterns likely result from a combination of topography and the tracks of the most common winter storms: there appear to be more frequent and larger storms that track to the northern end of Santa Cruz County, on average, and steep topography in the Santa Cruz Mountains and foothills at the back of the PVDB results in strong orographic effects.

In both basins, there is little hillslope runoff outside of the rainy season, and there is little runoff generated during the rainy season when precipitation during one month follows a dry month. This effect is more strongly pronounced in the PVDB than in the SLRB, mainly because there is less precipitation overall to the south, and the effect is strongest in both basins under the dry climate scenario. The lack of precipitation persistence during the dry scenario thus has a major influence on runoff generation when considered for a basin as a whole. Within each basin, there is considerable spatial variability in hillslope runoff for all climate scenarios. Considerable runoff is generated in parts of each basin during the normal and wet climate scenarios, but also under dry scenarios for some locations. There are sites within each basin where drainage areas of several hundred acres can generate enough runoff to justify development of a MAR project fed by stormwater, even under dry climate conditions.

For the SLRB, there is significant hillslope runoff generated under all three climate scenarios, with high variability throughout the basin. The areas generating the least runoff are generally on the western and northern side of the basin, even during wet climate conditions. In contrast, areas to the central and southern sides of the SLRB generate significant runoff even during dry conditions. There is considerably more variability in runoff generation in the PVDB, both spatially during any particular climate scenario, and in comparison between different climate scenarios. Areas generating the most runoff are located in the central part of the basin, within the City of Watsonville, and in the northern and eastern parts of the basin. Even under dry conditions, these areas generate significant runoff. Coastal and southern parts of the basin generate much less hillslope runoff.

In the SLRB, about 10% of the basin area (~35 km^2, ~8,700 acres) generate ≥12 inches of hillslope runoff each year, even under dry climate conditions, equivalent to 100 ac-ft for each 100 ac of drainage area. The fraction of the SLRB generating ≥12 in/yr of hillslope runoff increases to ~35% of the basin area during the normal climate scenario, and ~55% of the basin area during the wet climate scenario. Conditions in the PVDB are not as favorable, mainly because there is considerably less rainfall than in the SLRB under all three climate scenarios, yet there is still considerable opportunity to develop successful DCS-MAR projects. In the PVDB during a normal water year, about 5% of the basin area contributes ≥12 in/yr of hillslope runoff. But even an area generating 4 in/yr of hillslope runoff could contribute to 100 ac-ft/yr of DCS-MAR benefit if the water supply were collected from a drainage area ≥300 ac. During a normal climate scenario, 20% of the basin (equivalent to ~110 km^2 or ~27,000 acres) met this threshold. Less of the PVDB will provide enough runoff during dry years to support DSC-MAR projects,

but this mainly illustrates how important it is to assess, position, and design these projects on the basis of local conditions (drainage area, soils, runoff patterns, etc.).

Conclusion

There are many opportunities in the study region locate and develop managed aquifer recharge projects that are supplied with stormwater runoff. More water can be collected during wet years, of course, but that simply emphasizes the importance of developing and running these kinds of projects so that benefits can be achieved under favorable hydrologic conditions. The products of this work (maps, datasets) should be used mainly for screening purposes, complemented by direct assessments on a site-by-site basis. Maps and datasets specific to each basin are available for public access (download) through the Resource Conservation District of Santa Cruz County's website (http://www.rcdsantacruz.org/managed-aquifer-recharge). Results of this work have direct implications for this region, where communities must make do with limited local resources, but also may serve as a template for other parts of the state, where planning and implementation of new projects to improve the security and sustainability of groundwater resources is expected to be increasingly common.

Table of Contents

I. Project Motivation, Scope and Goals

A. Background and Motivation

Groundwater resources in California are increasingly stressed by rising demand, a changing climate, and shifting land use. The Sustainable Groundwater Management Act (SGMA, 2014) requires that basins across the state form groundwater sustainability agencies (GSAs), develop groundwater sustainability plans (GSPs), and implement practices that will help to maintain the supply and quality of water resources for coming generations. Managed aquifer recharge (MAR) is a strategy that can improve both the supply and quality of groundwater [*Bouwer*, 2002], routing excess surface water into aquifers using a variety of techniques.

Groundwater basins surrounding Monterey Bay, on California's central coast, are particularly vulnerable to increasing groundwater demand and decreasing supply. The region lacks large-scale infrastructure for multi-year surface storage, does not import water from other parts of the state, and is home to environmentally sensitive habitats (both onshore and offshore) that are influenced by declining groundwater resources. The region is also heavily dependent on groundwater, which supplies ~85% of regional freshwater needs, including municipal and extensive agricultural demands.

The primary goal of this project is to find sites in Santa Cruz and northern Monterey Counties where there may be good opportunities to improve groundwater resources using distributed stormwater collection (DSC) linked to MAR. Components of this approach have been applied in this and other regions [e.g., *Russo et al.*, 2014], but this is the first comprehensive and regional effort to map suitability for MAR and model potential for stormwater runoff to supply these projects. Results of this work have direct implications for this region, where communities must make do with limited local resources, but also may serve as a template for other parts of the

state, where planning and implementation of new projects to improve the security and sustainability of groundwater resources are expected to be increasingly common and important in coming years.

B. Project Components and General Approach

1. Project scope: Mapping and Modeling to Support DSC-MAR

This project has two main components: (1) quantify spatial variations in suitability for distributed stormwater collection linked to managed aquifer recharge (DSC-MAR), and (2) evaluate runoff conditions, based on a range of climate scenarios, to assess the potential benefits of stormwater collection. This project emphasizes the development and use of practical tools that can be applied by water managers, environmental stewards, and other stakeholders. We also seek to compile and generate datasets that can be used to update these calculations or conduct related analyses.

The two primary project components are addressed with standard techniques: a geographic information system (GIS) for mapping the suitability for DSC-MAR, and a process-based numerical model for quantification of stormwater runoff. In the following section, we describe the scope of these efforts, and discuss their applications and limitations.

2. GIS analyses for MAR suitability

A GIS is a computer-based mapping system, combining a geospatial database that uses a variety of data types and formats, visualization tools for displaying datasets, and scripting tools for processing and combining datasets to generate new coverages. The mapping component of this project was completed using ArcGIS v10.3, commercial software that is widely used for environmental resource assessment.

Our general approach for spatial assessment of MAR suitability is well established in the technical literature [e.g., *Chenini et al.*, 2010; *Jasrotia et al.*, 2007; *O'Geen et al.*, 2015; *Russo et al.*, 2014] (**Fig. I-1**). Individual datasets are acquired and imported into the GIS in digital format, with adjustments made as needed to the geographic projection, resolution, data gaps or errors, and/or units of measurement and display. An assessment is made as to how each parameter varies across the study region, and a classification scale is developed for simplified representation of the data. Multiple datasets are combined to identify locations where there is alignment of properties that are the most favorable for the processes or activities of interest (**Fig. I-1A**). In the case of suitability for DSC-MAR, we divided the assessment into two sets of coverages: surface and subsurface. Surface coverages included parameters such as elevation, soil types and properties, and the nature of bedrock (outcropping or subcropping below shallow soils). These datasets are available for the full study region (although, as described later, considerable processing and patching was required).

Subsurface coverages included hydrogeologic parameters such as geometry (lateral extent, thickness) of aquifers and confining layers, transmissive and storage properties, the thickness of soil and rock layers above the shallowest aquifer, and historic (recent) changes in groundwater levels (**Fig. I-IB**). These coverages were available only where agencies and municipalities had compiled and contoured data, generally in association with development of groundwater flow models. The scope of the current project was defined so that we would use existing subsurface coverages, rather than develop new coverages, for several reasons.

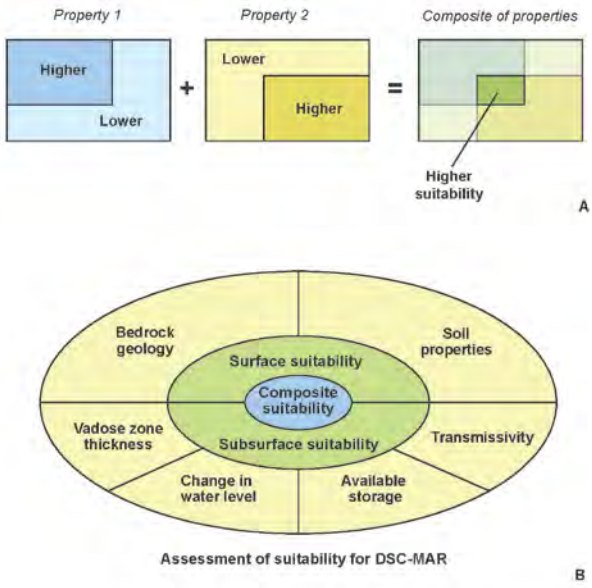

Figure I-1

First, this approach was consistent with the scope of the project in terms of staffing and time available, with the goal of producing maps, models, and interpretations for the full project region in about 24 months. Many person-years of effort had already been expended in recent years compiling, digitizing, and combining well log, outcrop, and other data, and in developing three-dimensional spatial coverages of subsurface information. It did not make sense to repeat this effort, particularly because earlier studies were completed by local experts (agency staff and their consultants), many of whom have decades of expertise working with the complex geology and hydrogeology of individual basins. In addition, using the same datasets that were developed for creation of hydrogeologic models meant that it would be possible to integrate results of our mapping and runoff modeling efforts with existing and ongoing subsurface modeling efforts, so

that scenarios developed through this project could be tested and updated as desired. We are providing digital versions of the datasets used for this project so that calculations can be revised as new data become available.

It is difficult to combine data types that use different field units and scales, e.g., infiltration capacity in m/day and vadose zone thickness (depth to water table) in m. In addition, our analyses needed to incorporate descriptive information on the presence or absence of aquifer units in the shallow subsurface. The approach we took for individual datasets was to assign values to a common index scale of 0 to 4, where lower values are less suitable for MAR. For some data coverages, we used the full index scale (e.g., effective transmissivity was rated using values of 0, 1, 2, 3, or 4), whereas other coverages were assigned an index using only part of this scale (e.g., available subsurface storage was rated using values of: 0, 2, or 4). The former approach was taken when observed/calculated values had a wide range (typically orders of magnitude) and there was confidence in the relative magnitude of the individual values. The latter approach was taken when the range of observed/calculated values was narrower and/or there was less confidence in our ability to distinguish between properties separated by relatively small values.

After indices were assigned for individual datasets, they were combined to derive an interpretation of MAR suitability based on (a) surface data (effective infiltration capacity of shallow soils, nature of bedrock geology), (b) subsurface data (effective transmissivity, available storage, vadose zone thickness, rate of recent changes in water levels), and (c) composite of all available data (combining surface and subsurface analyses). For the assessment of MAR suitability based on surface datasets, the effective infiltration capacity of shallow soils and the nature of bedrock geology were assigned equal weights. For analysis of MAR suitability based

on subsurface datasets, each of the four characteristics was assigned an equal weight. For composite analyses of MAR suitability using the complete ensemble of available data, surface and subsurface analyses were assigned equal weights. This means that individual surface datasets were weighted twice as heavily as individual subsurface datasets, because there were two surface datasets and four subsurface datasets. There was one exception to this last rule: for analysis of the Soquel Aptos Groundwater Basin (SAGB), the complete suite of subsurface data was available for only a small region near the ocean. We augmented the complete composite analysis for the SAGB with an additional composite analysis in which surface data were combined with effective transmissivity calculations, as the latter was available for a larger area than were other subsurface datasets. In this case, transmissivity data were weighted equally with surface datasets.

3. Runoff Modeling to Assess Potential Stormwater Supplies

We selected Precipitation Runoff Modeling System (PRMS) [*Leavesley et al.*, 1983; *S Markstrom et al.*, 2008; *S L Markstrom et al.*, 2015] to model basin runoff under a range of climate conditions. PRMS is an open-source program that is widely used, and can represent detailed soil, vegetation, and hydrologic properties at regional to local scales. Stormwater runoff from hillslopes is not the only water supply that could be used for MAR, but we chose to focus on this source because it can be accessed in many basins as part of broader efforts to control runoff, limit sediment export, and enhance environmental conditions as part of mitigation for climate change and urbanization. Collecting stormwater runoff is widely considered as part of low-impact development (LID) efforts, which link land planning and engineering, emphasizing conservation and use of on-site natural features to protect and improve water conditions. LID systems are often developed at a relatively small scale (e.g., pervious pavement along the edge of streets, or vegetated swales to collect runoff from parking lots), close to the source of runoff

generation, with the goal of slowing the movement of water across the landscape. Most LID projects are not monitored to assess performance, but a typical system might influence 1-10 ac-ft/yr of runoff. In contrast, regional-scale and highly engineered MAR systems (such as those operated in Orange County and Santa Clara County) infiltrate $>10^5$ ac-ft/yr. Our goal in the present study is to help identify locations where stormwater runoff from hillslopes could generate DSC-MAR benefits on the order of 10^2- 10^3 ac-ft/yr, a quantity intermediate between what is typically generated with LID and regional MAR systems. PRMS has not been used for this specific purpose in the past; additional goals of this study are to assess how well the model works for this purpose, and to gain a better understanding of data and technical requirements and limitations of this numerical tool.

C. Project Region and Coordinates

The geographic extent of this project comprises most of Santa Cruz County and a significant portion of northern Monterey County (**Fig. I-2**). The project area excludes three small parts of northern Santa Cruz County that drain surface runoff towards the north and west, into San Mateo County. The project area also includes small sections of San Mateo, Santa Clara, and San Benito Counties that drain into Santa Cruz County. The project area extends south into Monterey County, across the Elkhorn Slough drainage, because this area overlies (and is a potential supply for runoff and infiltration into) the Pajaro Valley Groundwater Basin [*Fugro West Inc.*, 1995]. The project region was subdivided for analysis based on topographic drainage (**Table I-1**), with some analyses applied across the full region, and others applied to subregions (as discussed in detail later in this report).

Table I-1. Project regions defined by topography and groundwater basins.

	Area (km^2)	Area (acres)	Groundwater basin [a]	MAR suitability (GIS) [b]	Runoff (PRMS) [c]
Full Project	1,386.5	342,602	NA	Surface	-
Northern Santa Cruz County (NSCC)	283.6	70,069	NA	Surface	-
San Lorenzo River Basin (SLRB)	351.4	86,826	Santa Margarita Groundwater Basin (SMGB)	Surface/subsurface	√
Mid-Santa Cruz County (MSCC)	209.2	51,685	Soquel Aptos Groundwater Basin (SAGB)	Surface/subsurface	(√)
Pajaro Valley Drainage Basin (PVDB)	541.1	133,706	Pajaro Valley Groundwater Basin (PVGB)	Surface/subsurface	√

[a] Groundwater basin as designated in this report
[b] Analyses completed using a GIS for suitability for managed aquifer recharge (MAR) using stormwater
[c] Analyses completed using a runoff model, PRMS, to assess potential for using stormwater as a source for MAR. √ = analysis complete and included in this report. (√) = analysis underway, with results to be added to the project website when ready.

Much of the data from the region incorporated into the GIS and modeling analyses are available in the State Plane Coordinate (SPC) georeference system. Although the SPC system is widely used by agencies in California, the project area extends across two SPC zones (zones 3 and 4), which would have caused problems working with numerous spatial data sets. For this reason, all data used in this study were projected onto a coordinate system of NAD 1983, UTM Zone 10N. In addition, any data acquired with spatial units of feet were converted to meters prior to merging with the GIS project.

D. Report Structure

In the next major section, we describe the technical methods used for this project, mapping using a GIS, and runoff modeling using PRMS. In discussing individual GIS coverages, we explain the origin of the various datasets, and how they were modified for use in this study. We describe runoff simulation using PRMS, including the basis for the model and the kinds of data it requires. We also discuss model calibration and the nature of meteorological data available for the study region, and explain how these were used to develop climate scenarios to assess of runoff under a range of hydrologic conditions.

Results are presented first for mapping of MAR suitability, staring with surface data that are available for the full project region, and then incorporating subsurface data that are available for limited parts of the project region. Runoff results are presented and assessed next. Finally, results from mapping and runoff analyses are combined to assess where conditions may be most favorable for development and operation of DSC-MAR systems.

II. Methods

A. Mapping Suitability for Managed Aquifer Recharge using a Geographic Information System

1. Digital Elevation Model (DEM) and Major Topographic Basins

The digital elevation model (DEM) used as the basis for analysis of MAR suitability and generation of stormwater runoff was assembled from three primary data sources: two provided by the United States Geological Survey [USGS, *U. S. Geological Survey*, 2014a], created using data from a variety of sources, and the third provided by Association of Monterey Bay Area Governments [AMBAG, *Digital Mapping Inc.*, 2011], based on regional LIDAR survey flown in 2010. The USGS data were gridded to create 1/9 arc-second (~3 m) and 1/3 arc-second (~10 m) products, referred to herein as the "USGS 3 m DEM" and the "USGS 10 m DEM." These data cover the vast majority of the full project region, with a few small gaps (discussed below). The AMBAG data were gridded to generate a DEM with 3 m resolution, but coverage of the project area was incomplete, with a notable gap in the Santa Cruz Mountains along the northeastern side of the project area. This DEM also displayed systematic "striping" when examined closely using the hillshade display, which would have influenced runoff calculations. We had access to one additional dataset that appeared initially to be useful: a 60-cm resolution DEM, based on the AMBAG LIDAR survey, supplied by Santa Cruz County. However, there were significant vertical offsets in this DEM compared to the 3 m and 10 m USGS coverages, and the very high resolution of the 60 cm DEM made it difficult to manage and manipulate.

The USGS 3 m DEM was selected as the primary topographic dataset because it had the relatively high resolution, few processing artifacts, and the almost complete coverage of the project region. However, examination of the USGS 3 m DEM revealed a series of data gaps in

the northernmost Santa Cruz County, and along the western side of the project area at the land-sea interface (**Fig. II-1**). These gaps were filled using the USGS 10 m and AMBAG 3 m DEMs (**Fig. II-2**). The AMBAG DEM data were clipped around the area of data gaps along the coast, processed using five-node averaging and a low-pass spatial filter (to remove striping), then mosaicked with the USGS 3 m DEM to fill gaps. Low-pass filtering results in loss of some information, but a check of elevation changes around the filtered areas suggests that smoothing shifted elevations by ≤4 cm. Bilinear interpolation was used during mosaicking, with the USGS 3 m DEM given precedence in areas of overlap. USGS 10 m data were clipped and mosaicked to cover gaps at the northern end of the project area.

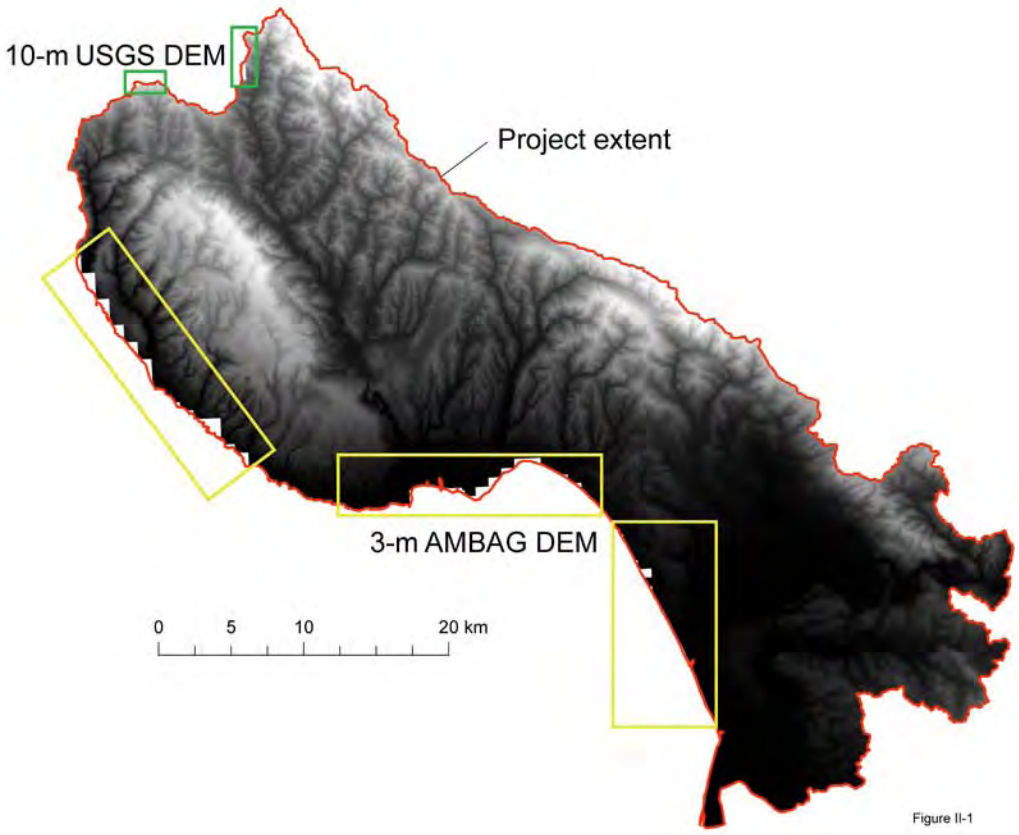

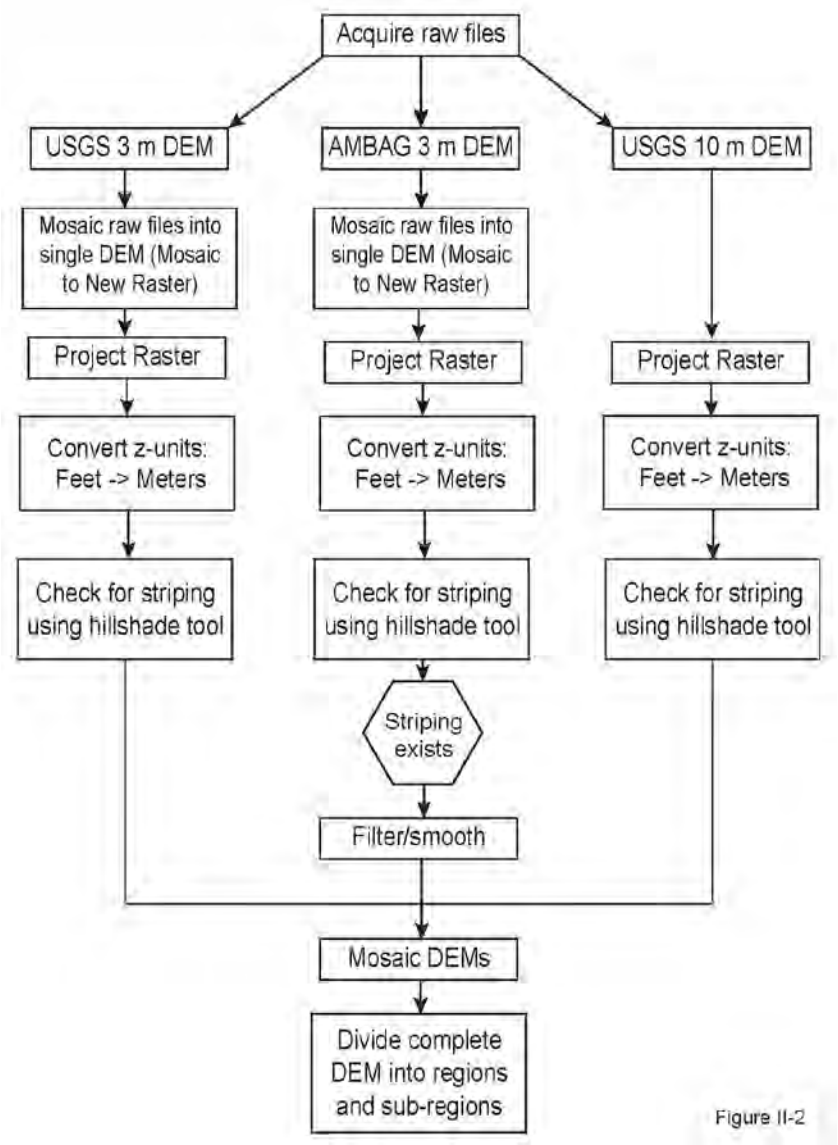

Figure II-2

The DEM was used for analysis of MAR suitability mainly as a screening tool, reasoning that areas with steep surface slopes would be more difficult and expensive to develop as infiltration sites. The DEM was used explicitly for runoff modeling, as described later.

The complete project area was subdivided into four major topographic basins (**Fig. II-3**, **Table 1-1**). These basins were defined on the basis of federally delineated hydrologic units, using USGS 1:24,000 topographic base maps, downloaded from the Watershed Boundary Dataset server [*U. S. Geological Survey*, 2014c].

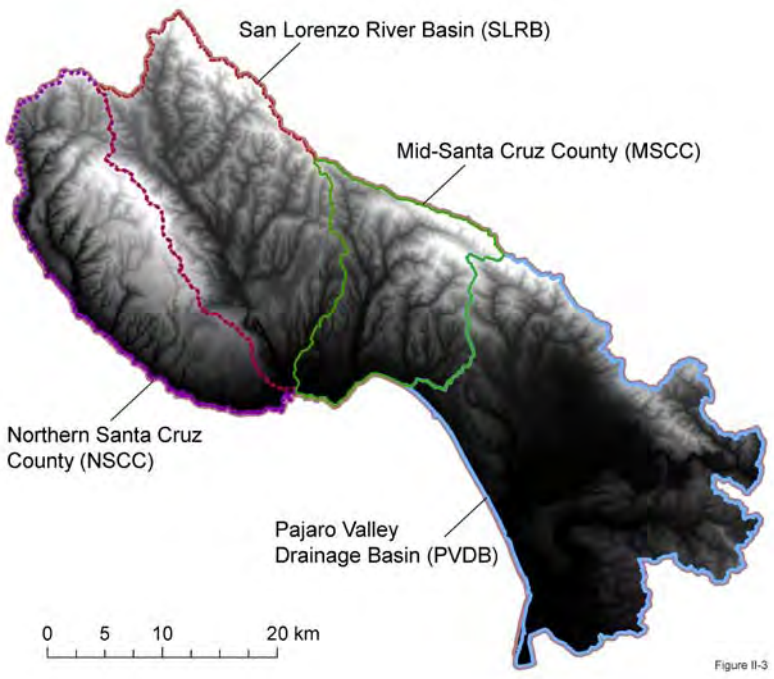

2. Soils Data

Soils data were compiled and processed for the full project region, with the primary data source being the U. S. Department of Agriculture's (USDA) Geospatial Data Gateway (https://gdg.sc.egov.usda.gov/GDGOrder.aspx), through which we acquired National Soil Conservation Service (NRCS) data from the Soil Survey Geographic (SSURGO) database [*Soil Survey Staff*, 2014]. Soils data were downloaded for the five counties covered by the project region: San Mateo (CA637), Santa Cruz (CA087), Santa Clara (CA646), San Benito (CA069), and Monterey (CA053). SSURGO datasets comprise spatial data for each county and a soil properties database in Microsoft Access format. Each county dataset is a single GIS shapefile that is divided into unique polygons representing different soil units. The spatial datasets do not include explicit information about soil properties; instead, each soil polygon is associated with a map unit symbol code (MUSYM) that can be used to cross-reference with information in the county database.

Using SSURGO data required that process information from each county database and link it to individual soil polygons. This required associating polygon data with independent tabular data, included with each county download, then generating a series of ASCII-format reports to list soil information of interest. Numerous report options were available (**Table II-1**), but none generated data in a simple tabular format as needed for processing. Once reports were generated and we confirmed data contents and format (which differed somewhat by county), we wrote Python scripts to extract, tabulate, and process soils datasets to generate coverages used for subsequent analyses. The result of this labor-intensive process is a series of useful data coverages, which were incorporated into our analyses, and are also included with the data distribution for this project for use with other applications.

Table II-1. Summary of soil reports from the SSURGO database used in this study.

Report name	Data included	Data used for MAR suitability [a]	Data use for runoff modeling [b]
Soil names, polygon sizes, fraction of area	Map unit name, map symbol, area (acres, %)	Unit name, area	Unit name, area
Wind erosion prediction	Fraction of sand/silt/clay (%), soil horizon thickness(es), texture, taxonomic order, albedo, fraction of area (%), slope	Soil horizon thickness	Soil horizon thickness, fraction sand/silt/clay
Physical soil properties	Soil thickness, fraction of sand/silt/clay (incomplete), bulk density, saturated conductivity (range), available water capacity, linear extensibility, organic matter, erosion factors, wind erodability group/index	Saturated conductivity	Soil thickness, saturated conductivity, available water capacity

[a] Data processed for use in calculation of MAR suitability, along with other datasets.
[b] Data processed to generate input for runoff modeling.

Soils data used for analysis of MAR suitability included unit names, areas, soil horizon thickness, and saturated conductivity (infiltration capacity). The latter was reported by layer and generally as a range of values (minimum, maximum). We calculated the effective infiltration

capacity (IC_E) of soils as the geometric mean of the stated range for each layer, followed by the harmonic mean of individual layers (weighted by layer thickness):

$$IC_E = \frac{\sum_{i=1}^{n} d_i}{\sum_{i=1}^{n} \left(\frac{d_i}{K_i^G} \right)} \quad (1)$$

where d = layer thickness, and $K^G = \sqrt{K_{\min} \times K_{\max}}$. This approach allowed for a range of possible soil characteristics to be represented, while giving more importance to vertical infiltration for layers having the lowest (limiting) infiltration capacity. Soils data were converted to SI units (m, m/d, etc.) during compilation and processing.

3. Bedrock Geology

Bedrock geology across the project region was assessed to determine whether individual units are likely to be aquifers contributing to regional water supply. Primary data for this analysis were developed from digital geological maps of Santa Cruz County [*Brabb et al.*, 1997], Monterey County [*Clark et al.*, 1997; *Wagner et al.*, 2002], and San Mateo County [*Brabb et al.*, 1998]. Each of these products comprises a map and explanation documentation, plus a set of digital (GIS) shape and database files. Each map is the product of compilation of dozens of data sources, including field data collected from natural outcrops, roadcuts, and well logs.

After acquiring the data and incorporating it into the GIS project, we developed a classification scheme for bedrock geology based on the presence or absence of units that are known to be aquifers, known to not be aquifers, or have the potential to be aquifers. Where units were not immediately recognizable as primary aquifer or confining units, additional research was completed to aid in classification.

An additional data set was integrated for assessment of the mid-Santa Cruz County, where the Purisima Formation is the primary aquifer. Although some units within the Purisima Formation are developed as aquifers in this area, others serve as confining units. For analysis of bedrock geology in this part of the region, we used an additional map of Purisima units that serve as shallow bedrock [*HydroMetrics WRI, Inc., pers. comm.,* 2015], overlying this map on top of the regional bedrock geology map, and thus giving it priority in classification. Detailed information on the nature and properties of individual Purisima Formation units was not available for other parts of the project region.

4. Aquifer Properties and Conditions

The primary subsurface data used in these analyses were the distribution and properties of aquifer and confining units. These data were analyzed and combined with surface data coverages to generate four subsurface datasets: transmissivity, available aquifer storage, vadose zone thickness above the water table, and recent changes in groundwater levels.

Data were acquired for the main groundwater basins in the project region (**Table I-1**) from agencies overseeing groundwater management in these areas. We assimilated data files that had been developed as part of regional groundwater modeling efforts, as these files had already taken into account information available from groundwater well logs, road cuts, stream channels, and other sources and developed three-dimensional stratigraphic and structural maps. In many cases, these stratigraphic and modeling projects were completed over many years by teams of investigators. By using the same data that had already been integrated for use with models, results of our work would be consistent with a common geological framework, and could be updated or incorporated into additional studies based on modeling and monitoring in these basins. On the other hand, this reliance on existing subsurface data coverages means that

assessment of MAR suitability based on subsurface data, and based on combined subsurface and surface data, is possible for just a fraction of each of the main drainage basins included in the full project region (**Fig. II-4**). Data sources, extent, and processing for each of these regions are described in the rest of this section.

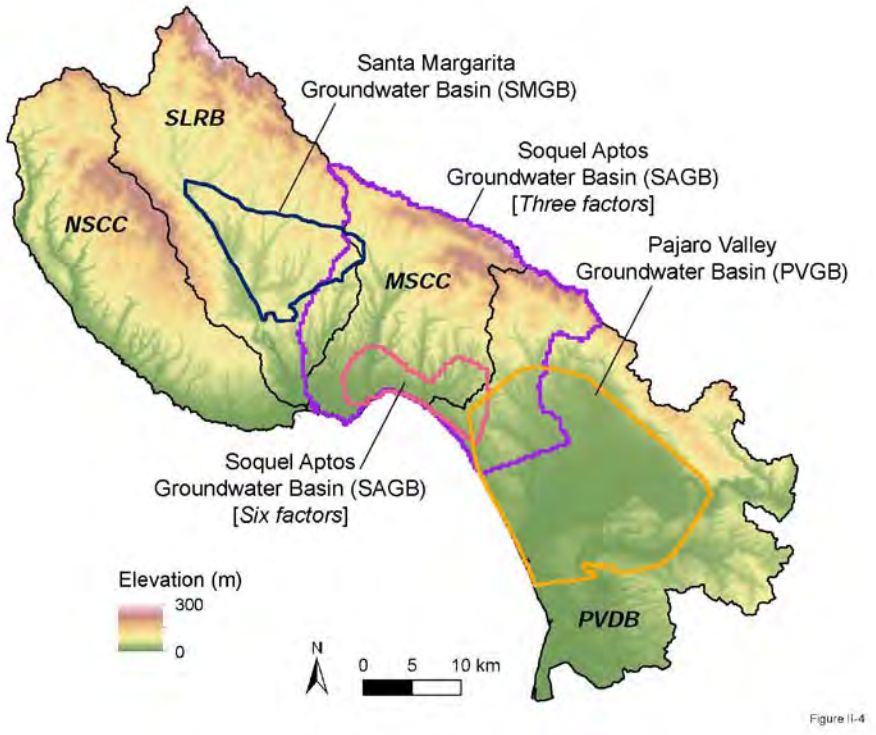

For the Santa Margarita Groundwater Basin (SMGB), located mainly in the San Lorenzo River Basin, data were developed by the Scotts Valley Water District (SVWD), the San Lorenzo Valley Water District (SLVWD), and their contractors for use in a series of groundwater models [*Kennedy/Jenks Consultants*, 2015]. For the Soquel Aptos Groundwater Basin (SAGB), located in mid-Santa Cruz County, model layers and geometric characteristics were acquired through consultants working with the Soquel Creek Water District (SqCWD) and Central Water District (CWD) [*HydroMetrics WRI, Inc., pers. comm., 2015-16*], and fundamental aquifer properties were assigned by unit from earlier studies [e.g., *Johnson et al.*, 2004]. There is an ongoing

surface water–groundwater modeling project being completed for this area, which will include revised/calibrated property assignments for subsurface units, but that work remains in progress. For the Pajaro Valley Groundwater Basin (PVGB), located mainly in southern Santa Cruz and northern Monterey Counties, subsurface data were developed from files associated with a recent groundwater model [*Hanson et al.*, 2014]. The horizontal resolution of subsurface analyses for the groundwater basins depended on the resolution of datasets developed for groundwater modeling; the size of these subsurface "pixels" was 33.528 m (110 ft) for the SMGB, 243.84 m (800 ft) for the SAGB, and 250 m (820.2 ft) for the PVGB.

The effective transmissivity of one or more aquifer layers (T_E) was calculated as the product of aquifer thickness and hydraulic conductivity, modified by the presence or absence of underlying aquifer or confining units. In general, greater transmissivity is better for managed recharge because it helps to transfer water laterally once that water reaches the aquifer(s), contributing to improved water supply and limiting mounding that could lead to saturation of shallow soils.

The same general approach was taken in all three of the main groundwater basins, but specific steps were modified slightly because of different ways in which aquifer and confining layer data were assembled for use in groundwater models. For the SMGB, there were five primary aquifer units (Santa Margarita, Monterey, Lompico, Butano, and Locatelli Formations) that were represented in seven model layers [*Kennedy/Jenks Consultants*, 2015]. In the SAGB, the Purisima Formation was divided into eight model layers, four of which were considered to be aquifers (Purisima subunits AA, A, BC, and DEF), in addition to stream and terrace deposits and the Aromas Formation [*Culkin et al.*, 2015; *Johnson et al.*, 2004]. In the PVGB, there were six

model layers, four of which represent aquifers (alluvial deposits, Upper and Lower Aromas Formation, and Purisima Formation) [*Hanson et al.*, 2014].

The effective transmissivity (T_E) was calculated as:

$$T_E = \left(K_1 \times b_1\right) + \sum_{i=2}^{n(K)} \left[\left(K_i \times b_i\right) \times I(i)\right] \quad (2)$$

where,

$$I(i) = 1 \quad \text{if} \left(K_i / K_{i-1}\right) \geq 0.5 \text{ and } K_{i-1} \geq 0.03 \text{ m/day}$$

$$I(i) = 0 \quad \text{if} \left(K_i / K_{i-1}\right) < 0.5 \text{ or } K_{i-1} < 0.03 \text{ m/day}$$

K = hydraulic conductivity, b = aquifer thickness, i = current model layer being considered, counting from the top-down at each X-Y location, and n is the total number of layers considered. I is an indicator function. I =1 when both $K_i/K_{i-1} \geq 0.5$, and $K_{i-1} \geq 0.03$ m/day. I = 0 when either one or both conditions are not met, and no deeper layers are considered (n is set to the current value of i, and summation is ended).

If K is sufficiently high, the tabulation of T values within each layer continues to the base of the aquifer system. This approach includes deeper geological layers (either aquifers or confining units) until their absolute or relative conductivity is low enough that penetration of infiltrating water to greater depths is unlikely. The net result is that calculated T_E values tend to be higher when there are adjacent layers of stacked aquifer units, all of which have favorable properties, and values of T_E tend to be lower when the shallowest layers have relatively low conductivity. This approach applies no penalty for "missing" layers in a particular location (e.g., in the case of an erosional unconformity); it simply considers all layers that are present at each location. The value of K = 0.03 m/day was chosen as a "screen" for inclusion of deeper aquifer layers based on the range of K values assigned to aquifer and confining units in the three groundwater basins.

Confining layers generally were assigned values lower than this threshold based on calibration of groundwater models (for the SMGB and PVGB) and assessment of pumping tests and other indicators of aquifer properties (for the SAGB).

Values of K used to determine T_E were obtained and assigned from agency and contractor reports and associated data files, as described earlier, but values of b (layer thickness) required additional calculations. The thickness of model layers was derived (at each X-Y location) by subtracting the lower elevation of each layer from the top elevation. However, the top elevation of each model layer was first screened and edited as needed to correct for overlap. In the case of the shallowest model layers, these sometimes had reported top elevations that were greater than ground elevation (as indicated by the DEM, after downsampling to the same spatial resolution as the groundwater model). This likely occurred because of interpolation between well records to determine layer elevations, especially when working with data from wells on either side of a valley. We used a downsampled DEM to clip model layers, so that no layer tops extended above the ground. Next, we used the bottom of each model layer to clip the top of underlying layers, if necessary. Overlap of this kind was usually ≤1 m, most likely a result of rounding errors, but there were larger overlaps in a few areas.

The availability of groundwater level data at from multiple times provided the greatest limitation on the spatial extent of analyses for subsurface MAR suitability. Groundwater level data were contoured by agency staff and consultants using measurements from wells, and these datasets never extended to the spatial limits of the associated groundwater basins. This created a particular challenge for the SAGB, for which water level data were available only for a small region close to the coast (**Fig. II-4**). For the SAGB, we completed two separate subsurface analyses, one that used only transmissivity (applicable to the full area for which aquifer units

were defined), and another for the small region for which all four subsurface datasets were available (transmissivity, available storage, vadose zone thickness, change in water level).

The space available for storage (S_A) was calculated for each *X*-*Y* location as the product of the specific yield of underlying aquifers (S_y) and the thickness of those aquifers that is not occupied by water (b_A), based on the most recent set of contoured water level elevations (**Table II-2**):

$$S_A = \left(S_{y1} \times b_{A1}\right) + \sum_{i=2}^{m(K)} \left[\left(S_{yi} \times b_{Ai}\right) \times I(i)\right] \quad (2)$$

where,

$$I(i) = 1 \quad \text{if } K_{i-1} \geq 0.03 \text{ m/day}$$
$$I(i) = 0 \quad \text{if } K_{i-1} < 0.03 \text{ m/day}$$

and b_A was calculated for each *X*-*Y* location as the lesser of the layer thickness and the difference between the top of the aquifer unit and the most recent groundwater level.

Table II-2. Summary water level data availability.

Groundwater basin	Area for which contoured water level data was available (km^2)	Year of most recent water level records	Year of earliest water level records
Santa Margarita Groundwater Basin	75.6	2014	1992
Soquel Aptos Groundwater Basin	4.8	2014	2009
Pajaro Valley Groundwater Basin	238.6	2010	1998

If a shallow aquifer unit is dewatered, calculation continues into the underlying unit until the water level is reached, provided that all overlying layers have $K \geq 0.03$ m/day. When $K < 0.03$ m/day, $I = 0$, and no deeper layers are considered (m is set to the current value of i, and

summation is ended). This is part of the same property screen used for calculation of T_E, reasoning that low K at depth will lead to perching of rapidly infiltrating water associated with MAR. In general, greater values of S_A are considered to be more favorable for placement of a DSC-MAR project.

Vadose zone thickness was calculated as the difference between the surface (ground) elevation and the most recent groundwater level. The surface elevation was determined from the downsampled DEM (corresponding to the resolution of subsurface data available for each groundwater basin). A very thin vadose zone could result in groundwater levels that mound and saturate shallow soils, which is not desired. A very thick vadose zone could require excessive infiltration before recharge occurs, delay delivery of water to an aquifer (contributing more water to ET), and/or allow for perching of infiltrating water by paleosols or thin confining layers, thus limiting infiltration and recharge benefits.

The temporal change in water level was calculated for the longest time period for which there was spatially extensive coverage. The time interval for which data were available varied basin by basin (**Table II-2**). In general, there were more data available from more recent times, and we selected data intervals that were long enough so that rates of change in groundwater levels could be represented. The shortest data interval was five years for the coastal region of the SAGB, 2009-14, which included the first three years of the recent drought. Water level data from different times were compared in each location for the shallowest aquifer layer. We took this approach so that we could assess the potential application of infiltration of excess surface water, but the emphasis on the shallowest aquifer layers in each location means that lowering of groundwater levels at depth may not be represented in the analysis.

B. Modeling Stormwater Runoff

1. Modeling overview

We simulated runoff and related processes using Precipitation Runoff Modeling System (PRMS), an open source and widely used water routing model [*Leavesley et al.*, 1983; *S Markstrom et al.*, 2008; *S L Markstrom et al.*, 2015]. PRMS is a deterministic, distributed-parameter model that represents many physical processes in computing water storage and transport on the landscape surface and in the shallow subsurface (**Fig. II-5**). We selected PRMS for this project because it can represent variability in hydrologic processes and conditions at spatial scales suitable for assessment of hillslope runoff, has a significant support community of users, and strikes a useful balance between simulation of fundamental processes and representation of the influence of these processes with parameterized equations and variables. Separate domains and models were developed for the San Lorenzo River Basin (SLRB) and lower Pajaro Valley Drainage Basin (PVDB). Work is in progress for the mid-Santa Cruz County region (overlying much of the Soquel Aptos Groundwater Basin), which is beyond the scope of the current project.

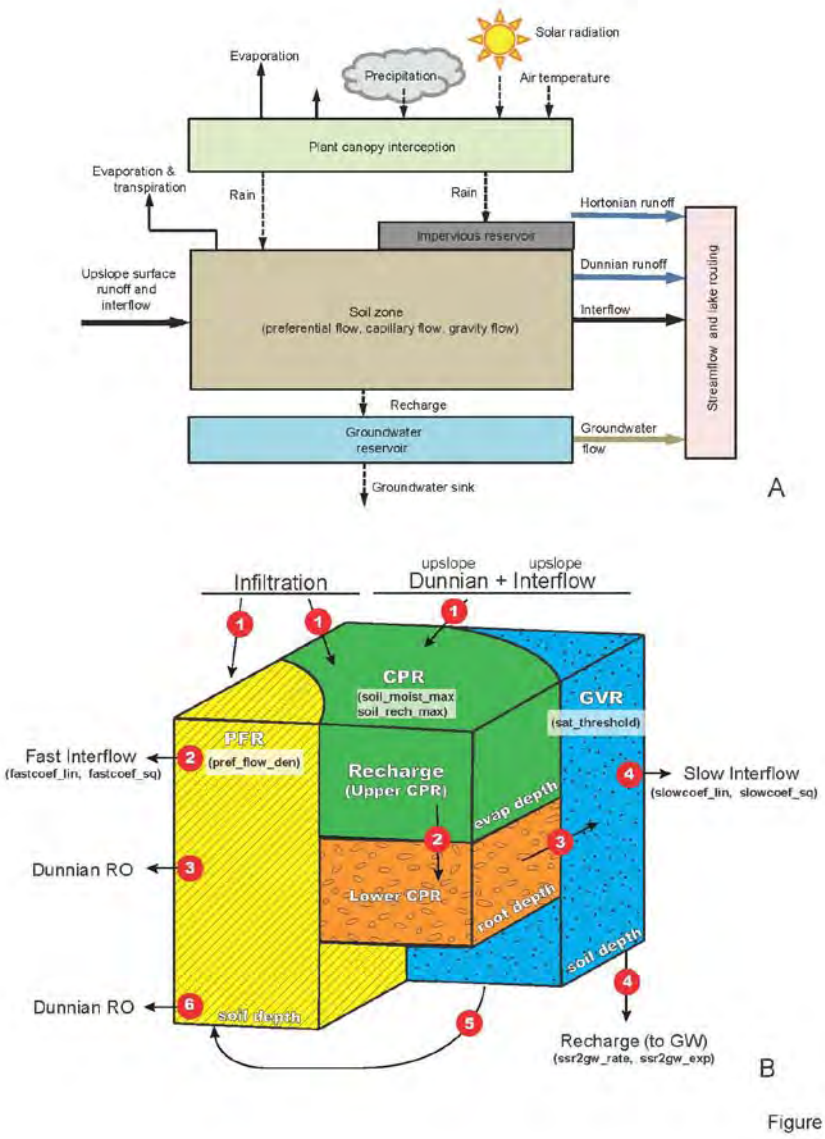

Figure II-5

PRMS requires that a topographic basin of interest be divided into a finite number of hydrologic response units (HRUs), within which water is routed, stored, and budgeted. Water applied to the landscape across a network of HRUs moves within and across the basin, eventually exiting as streamflow, evapotranspiration, or groundwater. PRMS is designed to represent hydrologic processes including: evaporation, transpiration, runoff, infiltration, and interflow, using energy and water budgets of the plant canopy, land surface, and soil zone. The model is driven by distributed climate information (temperature, precipitation, and solar

radiation). We ran PRMS simulations using daily time steps, the finest temporal resolution available with the model release used for this study (PRMS 4.01). In the following sections, we summarize steps needed to calculate preliminary parameter values, prepare input files, and calibrate results. Additional details are described elsewhere [*Young*, 2016].

2. HRU Concepts, Development and Cascades

HRUs are used to assign the geometry and properties for various water pathways and reservoirs. The soil comprises a set of complex, linked reservoirs (**Fig. II-5**), with consideration of separate but connected capillary, gravity, and preferential flow zones. Water is applied to each HRU as precipitation, and water can also enter an HRU as surface or subsurface flow from an adjacent HRU through a process known as a "cascade." At each daily time step, the water input to each HRU is separated into multiple runoff, interception, evaporation and infiltration components.

HRUs can be defined based on topography, soils, land use, vegetation, or a combination of these and other parameters. The delineation of HRUs and their property assignments are critical to simulation development, but there are limited tools available for this purpose. Thus considerable time was spent developing tools and protocols for creating a network of HRUs and assigning their hydrologic properties, after gathering and assimilation of essential datasets. In the rest of this section, we describe primary steps for HRU delineation and property assignments.

HRUs were delineated using the composite 3-m DEM. Because our primary goal was to assess contributions of stormwater runoff at a scale suitable for development of DSC-MAR systems, we targeted development of an HRU network for each basin made up of individual HRUs having an area of 0.1 to 1 km^2 (25 to 250 acres).

The elevation gradient was calculated at each raster location to determine the direction of steepest slope, rounded to the nearest 45° angular direction. Flow accumulation was calculated as the sum of upslope raster cells, leading to the creation of a digital stream channel network across the landscape when flow accumulation exceeded a predefined threshold. The delineation of this digital channel network is an iterative and interactive process, which continues until the desired density of channels is achieved. We compared the digital stream network to the USGS National Hydrography Database [*U. S. Geological Survey*, 2014b] to assess accuracy, and manually edited stream segments that were inconsistent with known flow paths. Editing was required mainly in areas having low topographic gradients and/or where water was artificially routed for agricultural use, in which vegetation or infrastructure patterns generated artifacts in the DEM. The digital channel network was subsequently subdivided and ordered into individual stream segments, each of which was associated with an HRU that could contribute runoff to that segment. The HRU delineation process can result in creation of apparent closed topographic regions, lacking a channel outlet. Most of these were caused by artifacts in the DEM and were "digitally filled" as part of the HRU creation process so that runoff could contribute to flow into an adjacent HRU, but some were found by inspection of aerial photographs to be lakes, quarries, or other small basins. Actual topographic depressions lacking an outlet were characterized in PRMS as "swales," from which there is no surface runoff [*S L Markstrom et al.*, 2015]. After creation of an initial set of HRUs within a topographic basin, most of which had an area consistent with our goal of 0.1 to 1.0 km^2, we divided or combined HRUs as needed so that all of them fell within the desired range of sizes.

HRUs can be connected to adjacent HRUs using a cascade network. Once the HRU set (size, boundaries) was finalized, we compared HRUs and the digital stream network to actual channels

("blue line streams") defined in the National Hydrography Dataset [*U. S. Geological Survey*, 2014b]. This allowed us to assess whether a digital stream channel corresponded to a natural stream channel that exists in the real world. If there was no corresponding blue line stream within 50 m of a digital channel (by comparison of stream centroids), we deleted the digital channel. If an actual channel existed within an HRU, PRMS routes hillslope flows within that HRU to the channel, then to the channel of the next downslope HRU and eventually out of the basin. In contrast, if an HRU does not contain an actual stream channel, then PRMS routes hillslope runoff from that HRU to the next downslope HRU, from where it can continue to flow across the landscape, infiltrate, etc. On this basis, each HRU that contains a blue line stream is classified as "channelized runoff-dominated," whereas other HRUs are classified as "hillslope runoff-dominated." We determined the HRU-to-HRU cascade links for HRUs that are "hillslope runoff-dominated," and HRU-to-stream cascade links for HRUs that are "channelized runoff-dominated."

3. HRU Parameter Assignments

PRMS requires assigning dozens of HRU parameters that are used to determine the nature of storage and flow within and between reservoirs and stream channels (**Table II-3**). Most PRMS parameters vary spatially but are constant in time, whereas others vary month to month, and still others are constant in both space and time. In addition, some parameters are assigned in terms of real world units, whereas others are classified according to rules governing water routing in PRMS. Some parameters were varied during calibration, whereas others were held constant (**Table II-3**). We discuss the formulation and selection of parameters in this section; calibration is discussed later.

Table II-3. Summary of PRMS parameters and values, organized by module.

PRMS module	Parameter	Units	SLRB	PVDB
basic physical	hru_area	acres (km^2)	5.7 - 245.7 (0.02 - 1.0)	1.0 - 266.9 (0.004 - 1.08)
	hru_aspect	degrees	49 - 262	0.1 - 291
	hru_elev	meters	4.0 - 839	2.3 - 781
	hru_lat	degrees N	37.0 - 37.2	36.8 - 37.1
	hru_slope	dec. frac.	0.03 - 0.72	0.00 - 0.65
	hru_type	-	0, 1, 3	1
strmflow - muskingum	hru_segment	-	0 - 859	0 - 953
	K_coef	hours	0.01	0.01
	obsin_segment	-	0	0
	segment_flow_init	-	0.0	0.0
	segment_type	-	0, 2	0
	tosegment	-	0 - 859	0 – 953
	x_coef	dec. frac.	1.0	1.0
subbasin	hru_subbasin	-	1 - 3	1 - 6
	subbasin_down	-	0, 2, 3	0, 1, 3, 4, 6
cascade	cascade_flg	-	1	1
	cascade_tol	acres	0.0	0.0
	hru_down_id	-	0 - 859	0 - 953
	hru_pct_up	dec. frac.	1.0	1.0
	hru_strmseg_down_id	-	0 - 859	0 - 953
	hru_up_id	-	1 - 867	1 - 1025
cascade gw	gw_down_id	-	0 - 859	0 - 953
	gw_pct_up	dec. frac.	1.0	1.0
	gw_strmseg_down_id	-	0 - 859	0 – 953
	gw_up_id	-	1 - 867	1 – 1025
gwflow	gwflow_coef	fraction/day	0.015	0.001
	gwsink_coef	fraction/day	0.035	0.6
	gwstor_init	inches	10.0	10.0
	gwstor_min	inches	0.0	0.0

	fastcoef_lin	fraction/day	0.001	0.001
	fastcoef_sq	-	0.001	0.001
	slowcoef_lin	fraction/day	0.001	0.001
	slowcoef_sq	-	0.001	0.001
	ssr2gw_rate	fraction/day	0.01 - 0.41	0.04 - 0.156
	ssr2gw_exp	-	2.0	1.8
	soil2gw_max	inches	0.0	0.0
soilzone	soil_rechr_init	inches	0.0	0.0
	soil_rechr_max	inches	0.041 - 0.098	0.072 - 0.286
	soil_moist_init	inches	0.0	0.0
	soil_moist_max	inches	0.11 - 20.95	0.65 - 64.8
	pref_flow_den	dec. frac.	0.0	0.0001 - 0.033
	sat_threshold	inches	0.41 - 33.16	0.116 - 7.64
	ssstor_init	inches	0.0	0.0
	soil_type	-	1 - 3	1 - 3
	transp_beg	cal month	1	1
	transp_end	cal month	13	13
transp-tindex	transp_tmax	°C	0.0	0.0
	potet_sublim	dec. frac.	0.5	0.5
	rad_trncf	dec. frac.	0.5	0.5
	smidx_coef	dec. frac.	0.06	0.02
srunoff-smidx	smidx_exp	1/inch	0.5	0.1
	hru_percent_imperv	dec. frac.	0.0 - 1.0	0.0 - 0.79
	imperv_stor_max	inches	0.05	0.05
	cov_type	-	0 - 4	0 - 4
	covden_sum	dec. frac.	0.0 - 0.90	0.0098 - 1.0
intcp	covden_win	dec. frac.	0.0 - 0.90	0.0098 - 1.0
	srain_intcp	inches	0.0 - 0.067	0.0361-0.067
	wrain_intcp	inches	0.0 - 0.067	0.0361-0.067
et – potet_hamon	hamon_coef	-	0.004 - 0.008	0.0064 - 0.0094

Basic topographic and geospatial parameters, such as HRU area and slope, were calculated by averaging raster values within each HRU. More complex parameters were calculated as a combination of contributing values. For example, the maximum amount of water available for transpiration (known in PRMS as, **soil_moist_max**, [L]), was calculated as:

$$\textbf{soil\_moist\_max} = AWC \times R \tag{3}$$

where *AWC* = available water capacity (fraction, [-]) and *R* = rooting depth [L]. Similarly, the water available for gravity drainage and/or interflow (**sat_threshold**, [L]) was calculated as:

$$\textbf{sat\_threshold} = (n - FC) \times d \tag{4}$$

where *n* = soil porosity [-], *FC* = soil field capacity [-], and *d* = soil thickness [L].

These and many other parameters were determined using soil and vegetation data for each HRU, and based on values reported in the literature (**Table II-4**). Soils data were derived from the SSURGO database [*Soil Survey Staff*, 2014], whereas vegetation and land use data were derived from the USDA Forest Service Classification and Assessment with LANDSAT of Visible Ecological Groupings (CALVEG) project [*USDA Forest Service*, 2014], augmented by the USDA, National Agricultural Statistics Service's Cropland Data Layer (CDL) [*USDA-NASS*, 2015].

Table II-4. PRMS parameter input as defined by soil and vegetation information

Soils

Soil PRMS input [a]	Sand	Loam	Clay	Source(s) [b]
Porosity, *n* (-)	0.35	0.45	0.50	1
Field capacity, *FC* (-)	0.15	0.30	0.40	1
Evap. depth (in)	0.59	0.59	0.59	2
Available water capacity, *AWC* (-)	0.07-0.15	0.05-0.19	0.10-0.20	3
Infiltration capacity, *IC* (in/day)	3.6 - 578	0.0 - 61.4	0.0 - 25.6	3

[a] Units listed are those used by PRMS. (-) = fraction, 0 to 1.
[b] 1 = Freeze and Cherry [1979], Fetter [2001], 2 = Heitmann et al. [2008]; 3 = Soil Survey Staff [2014].

Vegetation

Vegetation PRMS input [a]	Bare	Grasses	Shrubs	Deciduous	Confierous	Source(s) [b]
Rooting depth (in)	0	50	79	87	117	1
Coverage density (-)	0	100	55	35	35	2
Impervious fraction	1	0	0	0	0	3
Interception storage (in)	0	0.0672	0.0361	0.0490	0.0573	4

[a] Units listed are those used by PRMS. (-) = fraction, 0 to 1.
[b] 1 = Schenk and Jackson [2002], Canadell et al. [1996]; 2 = USDA Forest Service [2014]; 3 = Viger et al. [2010]; 4 = Crouse et al. [1996], Couturier and Ripley [1973], Garcia-Estringana et al. [2010], Fathizadeh et al., [2013], Klaassen et al. [1998], Reid and Lewis [2009].

SSURGO data includes information on multiple soil layers, requiring calculations to determine representative properties. Some of these properties were assigned on a highly detailed basis, whereas others were assigned by category. We used soil texture information for each soil category (weighted within each HRU) to assign PRMS soil types: *sand, loam* or *clay*. If the sand content was >50%, the assigned PRMS type was "sand." If sand content was < 50% and clay content was >40%, PRMS type was "clay." If neither of these conditions was met, PRMS type was "loam" (**Table II-4**). With the PRMS soil type in place, we assigned values of porosity and field capacity to each HRU.

The effective infiltration capacity (IC_E) for each soil polygon was calculated as described in Section II.A.2, then determined as a spatially weighted average for each HRU. Other soil parameters that were defined for multiple soil layers, like the available water capacity (*AWC*), were similarly weighted by both spatial representation in each HRU and depth representation of individual soil layers, weighted by layer thicknesses. Evaporation depth was assigned uniformly (**Table II-4**).

The CALVEG dataset was used as a primary coverage for land use and vegetation because it was the only available vegetation dataset that included percent cover. The CALVEG dataset also includes multiple detailed subcategories ("regional dominance") for classification of plant species and types of agricultural development (e.g., row crops versus fruit trees). However, the CALVEG dataset was found to have significant data gaps and inconsistencies in how vegetation type was assigned (entirely within in the Pajaro Valley Groundwater Basin), requiring additional processing and manipulation (**Fig. II-6**). We used the CDL data to fill gaps in the CALVEG data, but this required conversion and smoothing of CDL raster data, and reclassification of some of the data types to make them consistent with CALVEG classification. Because CDL data did not include information on percent vegetation cover, we applied median percent cover values for the same CALVEG vegetation types from the surrounding region in places where CALVEG data gaps were filled with CDL data. Once the conversion and reclassification of CDL data were complete, we applied a simple transform to convert vegetation types to the PRMS classification needed for runoff modeling (**Fig. II-7**). Many of the main CALVEG vegetation types mapped directly onto the PRMS classification (e.g., *Conifer* → *4. Conifer*, *Hardwood* → *3. Deciduous*, etc.), but for CALVEG cover types *Agriculture* and *Mix*, we used the regional dominance classification for each polygon to assign an appropriate PRMS vegetation/land use code.

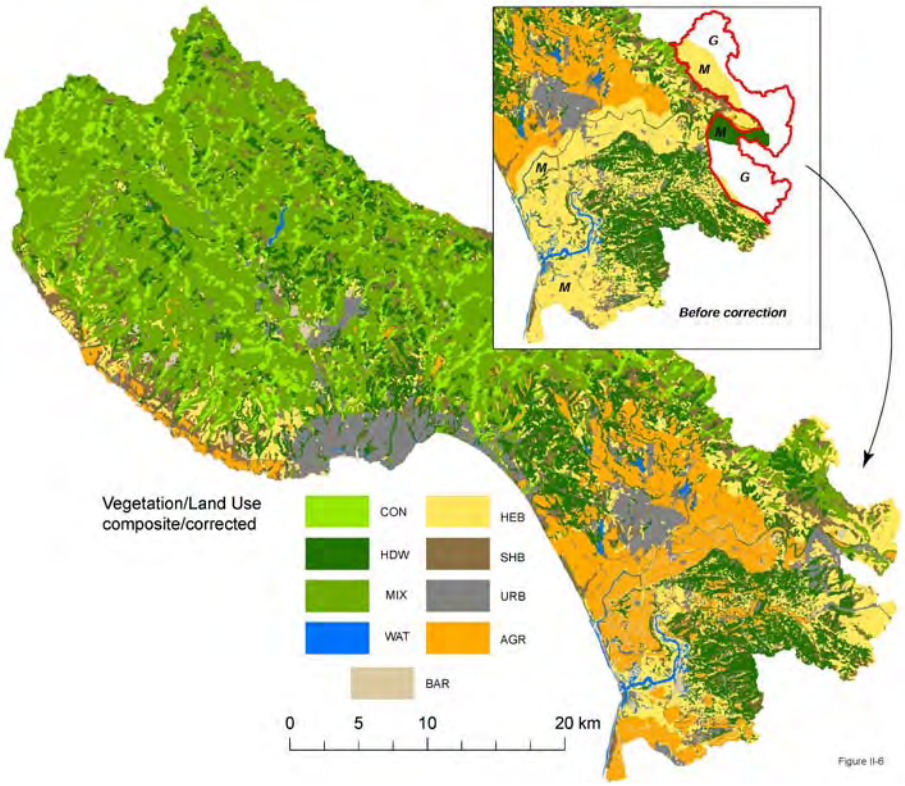

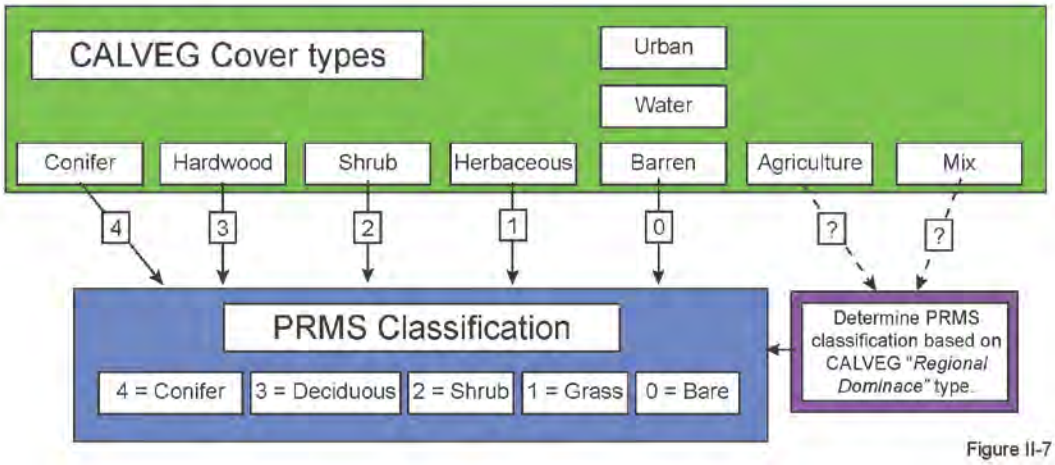

Figure II-7

The soil and vegetation input data, defined for polygons that do not correspond completely to HRUs, were used to assign representative properties to each HRU using area weighted or area-and-density weighted functions:

$$X_{HRU} = \frac{\sum_{i=1}^{n} x_i A_i}{\sum_{i=1}^{n} A_i} \text{ (area weighting)} \quad (5)$$

$$X_{HRU} = \frac{\sum_{i=1}^{n} x_i A_i D_i}{\sum_{i=1}^{n} A_i D_i} \text{ (area and density weighting)} \quad (6)$$

where X_{HRU} is a value assigned to an HRU, x_i is the soil or vegetation value for a polygon that is partly represented by the HRU, A_i is the area of the soil or vegetation polygon contained within the HRU, D_i is vegetation density, and n is the number of polygons that are partly or fully enclosed by the HRU.

Potential evapotranspiration (PET) was calculated using the Hamon method, whereby PET is computed based on mean daily air temperature and hours of sunshine [*Hamon*, 1961; *S L Markstrom et al.*, 2015]. A separate value for the **hamon_coef** parameter was assigned for each month of the year within each topographic basin, following proportionate scaling to match PET calculations from local meteorological stations. The percent impervious fraction within each HRU (**hru_percent_imperv**) was calculated using the composite vegetation/land use coverage for the study region, assigning an impervious fraction to each polygon and then weighting HRU values according (eq. 5).

Determination of linear soil routing coefficients (**fast_coef_lin**, **slow_coef_lin**, and **ssr2gw_rate**, **Fig. II-5**) required additional calculations. We had already determined effective infiltration capacity (IC_E) values based on SSURGO data. We separated IC_E values into quintiles and assigned a corresponding IC_{index} on a scale of 0 to 4 based on $\log_2$ scaling:

$$IC_{index} = \log_2(IC_E) - 2.3 \quad (7)$$

This approach is broadly consistent with rating of IC_E values as applied to calculations of MAR suitability (section III.A.2). Use of the $\log_2$ transformation preserves considerable variability in properties across the simulation domains, and prevents the highest IC_E values from overwhelming lower values during spatial averaging. Soil polygon values of IC_{index} were weighted by area within each HRU, and resulting values were used to scale the default PRMS linear soil routing coefficients.

4. HRU Variables

Primary PRMS variables, defined for each HRU at each (daily) time step are minimum temperature (*tmin*), maximum temperature (*tmax*), and precipitation (*precip*). In addition, we specified daily runoff as measured at stream gauging stations corresponding to stream channels within selected HRUs (*runoff*), for use in calibration and validation. Daily regional temperature and precipitation data were obtained from the Parameter-elevation Regressions on Independent Slopes Model (PRISM) project, covering the period of 1981-2014 [*PRISM Climate Group*, 2016]. PRISM data were interpolated on an 800-m, rectangular grid across the continental United States, based on observations from numerous meteorological data stations. After acquiring and parsing the datasets, clipping their extent to correspond to our project area for easier handling, we compared results from individual PRISM "pixels" to corresponding meteorological stations, confirming that the spatially continuous data honor direct observations. There were some offsets between values from one day to the next, mainly because of a mismatch between times used to define each meteorological "day." Days are defined at different stations as 12:00 to 12:00, 0:00 to 0:00, or 9:00 to 9:00. It is not possible to shift precipitation across individual data days to develop coverages using consistent day definitions, but assessment of cumulative precipitation across the project area indicates that the PRISM data comprise a

reasonable representation [*Young*, 2016]. Daily PRISM data values were averaged for each HRU (eq. 5), resulting in highly granular spatial and temporal resolution of critical inputs to PRMS (**Fig. II-8**).

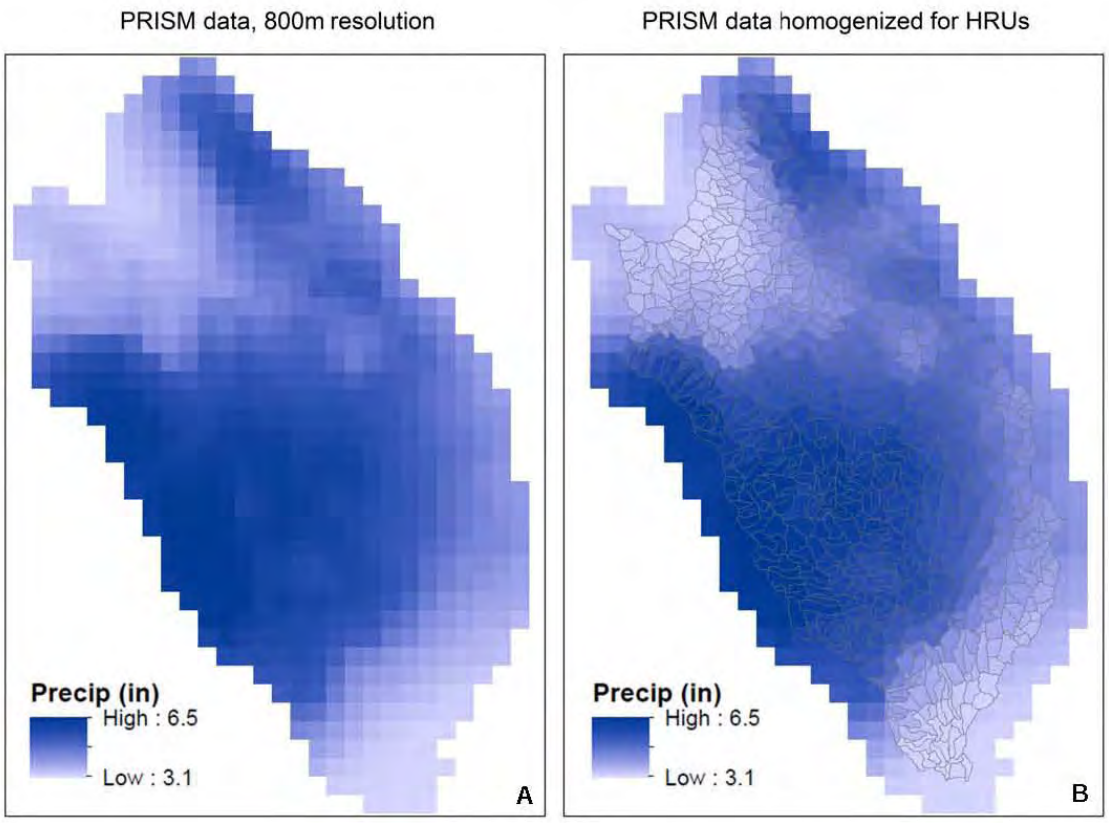

Figure II-8

5. Calibration and Validation

Calibration was completed by systematically modifying soil, streamflow, and other parameters, and comparing model output to measured streamflow runoff on monthly and annual timescales. Fit metrics are described below. Soil parameters and vegetation parameters assigned by type for rooting depth, coverage density, and interception storage varied spatially but were held constant in time. For initial conditions during calibration, we set water in soil reservoir storage to minimal values, and assigned nominal initial values for the groundwater reservoir

(**Table II-3**). Simulations were run for several years to allow "spin up" prior to calibration. Rainfall patterns are highly seasonal in the project area, which helped with assessment of rainfall-runoff response, because the start of each water year occurs after a 5-6 month dry period, essentially "resetting" soil reservoirs to relatively dry conditions.

We compared simulated and measured daily runoff values as well, mainly to assess the shape of the recession limbs of seasonal and event hydrographs, but chose to not develop formal metrics for calibration based on daily data. Using daily precipitation data limits the accuracy of daily runoff simulations, because precipitation records will frequently underrepresent storm intensity, which tends to be greatest for minutes to hours at a time. There is an additional problem when storm events cross multiple calendar days, which results in a longer and less intense event being represented in the simulation. Artificially low rainfall intensity and extended duration will tend to reduce soil moisture saturation, favoring infiltration and subsurface flow (interflow, gravity drainage, baseflow) rather than Dunnian runoff. The use of relatively small HRUs, which benefits representation of heterogeneities in landscape and vegetation conditions, also tends to favor infiltration and subsurface flows over surface runoff, because soil water routing options are assessed within each individual HRU at each time step, providing repeated opportunities for infiltration to occur. Thus the PRMS simulations are conservative with respect to hillslope runoff that might be collected for MAR, and will tend to under-predict channel runoff. Successful calibration for daily channel runoff would require meteorological (driving) data with a temporal resolution of hours or minutes, in addition to much shorter time steps in PRMS.

For the SLRB, we used a USGS gauging station on the San Lorenzo River, Santa Cruz, CA (#11161000) as the primary calibration data location, but also compared simulation results to

data collected upstream at Big Trees, CA (#11160500) (**Fig. II-9**). SLRB simulation output was considered in three separate time periods: six years of model start up and stabilization (WY82-87), 14 years of calibration (WY88-01), and 13 years of validation (WY01-14).

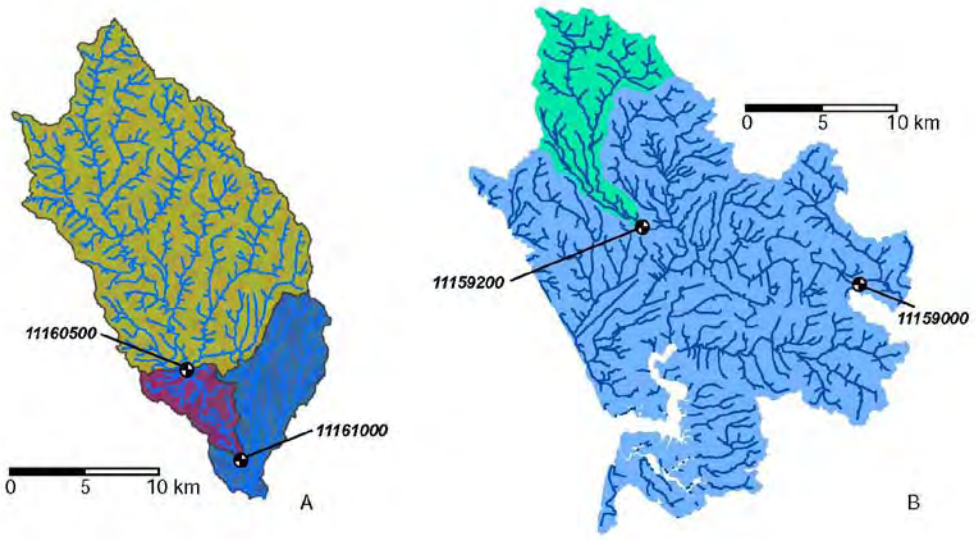

Figure II-9

For the PVDB, useful daily discharge data were available only for the USGS gauging station on Corralitos Creek at Green Valley Road, Freedom, CA (#11159200), which accounts for ~14% of the project basin (**Fig. II-9**). There is also a USGS gauge on the Pajaro River at Chittenden, CA (#1115900), but this represents drainage from a very small part of the project region, with most of the channel flow originating as drainage from 3,071 km^2 of the upper Pajaro River watershed. There has been a gauge operated periodically on the Pajaro River at the city of Watsonville, closer to the west side of the basin, but available data comprises stage rather than discharge and records are incomplete. For the PVDB, the calibration and validation periods were flipped relative to those used for the SLRB: 14 years of calibration (WY01-14), and 13 years of validation (WY88-00). The temporal order of calibration and validation periods should not matter, assuming that each of the periods has a broadly representative range of precipitation and flow conditions.

Calibration was completed using two primary metrics/tools to compare simulated to observed runoff: (a) cross-plots of simulated versus observed *runoff* (channel flow) at selected gauging points, with evaluation of monthly mean daily and annual discharge values, and (b) the normalized root mean square deviation (NRMSD) based on simulated and observed *runoff* values, calculated as:

$$NRMSD = \frac{\sqrt{\sum_{i=1}^{n} (x_i - o_i)^2 / n}}{(o_{\max} - o_{\min})^2} \quad (8)$$

where x_i is simulated *runoff*, o_i is observed *runoff*, n is the number of data points (months of mean values), and $o_{\max}$ and $o_{\min}$ are the maximum and minimum observed *runoff* values in the sample. For the monthly calibration, we considered NRMSD values only for six months during the rainy season each year (November-April), when most precipitation and runoff occurs, so that results are not biased by simulations of low flow conditions. This approach is appropriate for the current study, which is focused on hillslope runoff and the generation of a supply for distributed MAR projects. As part of the calibration process, we also considered mass balance across the multiyear simulations, verifying that soil and groundwater reservoirs did not systematically accumulate mass over the long term. PRMS does not model groundwater flow *per se*, but does route groundwater into a baseflow term as storage values increase. As a result, systematic increases in simulated groundwater storage can lead to unrealistic increases in baseflow.

Validation results are summarized with the same metrics used for calibration, but without any additional adjustment of PRMS parameters, focusing on monthly and annual flows. We also looked at daily streamflow records and simulated results, once again assessing the overall consistency and shapes of seasonal observed and simulated hydrographs.

6. Climate Scenarios

Once calibration was complete, we developed simulation catalogs based on data from the historic record (for which we had PRISM data) that were representative of "dry," "median" (*normal*), and "wet" water years. In each drainage basin (SLRB, PVDB), we calculated the non-exceedance probabilities, *p*, of total annual precipitation as:

$$p = \frac{m}{n+1} \tag{9}$$

where *n* is the number of years in the dataset and *m* is the rank (1 = largest). The non-exceedance probability is the fractional probability that the total annual precipitation for a given year will not be greater than a particular value.

We selected a set of water years at and surrounding the 20th, 50th, and 80th percentiles to represent "dry," "median" (*normal*), and "wet" conditions, with five years applied to the *dry* and *wet* scenarios and seven years applied to the *normal* scenario (**Fig. II-10**). Collectively, these catalogs span about 80% of the total range of climate conditions, from the 10th to the 90th non-exceedance probability. Ranking and year assignments for the climate scenarios were done independently for the SLRB and PVDB, based on PRISM records for each basin alone (**Fig. II-10**, **Table II-5**). Once the years for the three climate scenarios were defined, we randomized the order of the years within each scenario, then ran a single composite simulation for each basin that included all three of the climate scenarios. In each case, we ran two model "stabilization" periods using the *normal* climate scenario, so that there would not be a major influence from antecedent moisture conditions, one at the start of the composite simulation, and one between *wet* and *dry* climate scenarios (**Table II-5**).

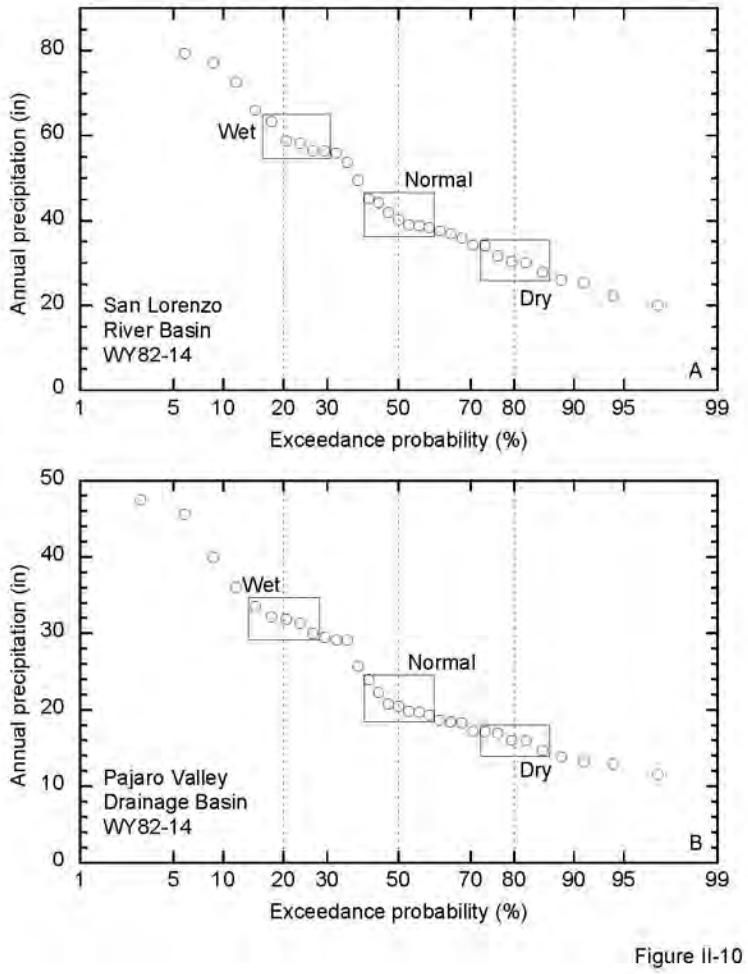

Figure II-10

We chose to represent different climate scenarios with this approach, rather than using results of regional climate models, for several reasons. First, by using the historic record as delineated with high-resolution (800 m, daily) PRISM data, we represented the complex nature of precipitation characteristics that have occurred in each basin: event intensity, duration, persistence, and spatial distribution. The observational record also contains information on temperature and precipitation, helping to reduce the number of degrees of freedom in exploring future conditions (warmer/cooler, wetter/drier). There is considerable disagreement among regional climate models as to whether future conditions may be wetter or drier, on average (e.g., Flint and Flint, 2014). In addition, even the finest-scale regional models tend to have spatial

resolution of 10-20 km, which would not provide useful information on how precipitation is distributed during wetter or drier periods. Given these uncertainties, it seems most useful to simulate a range of climate scenarios so that water managers and stakeholders can assess the extent to which DSC-MAR might be accomplished under dry, normal, and wet conditions.

Table II-5. PRMS climate scenarios based on daily PRISM data for each basin.

Purpose [a]	Climate scenario	SLRB	PVDB
Model stabilization	Normal	1984	2004
		1992	2001
		1999	1984
		2001	1985
		2002	1992
		2003	2003
		2004	1999
Analysis	Normal	1984	2004
		1992	2001
		1999	1984
		2001	1985
		2002	1992
		2003	2003
		2004	1999
Analysis	Wet	1986	2011
		1997	1997
		2005	1993
		2006	2005
		2011	1986
Model stabilization	Normal	1984	2004
		1992	2001
		1999	1984
		2001	1985
		2002	1992
		2003	2003
		2004	1999
Analysis	Dry	1988	1990
		1989	2013
		1991	1994
		1994	2012
		2012	1989

[a] Model stabilization helps to avoid a major influence from initial conditions, including antecedent moisture.

Once the climate scenarios were developed and simulations were completed, we analyzed model-generated outputs with an emphasis on relations between *precipitation* and *hillslope runoff*, including calculation of a hillslope runoff-precipitation ratio (*RPR*):

$$RPR = \frac{hillslope\ runoff}{precipitation} \tag{10}$$

where *hillslope runoff* = *interflow* + *surface runoff*. Although *interflow* and *surface runoff* are calculated separately within PRMS, we elected to combine these flows in *RPR* calculations because it is difficult to calibrate or develop observational datasets as groundtruth for these distinct hydrologic flows. In addition, both kinds of hillslope runoff could potentially contribute to development of DSC-MAR projects. The baseflow component of runoff was not considered to contribute in a significant way to supplying water for DSC-MAR systems, as this is water that is delivered to a stream or river channel from an underlying aquifer.

Our definition of *RPR* differs from the traditional runoff coefficient because the simulated *RPR* aggregates upslope runoff within downslope HRUs. This can lead to elevated *RPR* values, including *RPR* >1, when enough surface runoff from one HRU flows onto an adjacent HRU. This definition of *RPR* is beneficial for assessment of potential DSC-MAR project sites; parcels that receive runoff from the adjacent landscape and contribute additional runoff may be highly suitable locations, particularly if down-cascade parcels have surface and subsurface conditions that are amenable to rapid infiltration and storage of excess flows. To analyze the variability of *hillslope runoff*, we calculate statistics based on monthly and annual data drawn from all HRUs in a basin (mean monthly and annual values). Calculations of the range between 25th and 75th percentiles of these results are referred to as the "interquartile range." We also look at the distribution of *hillslope runoff* and *RPR* values across each basin to get a sense of heterogeneity and patterns. These calculations are restricted to the rainy season (November to April) of each

water year, as runoff during the dry season (even when there are occasional precipitation events) is unlikely to contribute significantly to DSC-MAR benefits.

III. Spatial Variations in Suitability for Managed Aquifer Recharge

A. Compiled Data and Index Classification

1. Digital Elevation Model

The composite digital elevation model provides ~3 m horizontal resolution for the full project region (**Fig. III-1**). Lowest elevations are found along the coast and within coastal estuaries, rivers, streams and bays, and the highest elevations are found in the Santa Cruz Mountains, particularly in the northern and eastern parts of the project region.

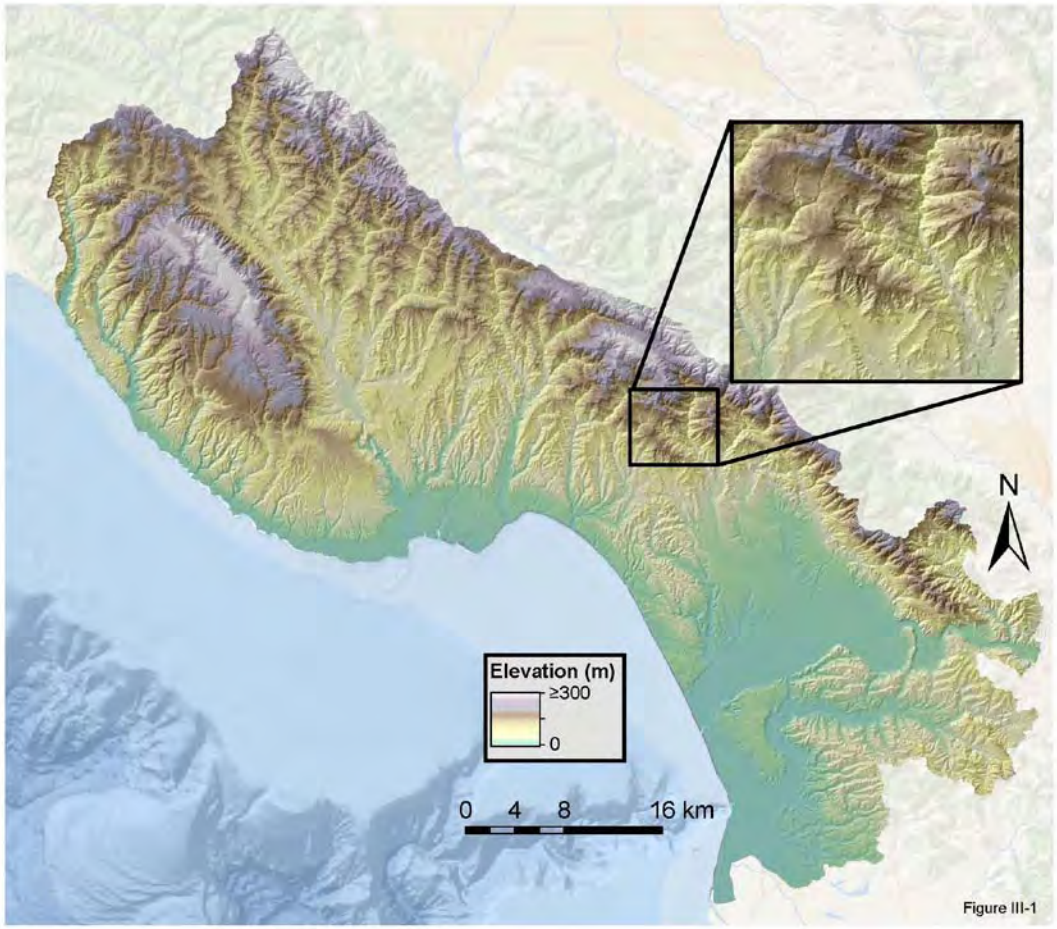

2. Soils Data

Soil data extracted from the SSURGO database delineate 5,270 individual polygons, ranging in size from 2.25×10^{-4} to 8.65×10^{3} acres, comprising 211 distinct soil types (**Fig. III-2**). The calculated effective infiltration capacity (IC_E) for these soils ranges from 0 m/day to 14.7 m/day, a range of more than three orders of magnitude. Assignment of a classification scale based on IC_E was accomplished by examining the distribution of calculated values (**Fig. III-2**), and exploring possible options for normalizing across the observed range. We chose a final index scale (0 to 4) based on a $\log_2$ transformation of IC_E values (**Fig. III-3**), with divisions at 0.25, 0.5, 1.0 and 2.0 m/day. This range was selected so that an intermediate value on the transformed scale (2) would correspond to an infiltration capacity value that was considered generally acceptable for an infiltration/recharge project (0.5 to 1.0 m/day). Lower values would not necessarily disqualify a site, particularly if other factors were favorable, but could limit project effectiveness. In general, soils having an IC_E index of 3 or 4 are coarser and correspond to stream channel, alluvial, and eolian (dune) deposits. In contrast, IC_E index scores of 0 or 1 tend to be found in present or ancient flood, wetland, or estuarine deposits (**Fig. III-3**).

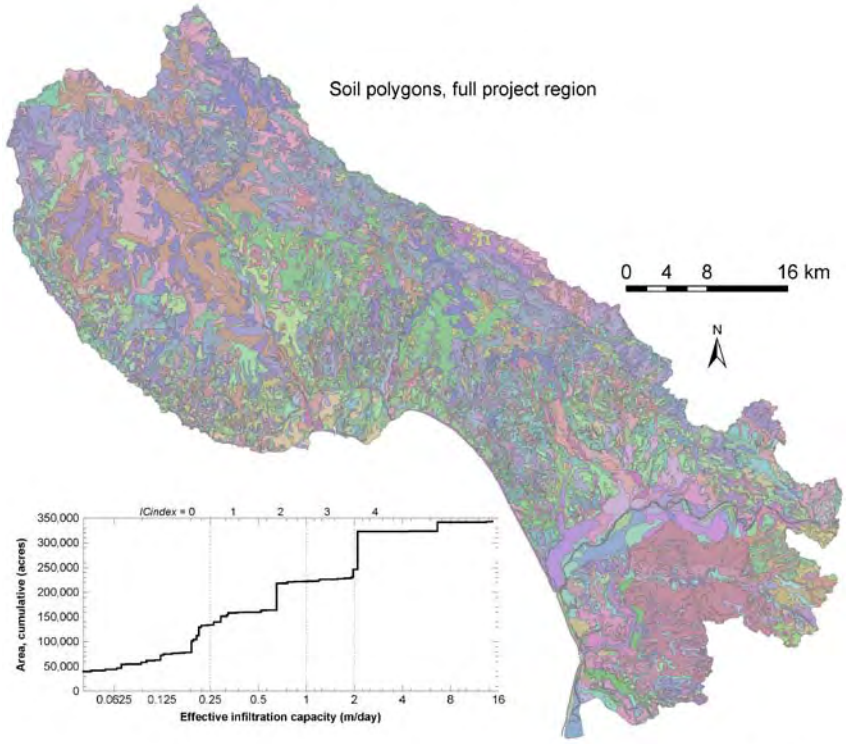

Figure III-2

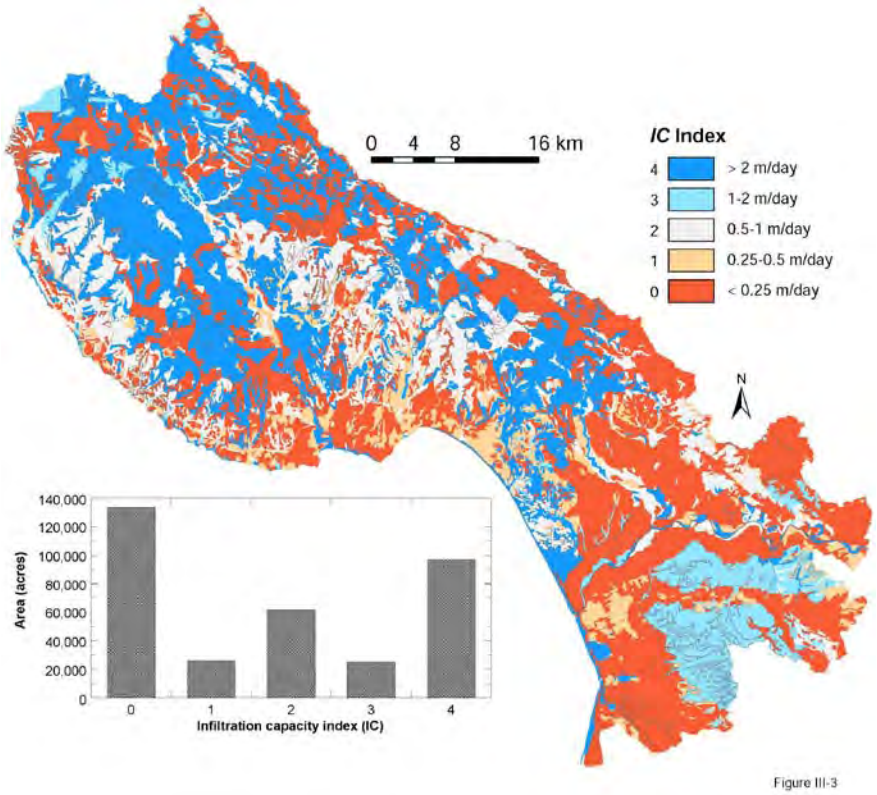

Figure III-3

3. Bedrock Geology

Compiled geological data yielded 1619 total polygons (**Fig. III-4**). Most of these are geological units, although the mapped designations also include lakes, estuaries, wetlands and other hydrologic/environmental features.

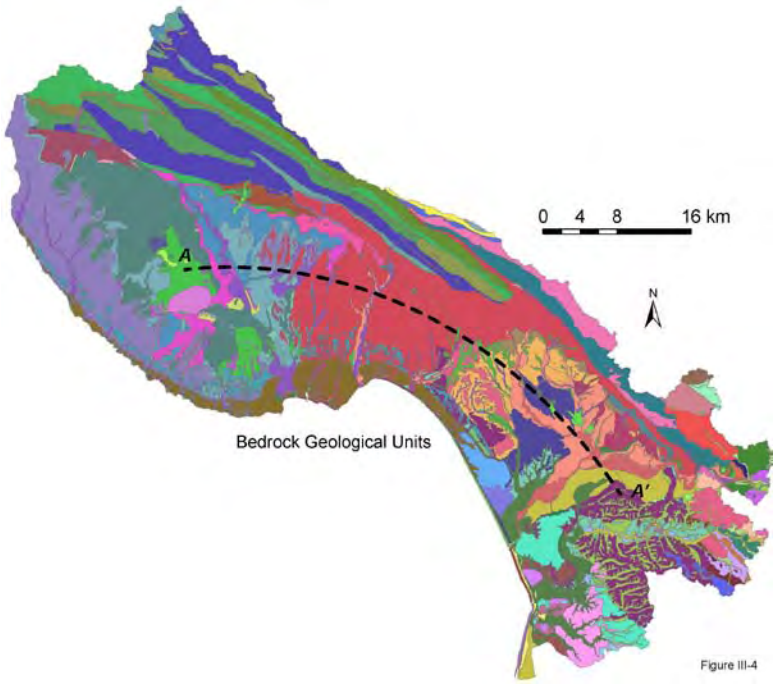

A conceptual cross section extending from northern Santa Cruz to northern Monterey Counties (**Fig. III-5**, M. Cloud, *pers. comm.*, 2008) illustrates several important characteristics of the bedrock geology in this region. The Santa Margarita Groundwater Basin (SMGB) is located mainly within the watershed of the San Lorenzo River, and its primary aquifers include the Santa Margarita, Lompico, Butano, and Locatelli Formations [*Kennedy/Jenks Consultants*, 2015]. These units contain thick sections of coarse deposits and generally have excellent aquifer properties. The Purisima and Monterey Formations in the SMGB have been developed for groundwater supply at a local scale (generally for domestic use), but these units are generally less productive than the primary SMGB aquifer units.

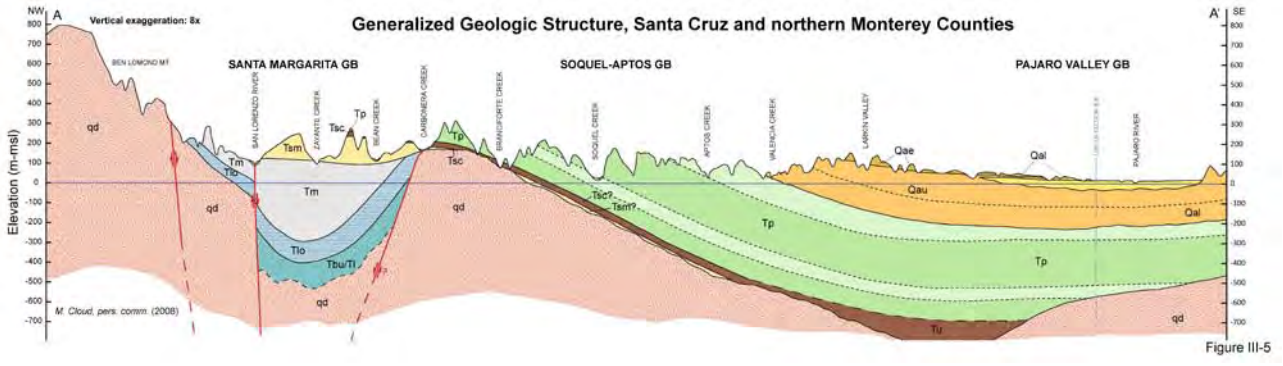

Figure III-5

In contrast, subunits of the Purisima Formation are the primary aquifer within the Soquel Aptos Groundwater Basin (SAGB) [*Johnson et al.*, 2004]. The Purisima Formation dips to the southeast across the southern part of the study region, where it is found underlying the Aromas Formation, alluvial/fluvial deposits, and eolian deposits that form primary aquifers in the Pajaro Valley Groundwater Basin (PVGB) [*Hanson*, 2003; *Hanson et al.*, 2014]. Within the PVGB, the Purisima is, once again, a secondary aquifer, used primarily for small scale supply to satisfy domestic and limited agricultural needs.

Bedrock geology was assigned an index on a scale of 0 to 4, where 0 = not an aquifer (confining unit or aquifer boundary), 2 = may be a primary aquifer, 4 = primary aquifer (**Fig. III-6**; **Table III-1**). Because development of the Purisima Formation as an aquifer varies throughout the study region, its assignment was more nuanced. Within the SAGB, individual Purisima Formation units were assigned to index values of 2, 3, or 4 depending on reported properties and importance for water supply [*Johnson et al.*, 2004]. In contrast, within the SMGB and PVGB, where individual Purisima Formation units are undifferentiated on most maps, this bedrock type was assigned an index of 3 (**Fig. III-6**).

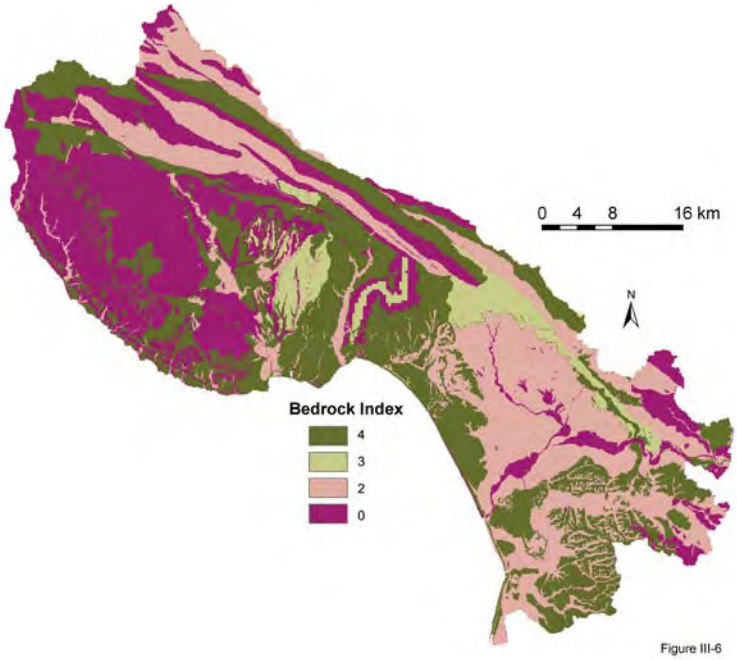

Figure III-6

Table III-1. Bedrock geology index assignments for full project region.

Bedrock Geology Index	Units [a]	Polygons [b]	Area (km^2) [c]
4 = Primary aquifer	MPe, Ppu, Qae, Qar, Qbs, Qce, Qcl, Qcu, Qd, Qds, Qc, Qc?, Qcm, Qcs, Qf, Qf?, Qfa, Qod, Tbl, Tblc, Tbm, Tbu, Tlo, Tlss, Tmm, Tp [d], Tps, Tsm	462	390
3 = Primary (minor) aquifer	Tp [d]	42	165
2 = May be primary aquifer	af, Ess, Orb, Ovq, Q, Q?, Qaf, Qaf?, Qal, Qb, Qcf. Qfl, Qls, Qms, Qmt, Qmt?, Qo, Qof, QT, Qt, QTc, Qtl, Qtw?, Qwf, Qyfo, Tl, Tmp, Ts, Tvq	615	433
0 = Not an aquifer (confining layer, other)	ch, db, Ebu, Ebu?, EOsj, ga, gd, gs, H2O, hcg, Jhg, Kcg, Kgr, Kgs, KJf, ls, m, Msh, Mv, Puc, Puc?, Pus, Pus?, qd, Qg, Qt?, Qyf, sch, Tbs, Tla, Tm, Tmb, Tms, Tsc, Tsl, Tsr, Tst, Tz, um	500	404

[a] Symbols for geologic units derived from data products used to develop index [*Brabb et al.*, 1997; *Brabb et al.*, 1998; *Clark et al.*, 1997; *Wagner et al.*, 2002].
[b] Number of individual bedrock polygons from geological maps within project area.
[c] Values rounded to nearest 1 km^2.
[d] Purisima Formation assigned bedrock geology index of 3 outside of the SAGB, because it is a minor aquifer in the SMGB and PBGB. Within the SAGB, the index assignment depended on the Purisima subunit preset in the shallow subsurface.

4. Aquifer Properties

i. Effective Transmissivity

The distribution of effective transmissivity (T_E) shows considerable variation, both within individual groundwater basins and when considered for the whole study region (**Fig. III-7**).

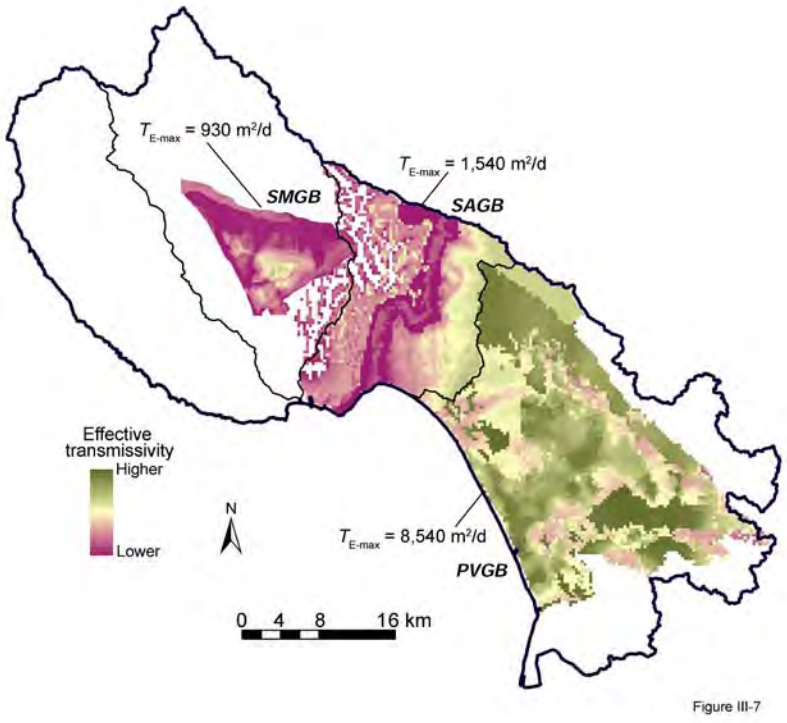

As described earlier, T_E values were calculated separately for each groundwater basin, using model layers that represent local stratigraphy (**Fig. III-5**). As a result, there are very different ranges of calculated T_E values in each basin. Areas for which T_E values can be calculated do not correspond to the topographic basin boundaries identified from regional DEMs. Instead, T_E values include only parts of each drainage basin, and in each case extend into an adjacent drainage basin (**Fig. III-7**). T_E values for the SMGB and PVGB were calculated using hydraulic conductivity values developed recently for use in groundwater models [*Hanson et al.*, 2014; *Kennedy/Jenks Consultants*, 2015], which defined both aquifer and confining layer geometries and formation/layer properties through calibration. In contrast, layer geometry information was

available for the SAGB based on an ongoing modeling project [*HydroMetrics, Inc., pers. comm., 2015*], but these models have not yet been run or calibrated. Instead, we assigned properties by layer for the SAGB based on an earlier compilation and assessment of typical values for the basin [*Johnson et al.,* 2004].

T_E values were rated using a transmissivity index (0, 1, 2, 3, or 4), with unique scales assigned to each groundwater basin (**Table III-2**). We initially attempted to develop a single index transformation for the full project region, but found that this made it difficult to distinguish between areas having significant differences in T_E values. Although the SAGB and PVGB share a common overall stratigraphy (**Fig. III-5**), with the Purisima and Aromas Formations comprising primary aquifers, the upper limit of calculated T_E values in these two basins differed by more than a factor of 5 (**Fig. III-7**). The Aromas aquifer is not present in much of the SAGB today because of uplift, folding and erosion, except at the southeastern edge of the basin. The Purisima aquifer is present throughout much of the PVGB, but it is near the surface mainly along the northeastern (inland) side of the basin, close to the San Andreas Fault. Because the Aromas aquifer has comparatively favorable properties, use of the Purisma aquifer is limited in the PVGB.

Table III-2. Transmissivity index assignments for the three main groundwater basins in the study region.

Transmissivity Index [a]	Santa Margarita Groundwater Basin		Soquel Aptos Groundwater Basin		Pajaro Valley Groundwater Basin	
	Range (m^2/day)	Area (km^2)	Range (m^2/day)	Area (km^2)	Range (m^2/day)	Area (km^2)
0	0 to <25	38.79	0 to <75	83.00	0 to <75	1.42
1	25 to <70	14.32	75 to <100	9.33	75 to <250	16.06
2	70 to <100	6.63	100 to <250	51.55	250 to <450	76.06
3	100 to <150	4.66	250 to <450	28.30	450 to <3300	216.65
4	≥150	11.88	≥450	146.80	≥3300	54.62

[a] Indices were assigned based on consideration of the range of values found in each groundwater basin. Although the SAGB and PVGB share some of the same general stratigraphy (Fig. III-5), the Purisima aquifer is more important in the SAGB, whereas the Aromas aquifer is more important in the PVGB.

In the SMGB, the highest T_E values are in the central and southeastern parts of the basin, with patches of elevated values to the west and along the northwestern edge of the basin (**Fig. III-8**). Lower transmissivity values are found mainly where the Monterey Formation (which has relatively poor aquifer properties compared to primary SMGB aquifers) or the Santa Cruz Mudstone outcrops, limiting connection to underlying units. The pattern of higher and lower T_E values suggests influence from ancient drainage patterns, because uplift, deformation, and erosion have removed some units and helped to create unconformable connections between others.

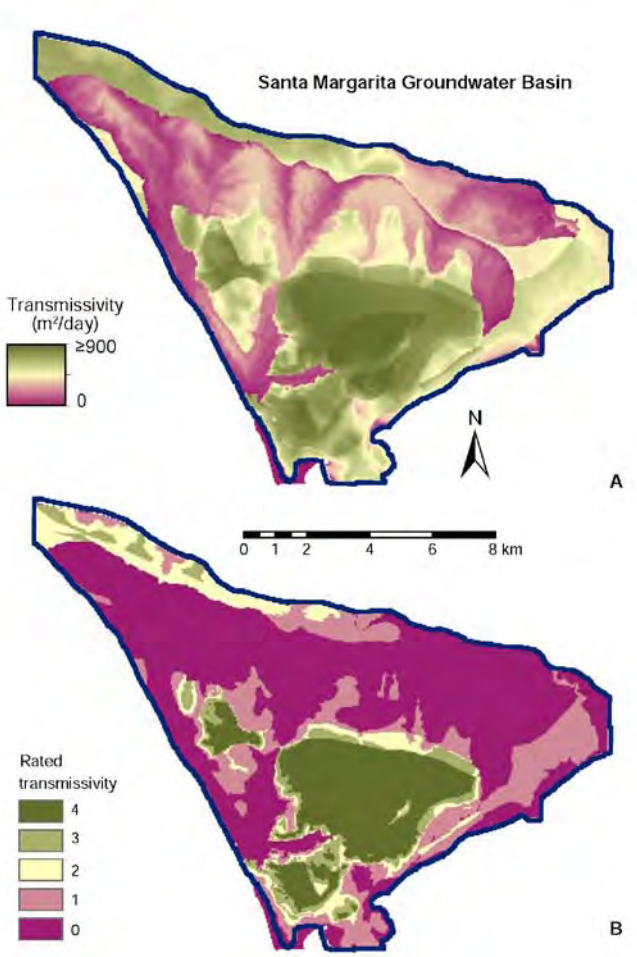

Figure III-8

In the SAGB, the highest T_E values (>1,500 m^2/day) are found along the eastern side of the basin, where the SAGB merges with the PVGB (**Fig. III-9**), including areas where both the Aromas and Purisima aquifers are the shallowest bedrock units. The Purisima aquifer units tend to have lower hydraulic conductivity than does the Aromas aquifer, but the Purisima aquifer can be quite thick in the eastern SAGB. T_E values tend to be much lower through the central and western part of the SAGB, and especially along a band of confining layers [Purisima subunits B and D,*Johnson et al.*, 2004] that are exposed through the central part of the basin (**Fig. III-9**). Transmissivity data are available for essentially all of the SAGB, but other subsurface coverages are more restricted spatially, particularly information on recent water levels. This limits the spatial extent of the full subsurface and composite analysis for MAR suitability in the SAGB (**Fig. III-9**).

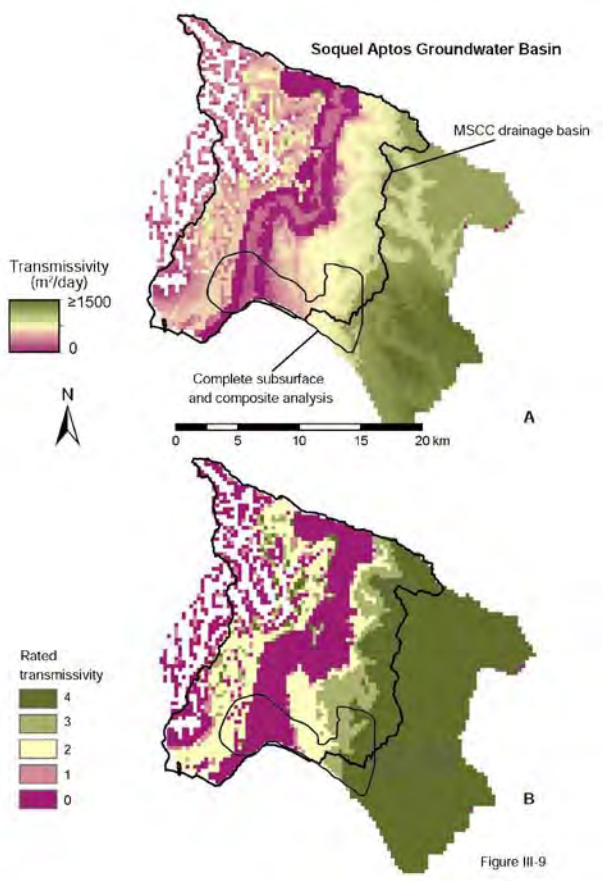

In the PVGB, there are high T_E values distributed throughout the basin, including the northern and eastern edges, the central and southern basin, and along the coast (**Fig. III-10**). Some calculated transmissivity values exceed 8,500 m^2/day, and T_E is generally greatest where the Aromas aquifer is in contact with the ground surface, where there is little or no confining layer separating the shallow Alluvial aquifer from the underlying Aromas Formation, or where the Purisima aquifer is especially thick. Lower transmissivity values are found mainly where there are low-conductivity confining layers between the Alluvial aquifer and the underlying Aromas aquifer. Because T_E values are so high in general across the PVGB, the map of rated values is skewed to the high end of the rating scale (**Fig. III-10B**, **Table III-2**). The three remaining subsurface coverages (available storage, vadose zone thickness, and changes in water level) are available for much of the PVGB; but as in the SAGB, the dataset that limits the full subsurface and composite analysis for the PVGB is contoured water levels (**Fig. III-10**).

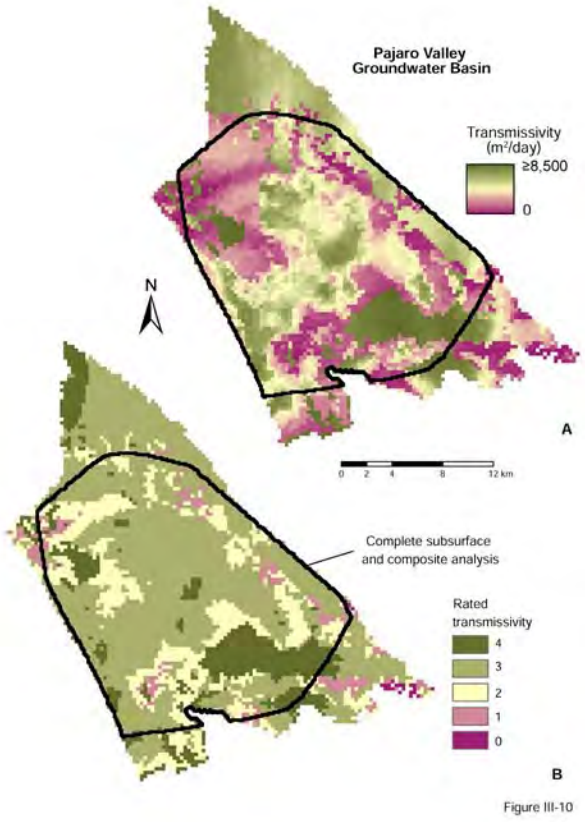

Figure III-10

ii. Available storage

Calculated values of available storage, S_A, in the three groundwater basins (**Figs. III-11** to **III-13**) are much less variable than is transmissivity, mainly because aquifer specific yield varies less in magnitude than does hydraulic conductivity. The highest values of available storage (S_A = 17 m) are found in parts of the PVGB. Although this may not seem to be much space for an aquifer with S_y =0.1, 17 m of available storage corresponds to 170 m of dewatered aquifer. Based on the range of storage values calculated in all three basins, a single rating scale was developed for S_A across the full project region (**Table III-3**). This index scale contains just three values (0, 2, 4) because the total range in S_A values was modest, and it was not clear that contoured water level data (used to calculate S_A) were reliable enough to justify finer distinctions.

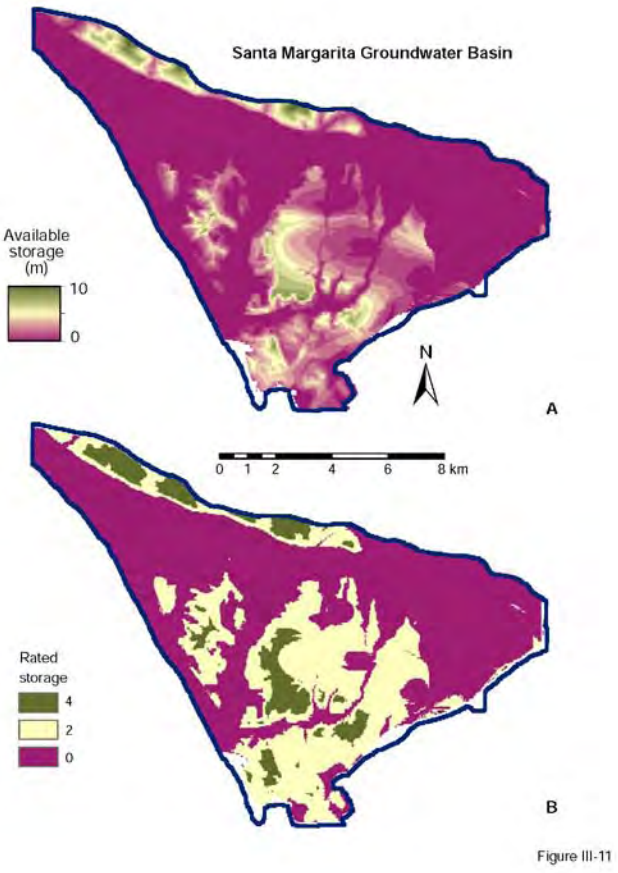

Figure III-11

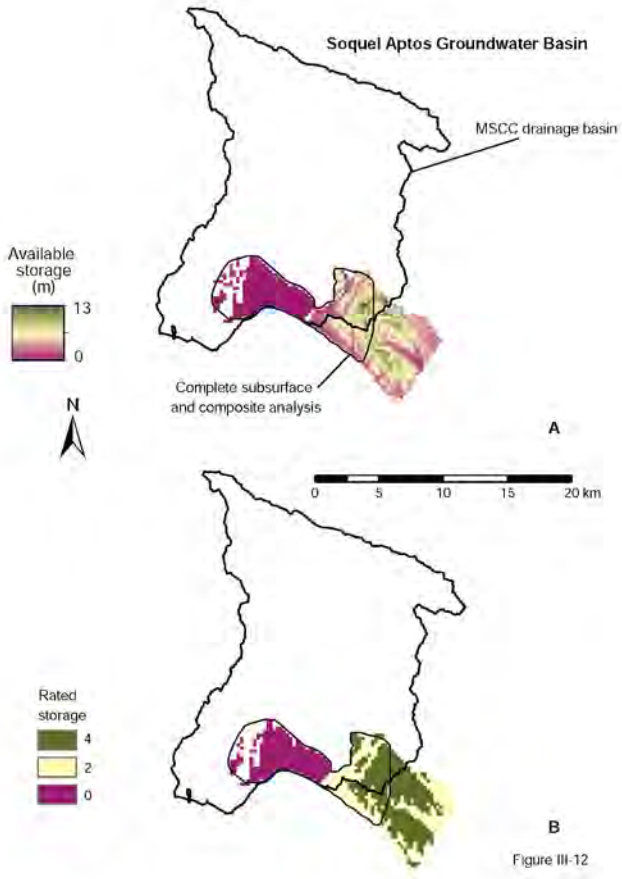

Figure III-12

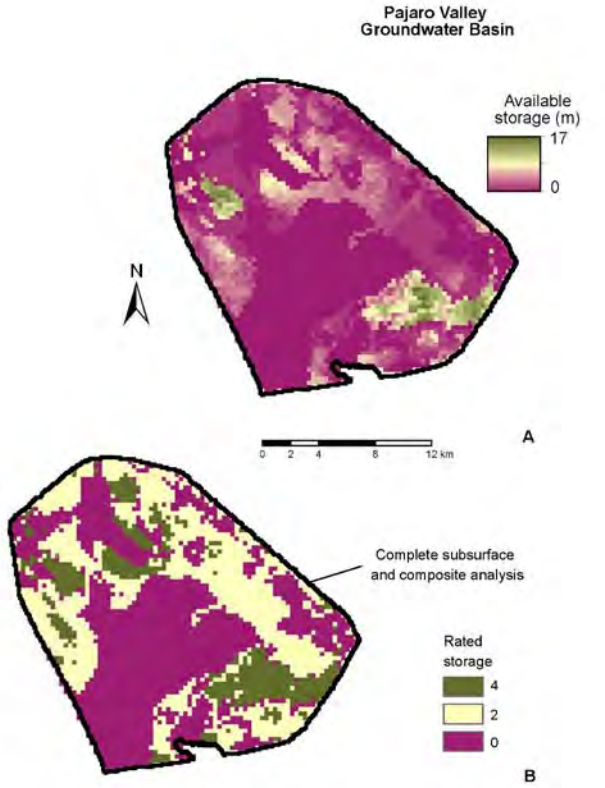

Figure III-13

Table III-3. Available storage index assignments for the three main groundwater basins in the study region.

Available storage, S_a [a]		Santa Margarita Groundwater Basin	Soquel Aptos Groundwater Basin	Pajaro Valley Groundwater Basin
Index	Range (m)	Area (km^2)	Area (km^2)	Area (km^2)
0	< 1	45.29	16.59	115.20
2	1 to < 5	23.19	22.12	86.80
4	≥ 5	5.59	27.05	33.13

[a] Indices were assigned based on consideration of the range of values found across the study region, with a single scale used for all groundwater basins. Because there was a relatively narrow range of available storage values, 0 to 17 m, we use three indices extending across the same range as indices used for other MAR suitability metrics (0 to 4).

In the SMGB, the highest S_A values are found in the northeastern edge and near the center and southern parts of the basin, but ~70% of the total area has $S_A \leq 1$ m (**Fig. III-11**). Low values of available storage occur, in part, because much of the outcropping bedrock in the SMGB is the Monterey Formation or the Santa Cruz Mudstone, both of which have relatively poor aquifer properties. In addition, the available storage calculation is based on contours of water level from shallow aquifer units. As discussed in the methods section, water level contours that are interpolated across valleys between topographic highs tend to be shallow, in some cases being placed above the ground surface. Although this is (in part) an artifact of contouring, it suggests that relatively less space is likely to be available for storage of MAR water in topographic lows.

In the SAGB, S_A was calculated only for a small area near the coast, where water level contours were available (**Fig. III-12**). In general, Purisima aquifer units in this area tend to have relatively little available storage both because of aquifer properties and because water levels are to some extent "pinned" by sea level. There are lower water levels in the Aromas aquifer in the eastern part of the SAGB, resulting in higher available storage values.

S_A also tends to be relatively low in much of the PVGB, with values >5 m occurring mainly in patches in the northern and southern parts of the basin (**Fig. III-13**). Areas having the lowest storage values and rating tend to be in the flood plain of the Pajaro River and Corralitos Creek, and around the Watsonville Sloughs, where confining layers below the Alluvial aquifer limit access to underlying units. In contrast, many regions along the edges of the basin (comprising >50% of the analyzed area) have moderate to high S_A values (**Fig. III-13**).

iii. Vadose zone thickness

The vadose zone thickness (T_{vz}) was calculated as the distance between the ground surface and the most recent contoured groundwater levels. Median values for T_{vz} are ~60 m in the SMGB, ~65 m in the SAGB, and ~40 m in the PVGB. A small number of calculations lead to apparent negative values of T_{vz}, comprising 3% of the area analyzed in the SMGB, 0.2% of the small area analyzed in the SAGB (limited by the extent of water level contour data), and 0.8% of the area of the PVGB. For the SAGB and PVGB, the largest magnitude negative values are -2 m and -8 m, respectively, suggesting that these are likely to have resulted from small errors in interpolation of water level observations. But in the SMGB, almost half of the negative T_{vz} values extend from -8 to -48 m. It is unlikely these higher magnitude T_{vz} values are real, as they are found mainly where groundwater levels determined from wells located in hilly areas were interpolated out and across adjacent valleys. MAR projects are unlikely to be successful if placed in topographic depressions that are surrounded by elevated groundwater levels, so these areas with negative or very low vadose zone thickness are categorized as being less suitable for MAR (**Table III-4**). Values of $T_{vz} \geq 80$ m were also considered to be less desirable for MAR infiltration projects, because a thick vadose zone provides more opportunity for shallow storage of soil water and/or the presence of perching layers. We categorized T_{vz} values ≥ 5 m and <20 m as ideal for infiltration leading to MAR, being thick enough to avoid complications due to mounding, yet deep enough to allow significant travel time from the surface, potentially contributing to nutrient cycling and other processes that may improve water quality.

Table III-4. Vadose zone thickness index assignments for the three main groundwater basins in the study region.

Vadoze zone thickness, T_{vz}[a]		Santa Margarita Groundwater Basin	Soquel Aptos Groundwater Basin	Pajaro Valley Groundwater Basin
Index	Range (m)	Area (km^2)	Area (km^2)	Area (km^2)
0	$T_{vz} \leq 0$, $T_{vz} \geq 80$	32.24	24.62	65.41
1	$60 \leq T_{vz} < 80$	8.98	13.02	31.32
2	$0 < T_{vz} < 5$, $40 \leq T_{vz} < 60$	13.19	15.28	62.05
3	$20 \leq T_{vz} < 40$	11.44	9.33	69.22
4	$5 \leq T_{vz} < 20$	9.49	3.51	65.45

[a] Indices were assigned based on consideration of the range of values found in each groundwater basin and across the full project region. The most favorable ratings were assigned to vadose zone thicknesses that are low enough to allow relatively rapid infiltration into underlying aquifers, but high enough to allow some water-soil interaction (including processing of potential contaminants) during transport.

T_{vz} values in the SMGB are greatest along the northern edge of the basin, especially along topographic highs, and are considerably lower in drainages that end towards the south (**Fig. III-14**). The highest rated T_{vz} values tend to occur along the sides of drainages, where calculated depths to the water table are intermediate between deeper and shallower extremes.

As with other subsurface factors depending on the extent of water level data, T_{vz} values in the SAGB were calculated only for a small region near the coast (**Fig. III-15**). Relatively high rated values for T_{vz} were assigned along the boundary between the basin and ocean. In the PVGB, the greatest vadose zone thicknesses were found in elevated areas along the northern, eastern, and southern margins of the analysis (**Fig. III-16**). Lower T_{vz} values were calculated near the center of the basin, including large areas in the flood plain of the Pajaro River and along drainages for Corralitos Creek and the Watsonville Sloughs. As a result, indices assigned for T_{vz} across the PVGB tended to be highest near the basin center and close to the coast (**Fig. III-16**).

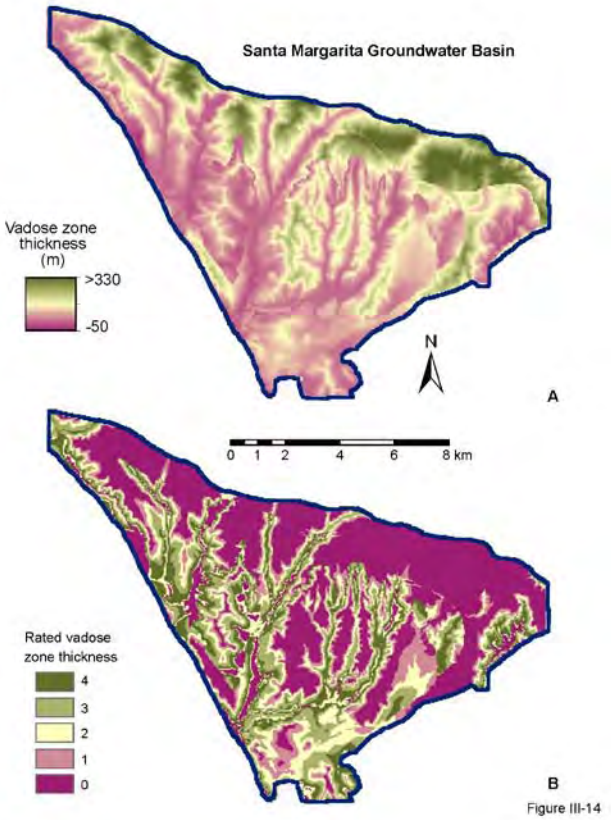

Figure III-14

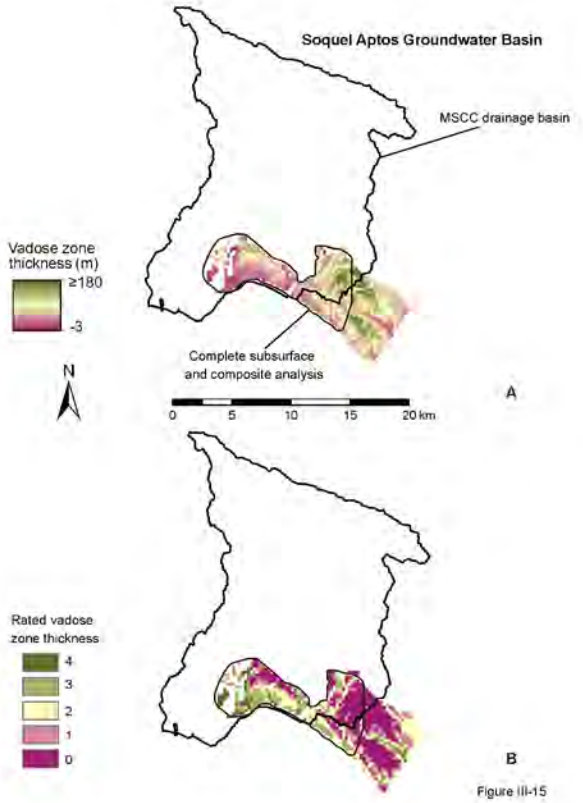

Figure III-15

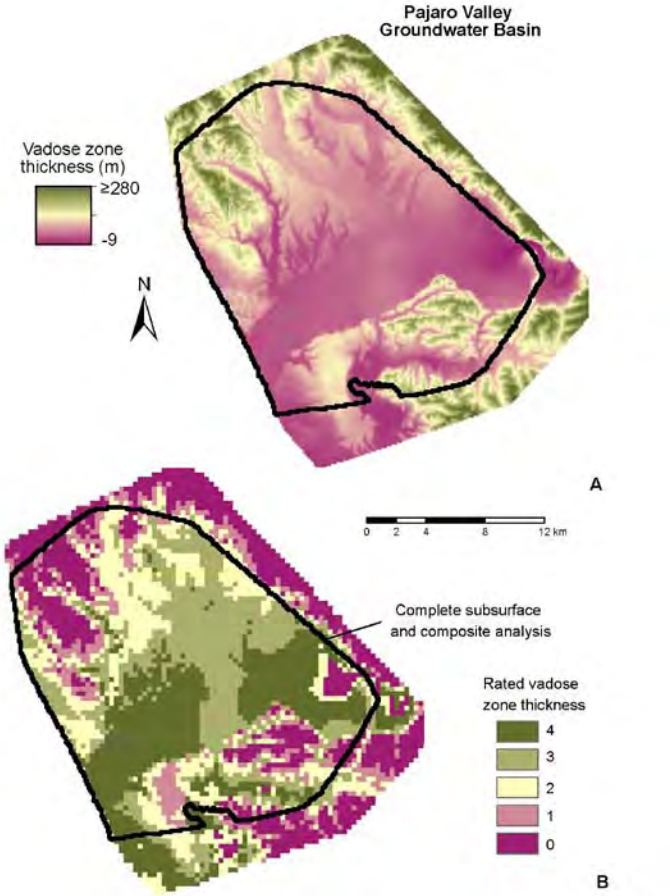

Figure III-16

iv. Changes in groundwater levels

Data on groundwater levels were used to assess which areas might benefit from recharging recently emptied pore space in an aquifer, based on a comparison of contoured water level data from multiple years (**Table II-2**). The lateral extent of this analysis was based on the region over which water levels had been contoured, and in each case, the analysis was applied to the shallowest aquifers for which there were data from multiple years. Values were calculated by subtracting elevations at an earlier time from elevations at a later time, resulting in negative values when water levels had become lower, and positive values when water levels had become higher. Because the time period represented in this analysis varied by basin, we normalized the data to calculate the apparent rate of change in water level, before scaling values using a

common index (**Table III-5**). We chose a three-point index (0, 2, 4) based on the relatively narrow range in calculated rates of change and the approximate nature of the method used to make these calculations (comparing contour maps based on well data).

Table III-5. Recent water level change index assignments for the three main groundwater basins in the study region.

Rate of change of water level, ΔW [a]		Santa Margarita Groundwater Basin	Soquel Aptos Groundwater Basin	Pajaro Valley Groundwater Basin
Index	Range (m/yr)	Area (km^2)	Area (km^2)	Area (km^2)
0	$\Delta W \geq 0$	55.62	27.11	109.37
2	$-0.5 < \Delta W < 0$	12.03	6.01	61.01
4	$\Delta W \leq -0.5$	7.70	3.45	66.12

[a] Indices were assigned based on consideration of the range of values found across the study region, with a single scale used for all groundwater basins. Because time periods for which data were available differed by basin (**Table II-2**), the annual rate of change in water level was used as the primary metric.

In the SMGB, most of the basin experienced little or no change in groundwater levels in the shallowest aquifers during the period assessed, 1992 to 2014 (**Fig. III-17**). This does not mean groundwater levels at depth remained constant during this time, but it may be difficult for infiltrating water from the surface to reach dewatered aquifers in many parts of the basin. Areas with the greatest apparent decrease in shallow groundwater levels are clustered mainly around the northern and eastern sides of the SMGB, with additional areas of decrease to the south (**Fig. III-17**). For the small area of water level data assessed in the SAGB, covering the period of 2009 to 2014, water levels generally increased (**Fig. III-18**). Proximity to the ocean creates challenges for the use of water level data in this area, tending to limit the extent of water level movement. Within the area analyzed in the SAGB, the greatest decreases in water levels are found in more inland locations (**Fig. III-18**).

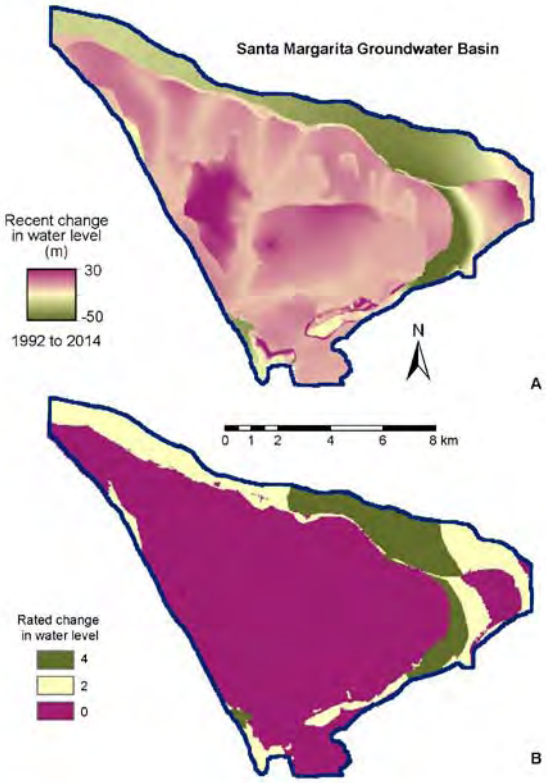

Figure III-17

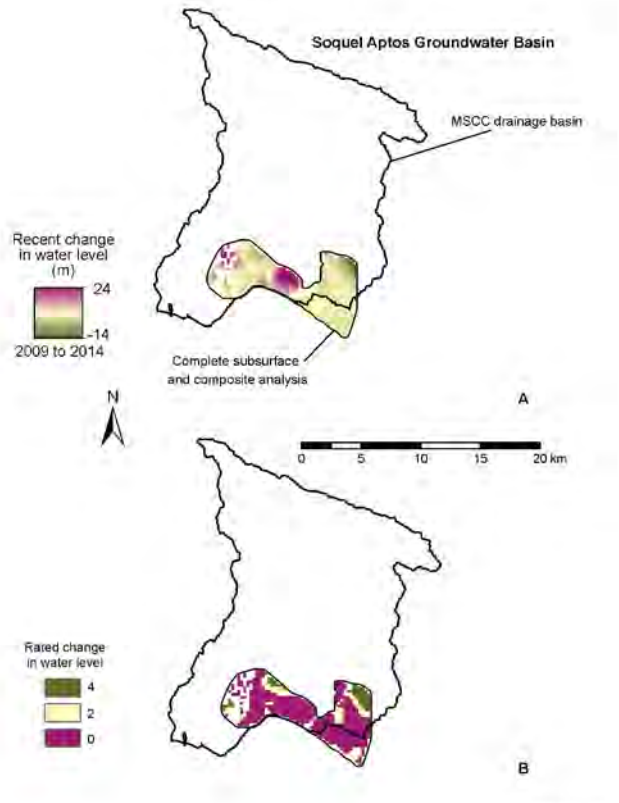

Figure III-18

A larger area was analyzed for changes in water levels in the PVGB for the period of 1998 to 2010 (**Fig. III-19**). The areas in which water levels decreased the most are along a north-south trend through the center of the basin, and along the southern edge of the area analyzed. The data suggest that shallow water levels have increased along the western side of the basin, including areas near to the ocean (**Fig. III-19**).

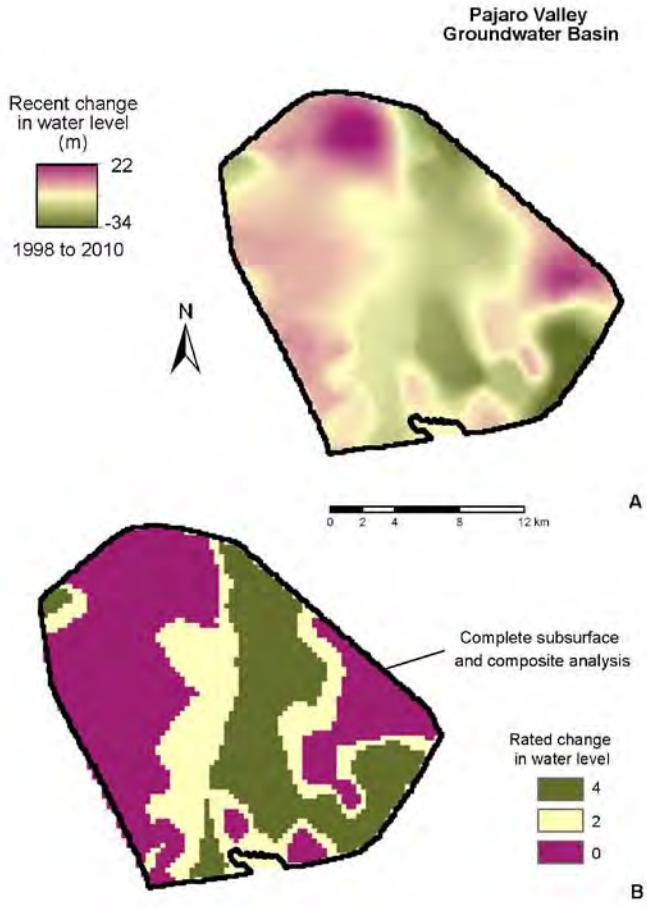

Figure III-19

B. Maps of Suitability for Managed Aquifer Recharge

1. Surface MAR suitability

We combined soil and bedrock geological information across the project region, giving each of these indicators an equal weighting, resulting in a map of MAR suitability based only on surface data (**Fig. III-20**, **Table III-6**). Of the full 1387 km^2 project area, 35% (481 km^2, 119,000 acres) is rated as above the central value (≥5 on an index scale of 0 to 8). Examination of the map shows that areas that are suitable to highly suitable for MAR based on shallow data (sandy soil underlain by primary aquifers) are distributed throughout the study region, sometimes in large swaths, but often in small patches.

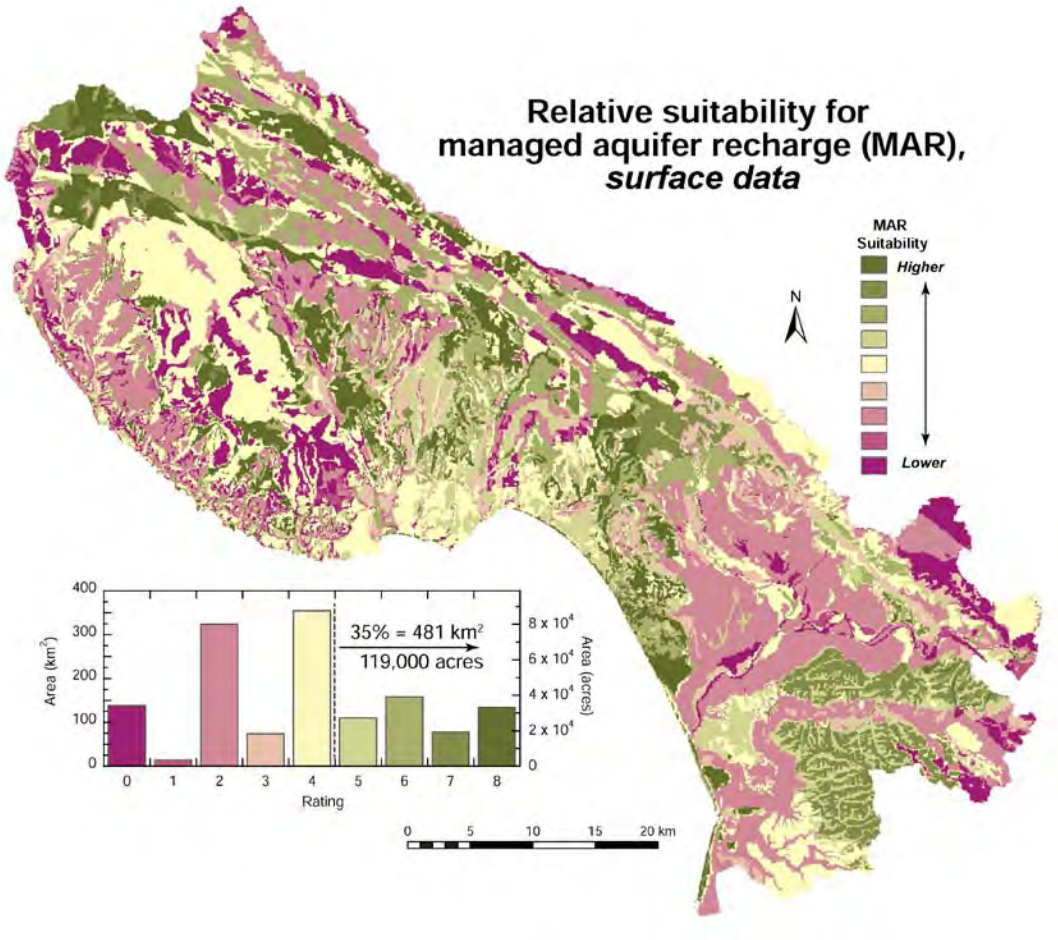

Figure III-20

Table III-6. Summary of MAR suitability analyses using surface data (soils, bedrock geology).

MAR suitability [a]	Northern Santa Cruz County (NSCC)		San Lorenzo River Basin (SLRB)		Mid-Santa Cruz County (MSCC)		Pajaro Valley Drainage Basin (PVDB)	
	(km^2)	(% of area)	(km^2)	(% of area)	(km^2)	(% of area)	(km^2)	(% of area)
Q1	55.1	19.4	45.1	12.8	17.1	8.2	35.3	6.5
Q2	61.4	21.6	81.3	23.1	28.6	13.7	226.6	41.9
Q3	110.6	39.0	112.8	32.1	82.7	39.6	158.2	29.2
Q4	56.5	19.9	112.3	32.0	80.8	38.6	120.9	22.3

[a] MAR suitability calculated from soils and bedrock geology data on a relative scale, converted to equivalent index quartiles: $0 \le Q1 < 25\%$, $25 \le Q2 < 50\%$, $50 \le Q3 < 75\%$, $75 \le Q4 \le 100\%$.

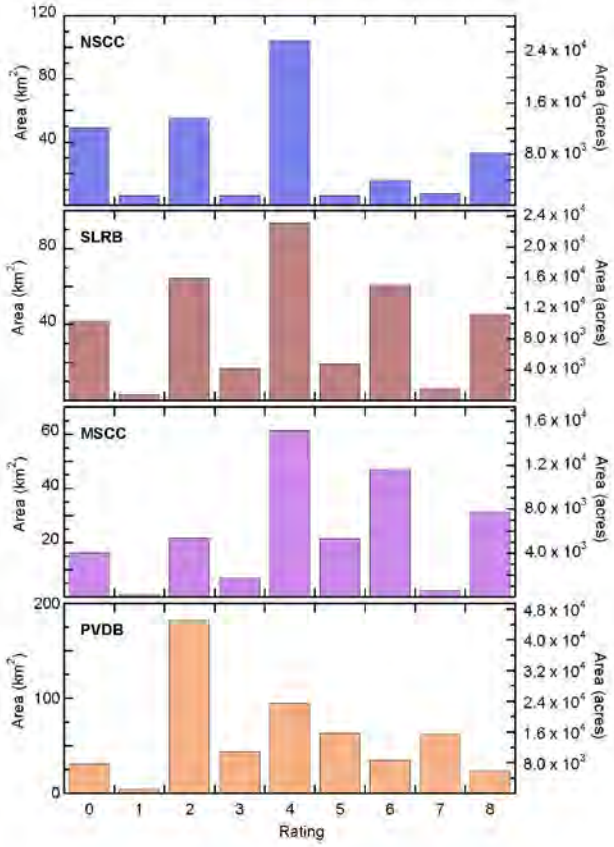

Figure III-21

Conditions differ within individual parts of the study region (**Figs. III-20** and **III-21**). The northern Santa Cruz County region has the lowest fraction of area rated as suitable for MAR based on surface data, mainly because there are limited groundwater development opportunities, with aquifers comprising mainly small alluvial valleys between outcrops of terrace deposits and non-aquifer bedrock (**Fig. III-6**). Many of the soils in this subregion have a high infiltration

capacity (**Fig. III-3**), but aquifer conditions are limited and/or poorly known. Small aquifers in this area may still be important for domestic and local agricultural use, but there are better opportunities in other parts of the region for managed recharge. The other three subregions (SLRB, MSCC, and PVDB) have significant areas with moderate to high MAR suitability, based on surface data, but as shown later, there are significant regional differences between and within the major groundwater basins. The fraction of landscape that is suitable to highly suitable for MAR based on surface data is considerably lower when screened for areas having a surface slope <10° (**Fig. III-22**, **Table III-7**). It is easy to forget how much of the study region is mountainous and steep, because most of its population and agricultural centers occupy flat areas.

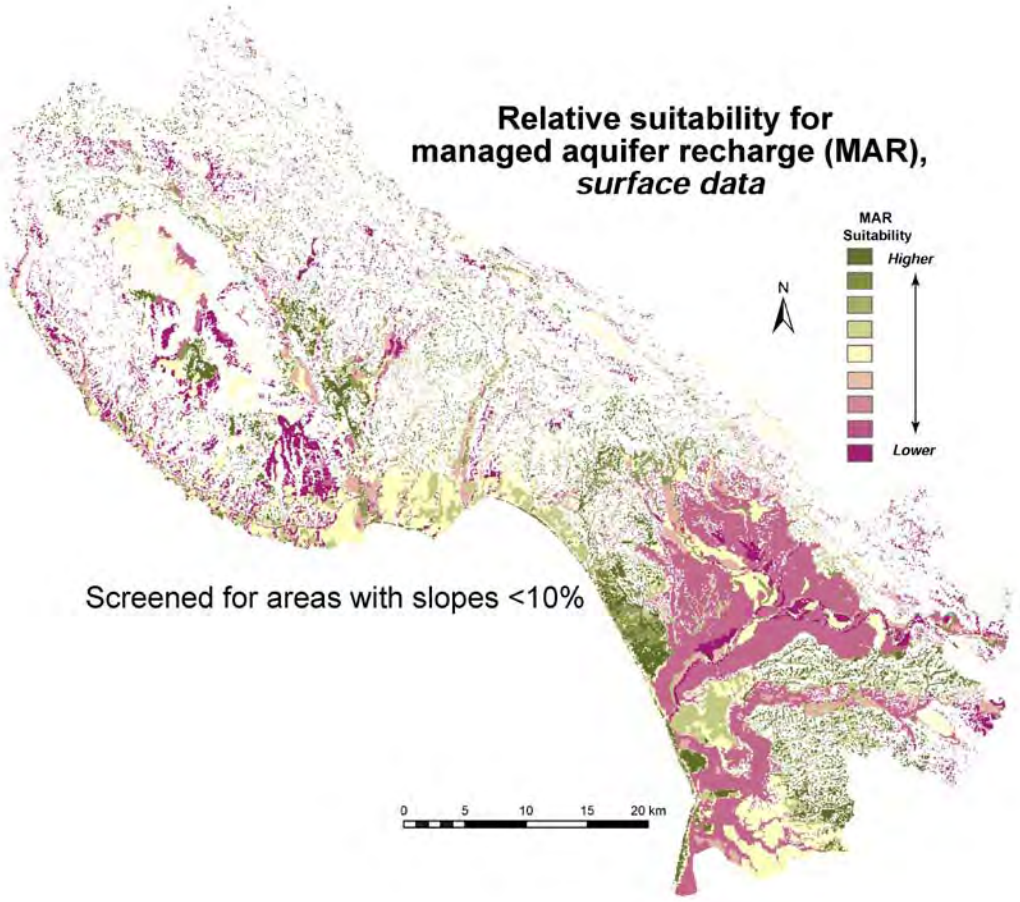

Figure III-22

Table III-7. Summary of MAR suitability analyses using surface data (soils, bedrock geology), screening for areas with surface slopes <10%.

MAR suitability [a]	Northern Santa Cruz County (NSCC)		San Lorenzo River Basin (SLRB)		Mid-Santa Cruz County (MSCC)		Pajaro Valley Drainage Basin (PVDB)	
	(km^2)	(% of area)	(km^2)	(% of area)	(km^2)	(% of area)	(km^2)	(% of area)
Q1	24.8	27.3	11.3	14.9	3.8	6.2	14.4	4.6
Q2	14.6	16.1	20.4	27.0	8.6	14.0	157.8	50.6
Q3	37.5	41.3	22.5	29.7	34.9	56.8	86.5	27.8
Q4	13.9	15.3	21.5	28.4	14.1	23.0	52.9	17.0

[a] MAR suitability calculated from soils and bedrock geology data on a relative scale, after screening out all areas having steep surface slopes, converted to equivalent index quartiles: $0 \le Q1 < 25\%$, $25 \le Q2 < 50\%$, $50 \le Q3 < 75\%$, $75 \le Q4 \le 100\%$. For these calculations, % of area applies to areas having surface slopes <10%.

Most of these are near the coast, but there are also small patches of flat ground at higher elevations (**Fig. III-1**). The prevalence of steep slopes is especially apparent in the SLRB subregion, where only 22% of the area has a surface slope <10°. In contrast, within the PVDB, a much larger alluvial basin, 58% of the ground has a slope <10°. Only a few acres may be needed to accomplished infiltration objectives associated with individual DSC-MAR projects, and there are many local areas having moderate to high MAR suitability based on surface data in all three of the major groundwater basins (**Fig. III-22**, **Table III-7**). These areas are most extensive in the PVDB, especially along the coast, on either side of the Elkhorn Slough drainage, south of the Pajaro River, and in the northern part of the basin (Corralitos, Freedom). But there are also numerous 1-4 acre areas of elevated MAR suitability distributed across the SLRB and MSCC region.

2. Subsurface and composite MAR suitability

We combined analyses of surface and subsurface datasets to develop more comprehensive maps of MAR suitability across the study region. As noted earlier, subsurface and composite maps could be generated for the smallest areas defined by the data sets used, so subsurface and composite maps cover smaller areas than do the surface maps. Subsurface data are available only where detailed analyses have been completed by local agencies, including assessment of well

logs, water levels, aquifer tests and other information, generally in association with development of a groundwater model. This limitation is particularly important in SAGB, where only a small area near the ocean is represented with a complete subsurface analysis; modeling currently underway should be helpful in developing useful subsurface data over much of the SAGB.

Results for the full project region and individual groundwater basins show considerable variability (**Fig. III-23**). It is especially useful to compare this map to that showing regional MAR suitability analyses based only on surface data (**Fig. III-20**). Surface and composite maps are generally similar when entire basins are considered, but there are important differences at a spatial scale of ≤10 acres, the typical size range for individual DSC-MAR infiltration projects.

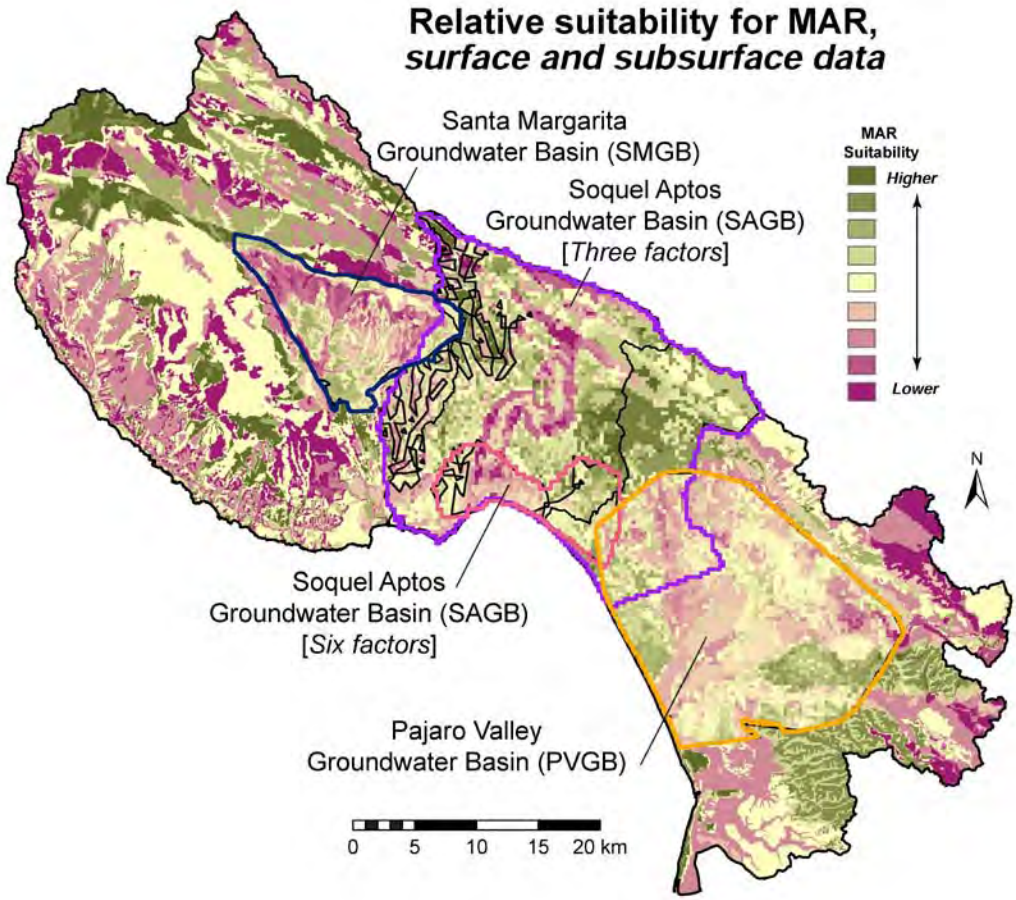

Figure III-23

In the SMGB, subsurface suitability is highest near the center, southern, and northern edges of the groundwater basin (**Fig. III-24**). This includes much of the developed part of the basin. Moderate to elevated composite suitability values are mapped across ~40% of the SMGB (**Table III-8**). Areas that are less suitable for MAR in the SMGB based on the composite analysis were generally those having less favorable soils and/or bedrock geology (**Figs. III-3**, **III-4**, and **III-20**). In other words, given generally good aquifer conditions in this basin, the surface factors are most important in distinguishing between more and less suitable DSC-MAR locations.

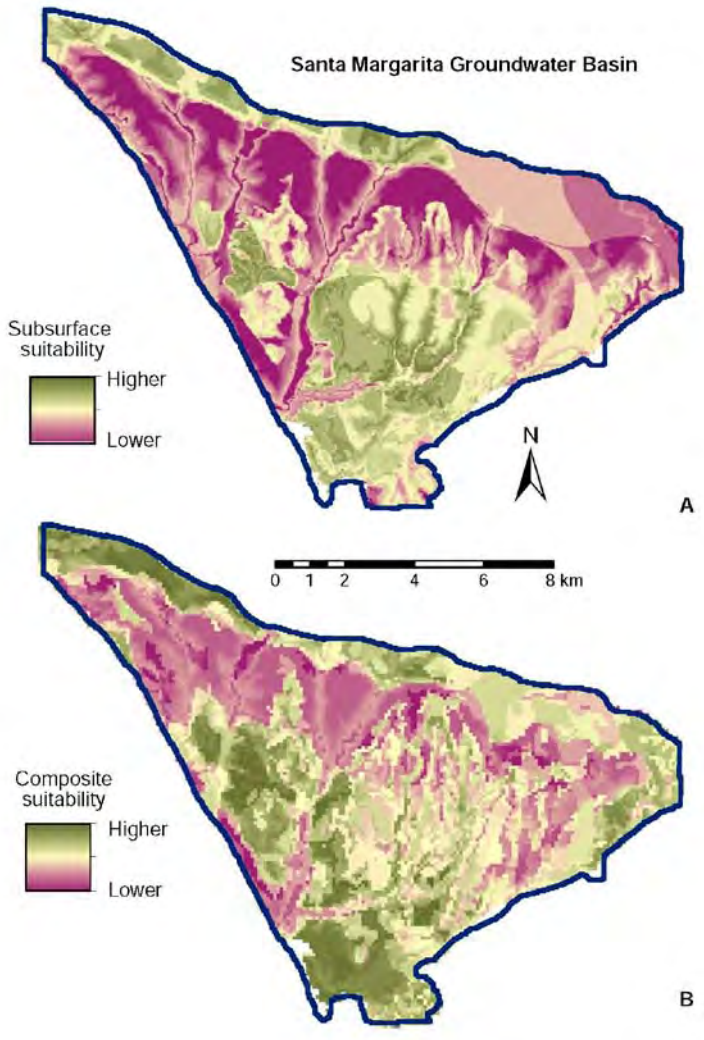

Figure III-24

Table III-8. Summary of MAR suitability analyses using a combination of surface and subsurface data.

MAR suitability [a]	Santa Margarita Groundwater Basin (SMGB)		Soquel Aptos Groundwater Basin (SAGB), three factors [b]		Soquel Aptos Groundwater Basin (SAGB), six factors [b]		Pajaro Valley Groundwater Basin (PVGB)	
	(km^2)	(% of area)	(km^2)	(% of area)	(km^2)	(% of area)	(km^2)	(% of area)
Q1	17.85	24.1	25.27	8.0	2.44	6.7	5.43	2.3
Q2	26.44	35.7	55.47	17.5	15.99	43.8	128.02	55.0
Q3	24.76	33.5	144.48	45.5	13.56	37.1	83.97	36.1
Q4	4.95	6.7	92.34	29.1	4.52	12.4	15.29	6.6

[a] MAR suitability calculated on a relative scale, converted to equivalent index quartiles:
$0 \le Q1 < 25\%$, $25 \le Q2 < 50\%$, $50 \le Q3 < 75\%$, $75 \le Q4 \le 100\%$.

[b] For the "three factor" analysis in the SAGB, only transmissivity was used to represent subsurface properties, being available for the full basin (**Fig. III-7**). A complete "six factor" analysis was completed for a smaller SAGB area (**Fig. III-9**), using the standard two surface factors (soils and bedrock geology) and four subsurface factors (transmissivity, storage, vadose zone thickness, and recent changes in water levels).

In the SAGB, subsurface suitability was calculated for a small region near the coast, and a composite analysis was completed two ways: with three factors (soils, bedrock geology, and transmissivity), and with six factors (as for composite analyses in the other basins) (**Fig. III-25**).

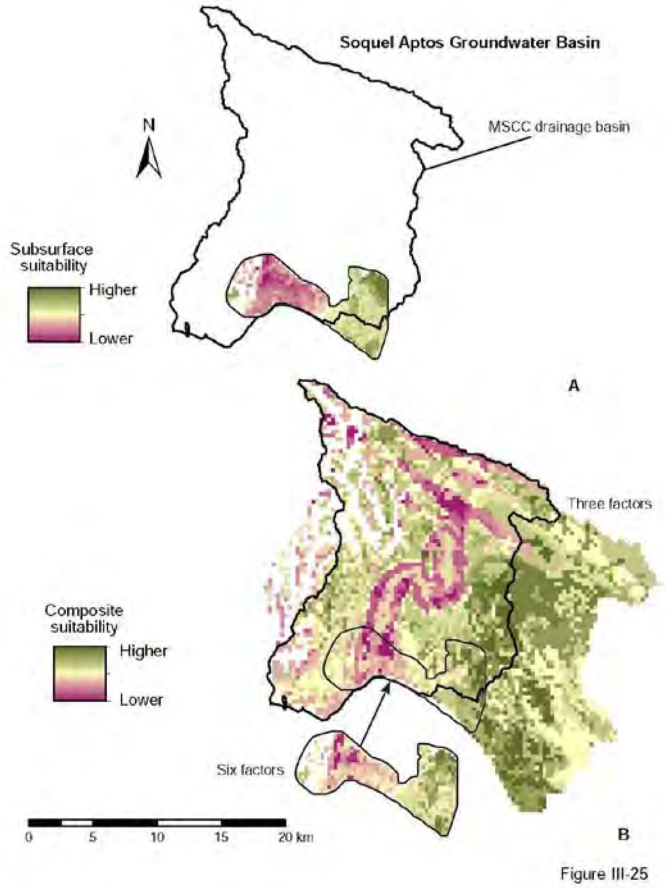

Figure III-25

The composite analysis with six factors tends to screen out small areas that were previously identified from surface analyses as being suitable for MAR (**Fig. III-20**), whereas the composite analysis with three factors shows a broader regional pattern. Much of the basin is moderately to highly suitable for MAR, with the primary exceptions being areas underlain by Purisima subunits having poor aquifer properties (and therefore function as confining layers). The eastern side of the basin tends to be more suitable for MAR, but there are zones of high suitability scattered throughout. In the PVGB, subsurface MAR suitability (**Fig. III-26**) deviates significantly from surface MAR suitability (**Fig. III-20**), particularly in the central and eastern parts of the basin. In these areas, lower suitability around the flood plain of the Pajaro River, the Watsonville Sloughs, and other aquatic systems. But these low indices can be offset significantly by aquifer conditions that appear to be highly suitable for DSC-MAR. In the composite analysis of MAR suitability for the PVGB (**Fig. III-26**), there are moderately to highly suitable areas distributed throughout the basin, especially along the northern coast and south of the Pajaro River, but also adjacent to the hills bounding the eastern side of the basin.

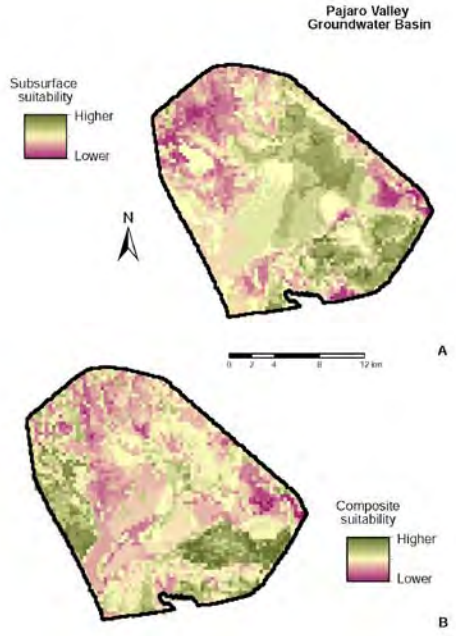

Figure III-26

IV. Simulation of Stormwater Runoff

A. Parameter Assignments, Calibration, and Validation

The ranges of parameter values used for simulation of stormwater runoff in the SLRB and PVDB are summarized in **Tables II-3**, **II-4**, and **IV-1**. NRMSD metrics are reported for calibration based on two time periods, the full year and the wet months of each year (November - April) (**Table IV-2**). The full-year metrics include data from the full year, whereas the wet-monthly results avoid bias from dry periods, when there is not likely to be much hillslope runoff that contribute to DSC-MAR.

Table IV-1. PRMS calibration parameters, ranges and final values.

Parameter	PRMS units [a]	Description	Calibration range [b]	Final value(s) [c]	
				SLRB	PVDB
K_coef	hr	Muskingum coefficient (travel time)	0.01 - 1.0	0.01	0.01
x_coef	(-)	Muskingum coefficient (attenuation)	0.2 - 1.0	1.0	1.0
gwflow_coef	(-)/day	Baseflow linear routing coefficient	0 - 0.5	0.015	0.001
gwsink_coef	(-)/day	GW extraction linear routing coefficient	0 - 0.8	0.035	0.6
fastcoef_lin	(-)/day	Preferential flow linear routing coefficient	0.001 - 1.0	0.001	0.001
slowcoef_lin	(-)/day	Gravity soilzone linear routing coefficient	0.001 - 0.5	0.001	0.001
slowcoef_sq	-	Gravity soilzone non-linear routing coefficient	0.001 - 0.35	0.001	0.001
ssr2gw_rate	(-)/day	Gravity soilzone drainage coefficient (to GW)	0.01 - 1.2	0.01 - 0.41	0.004-0.156
ssr2gw_exp	-	Gravity soilzone drainage exponent (to GW)	0.0 - 3.0	2.0	1.8
soil_moist_max	in	Max normalized water volume of capillary soilzone (AWC x rooting depth)	0.05 - 100	0.11 - 20.95	0.65-64.8
pref_flow_den	(-)	Fraction of the total soil depth in which preferential flow occurs	0.0 - 0.5	0.0	0.0001 – 0.033
sat_threshold	inn	Max normalized water volume of gravity + preferential soil zones: *(n-FC) x soil depth*	0.3 - 179	0.41 - 33.16	0.116 – 7.64
smidx_coef	(-)	Hortonian runoff contributing area coefficient	0.001 - 0.06	0.06	0.002
smidx_exp	in^{-1}	Hortonian runoff contributing area exponent	0.3 - 1.0	0.5	0.1

[a] Units used by PRMS

[b] Range of values that was explored to improve calibration fit

[c] Single values are uniform across drainage basin. Range of values indicates scaling for each HRU, based on available soils data, as described in the text.

Calibration was accomplished independently for the SLRB and PVDB by sequentially modifying a subset of parameters, first with a focus on replicating annual flows, and then emphasizing monthly channel discharge. The primary parameters adjusted for the annual calibration were **gwflow_coef** and **gwsink_coef**. Like parameters related to ET, these parameters govern the rate by which surface water "leaves" the topographic basin, becoming groundwater, and thus is not represented in channel flow data. For monthly channel runoff, the primary

calibration parameters include the horizontal routing (interflow) coefficients (**slowcoef_lin**, **slowcoef_sq**), the vertical routing (gravity drainage) coefficients (**ssr2gw_rate**, **ssr2gw_exp**), and the maximum soil zone storage parameters (**soil_moist_max**, **sat_threshold**). We found it necessary to minimize horizontal routing coefficients to match the observed hydrograph responses for small and moderate precipitation events.

Table IV-2. PRMS calibration and validation time periods and results summaries, SLRB and PVDB.

SLRB

Time period [a]	Purpose	Wet months [b]		Annual	
		N months	NRMSD	N years	NRMSD
WY88-01	Calibration - initial	84	0.158	14	0.109
WY88-01 [c]	Calibration - final	82	0.137	12	0.106
WY02-14	Validation - initial	78	0.246	13	0.100
WY02-14 [c]	Validation - final	76	0.212	11	0.100

[a] WY = water year, calibration/validation follows model stabilization period of WY82-87
[b] Data compiled on a monthly basis for November - April of each water year
[c] Data neglected for two months of relatively extreme rainfall, as described in text

PVDB

Time period [a]	Purpose	Wet months [b]		Annual	
		N months	NRMSD	N years	NRMSD
WY01-14	Calibration	84	0.064	14	0.102
WY88-00	Validation	78	0.098	13	0.168

[a] WY = water year, calibration/validation follows model stabilization period of WY82-87
[b] Data compiled on a monthly basis for November - April of each water year

In general, there is little observed hydrograph response to these events, but the simulations had significant responses unless **slowcoef_lin** and **slowcoef_sq** were set at the lower end of their standard ranges (**Table II-3**). The vertical routing coefficients and soilzone storage terms were adjusted to improve the monthly calibration, helping to assure that water was delivered to stream channels as observed. We found that the simulated basin response tended to be independent of initial conditions after the first few water years; we ran a six-year stabilization period before attempting calibration or validation.

A comparison of observed and simulated runoff illustrates the consistency of PRMS calibration for the SLRB (**Fig. IV-1**, **Table IV-2**). Calibration on annual data was broadly successful, although there is a systematic offset for WY97 and WY98, with simulated values being lower than observed. These offsets result mainly from simulated channel runoff during two months, Jan 97 and Feb 98. These months had the greatest precipitation during the calibration period, yet simulated runoff was consistently below that observed. In fact, simulated channel runoff was lower during these months than during three other months for which there was less rainfall. We were not able to find a combination of PRMS parameters that allowed a good match to runoff from these two months without making the fit significantly worse for the calibration period overall. We suspect that the misfit for these two months results from the artificially low precipitation intensity represented in the PRISM data, as discussed earlier, which tends to favor infiltration and slower runoff modes rather than Hortonian overland flow.

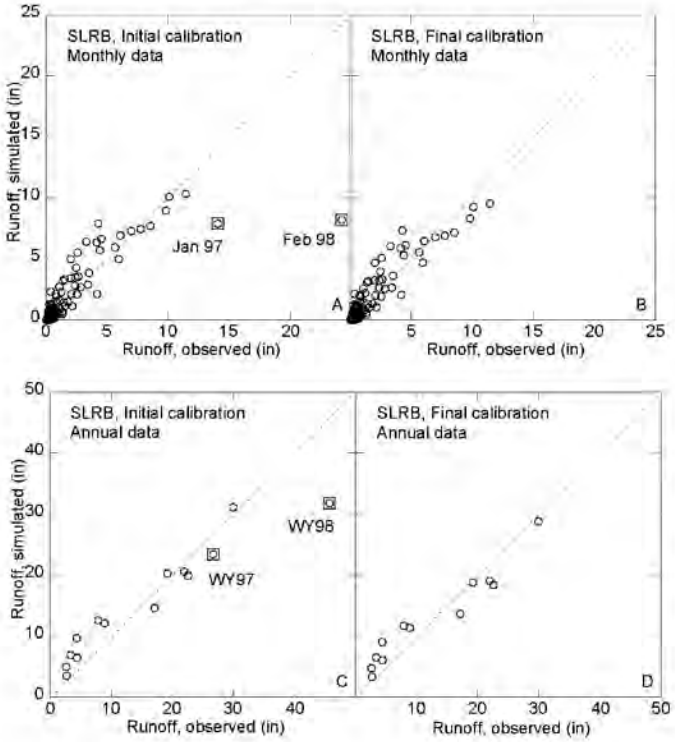

Figure IV-1

The primary goal of this project is to assess potential for distributed stormwater collection to support managed aquifer recharge (DSC-MAR). As a consequence, we are most interested in identifying locations where DSC-MAR projects are most likely to be successful during normal to dry years; there is likely to be plenty of water for DSC-MAR projects during wet years. For this reason, we avoided calibrating the simulations to extremely wet periods, at the expense of fitting normal and dry periods, and removed Jan 97 and Feb 98 from calculation of fit statistics and updated the calibration (**Fig. IV-1**). This required that we also remove WY97 and WY98 from assessment of annual calibration metrics. The updated calibration fit was improved somewhat, as was the fit for the subsequent period of validation (**Table IV-2**).

The period of validation for the SLRB simulation shows results that are similar, in many respects, to those from calibration (**Fig. IV-2**, **Table IV-2**). The NRMSD fit metric for annual hydrographs is slightly better than for the calibration period, but the results for wet months (November to April of each water year) were worse (**Table IV-2**). Some of the increased NSMSD metric for monthly data resulted from flows during two consecutive months, Dec 02 and Jan 03.

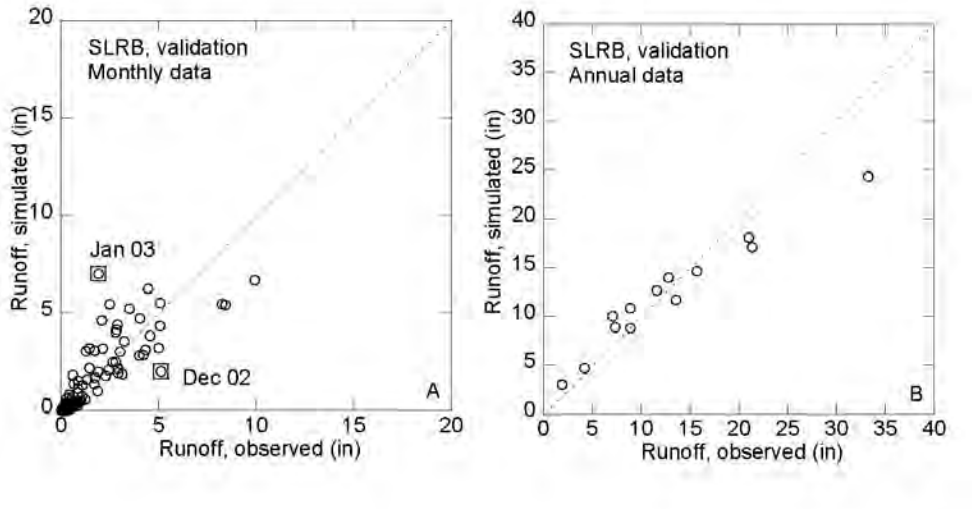

Figure IV-2

Simulated flows for these months were underpredicted and overpredicted, respectively. These were relatively high-precipitation months when, once again, PRMS routed water across the landscape more slowly than was observed. No adjustment was made to the calibration on this basis, but (out of curiosity) we removed these two months and their associated years from post-simulation calculations and updated the validation fit statistics, generating a modest improvement (**Table IV-2**).

For the PVDB, we reversed the periods of calibration and validation relative to those used for the SLRB (**Table IV-2**). In principle, it should not matter which periods are used for calibration or validation, provided that both represent a range of representative hydrologic conditions. Calibration and validation results for the PVDB appear to be reasonable, with scatter about a 1:1 line of observed and calibrated values (**Fig. IV-3**). The NRMSD fit statistics for wet month flows are lower (better) for the PVDB than those for the SLRB, but as in the SLRB, there are several pairs of consecutive months in which observed flow is higher than simulated in one month, then observed flow is lower than simulated in the next month. We found more deviation between simulations and observations at higher flows during the validation period (**Fig. IV-3**), in part because this period was somewhat wetter overall. As with the SLRB, the calibration of PRMS parameters for the PVDB was deemed satisfactory, and we next ran simulations to explore runoff and infiltration responses to different climate scenarios.

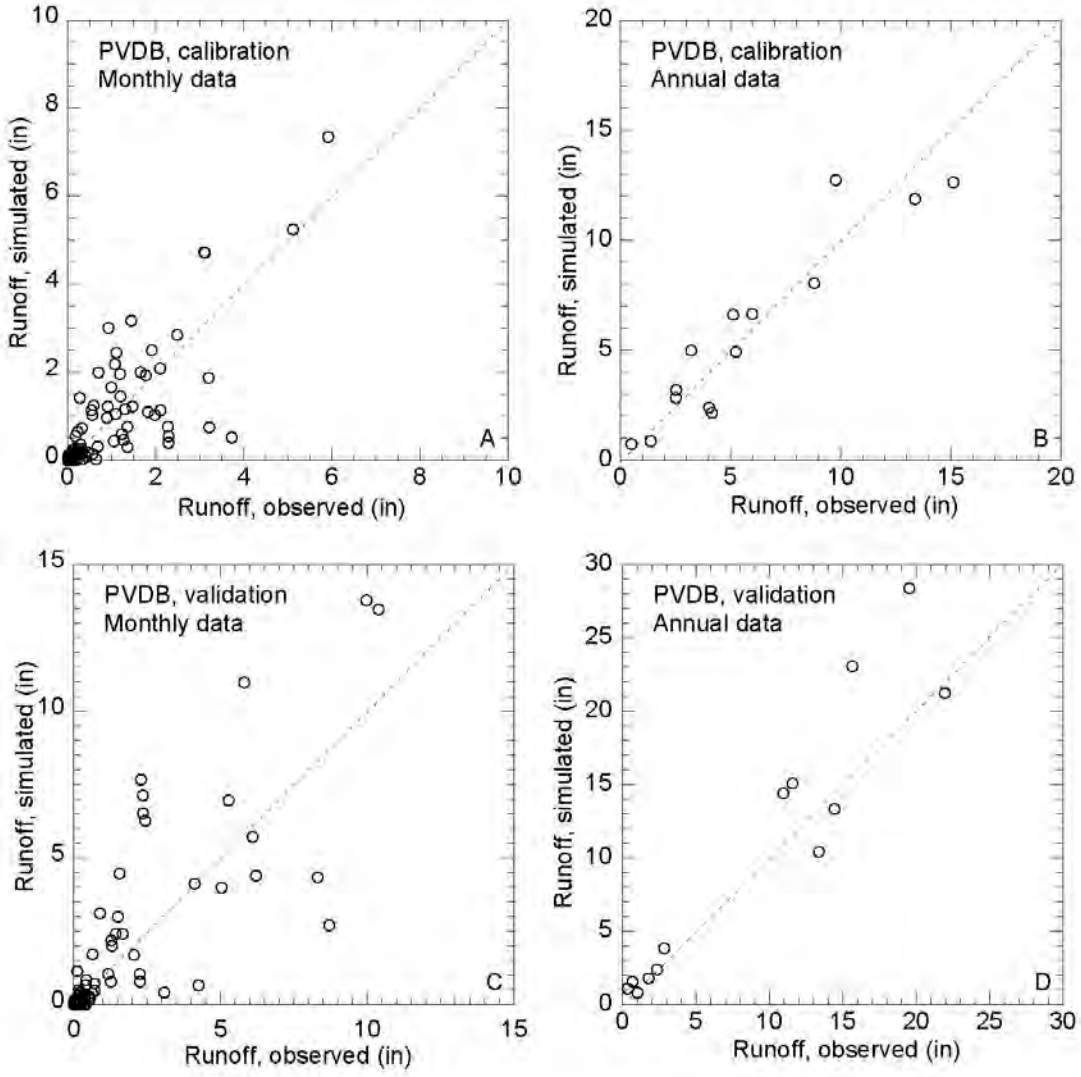
PVDB, calibration
Monthly data
Runoff, simulated (in)
Runoff, observed (in)
A
PVDB, calibration
Annual data
Runoff, simulated (in)
Runoff, observed (in)
B
PVDB, validation
Monthly data
Runoff, simulated (in)
Runoff, observed (in)
C
PVDB, validation
Annual data
Runoff, simulated (in)
Runoff, observed (in)
D

Figure IV-3

B. Precipitation during Climate Scenarios

Variations in monthly and annual precipitation for *dry*, *normal* and *wet* climate scenarios (**Table II-2**) illustrate important characteristics for both basins (**Figs. IV-4** and **IV-5**). There is more precipitation overall in the SLRB than in the PVDB, illustrating a north-to-south gradient across the study region. As result, there are relatively few months that exceed a basin-wide average precipitation of 50 ac-ft/100 ac in the PVDB (equivalent to ~6 in/month of rain), even under *wet* conditions, whereas this threshold is met in the SLRB much more frequently, even under *normal* conditions.

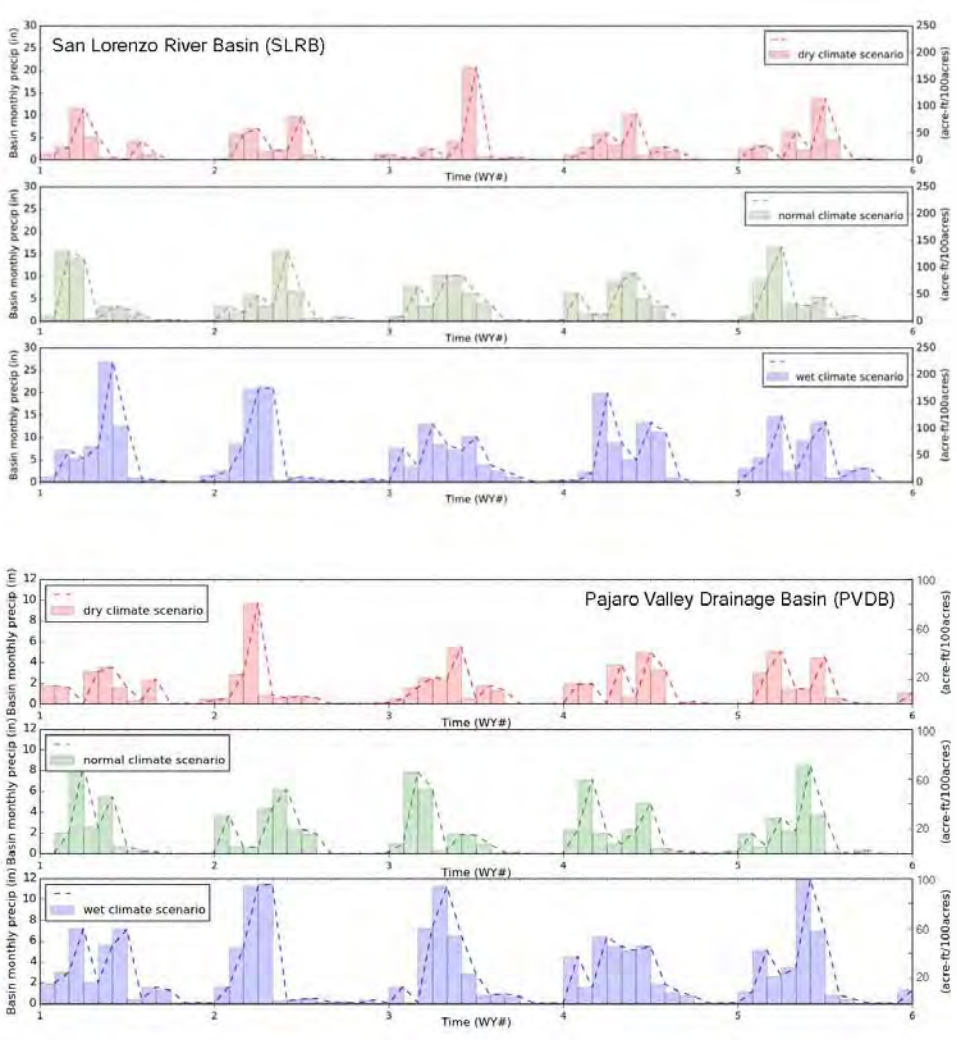

Figure IV-4

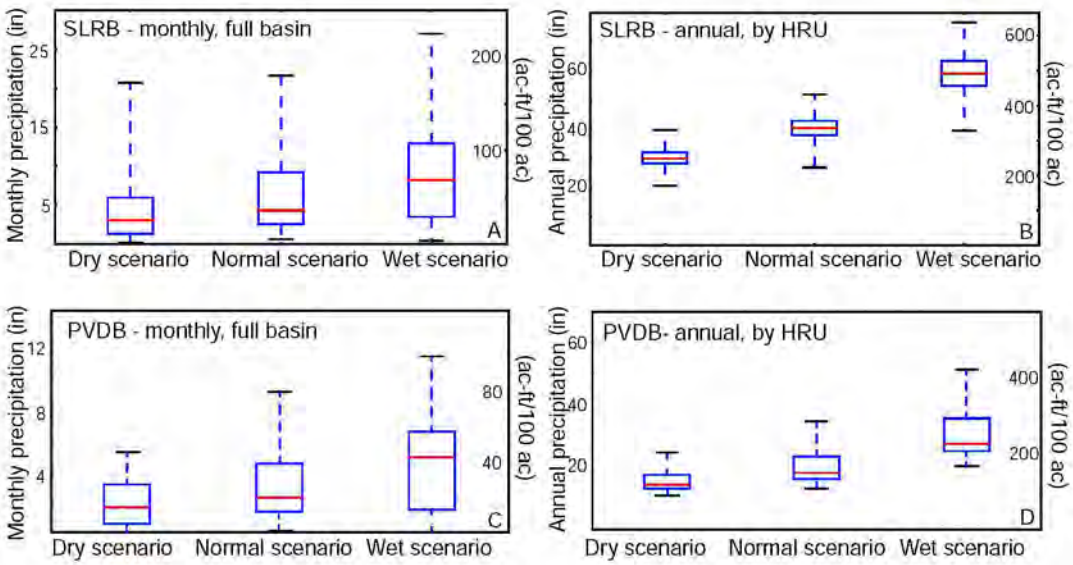

Figure IV-5

Under all climate scenarios in both basins, most precipitation falls during the wet season, November-April (month 2 to month 7 of each water year). Within both basins, there are occasional months with significant precipitation even during the *dry* scenario, often resulting from a single major precipitation event. But in addition to having more rain per month, the *normal* and *wet* climate scenarios tend to have greater persistence in rainy months (**Fig. IV-4**). Typical precipitation more than doubles from *dry* to *wet* conditions in both the SLRB and the PVDB, but values are considerably lower overall in the PVDB (**Fig. IV-5**).

The spatial distribution of precipitation is consistent for each basin under different climate scenarios (**Fig. IV-6**). In the SLRB, there is much greater precipitation along the western and eastern boundaries of the basin, with much less precipitation near the coast and at the northwestern edge of the basin. The spatial trends are somewhat simpler in the PVDB, with a strong north-to-south gradient and higher precipitation in areas of higher elevation (**Fig. IV-6**). In both basins, these patterns likely result from a combination of topography and common winter storm tracks: there appear to be more frequent and larger storms that track to the northern end of

Santa Cruz County, on average, and steep topography in the Santa Cruz Mountains and foothills at the back of the PVDB results in strong orographic effects.

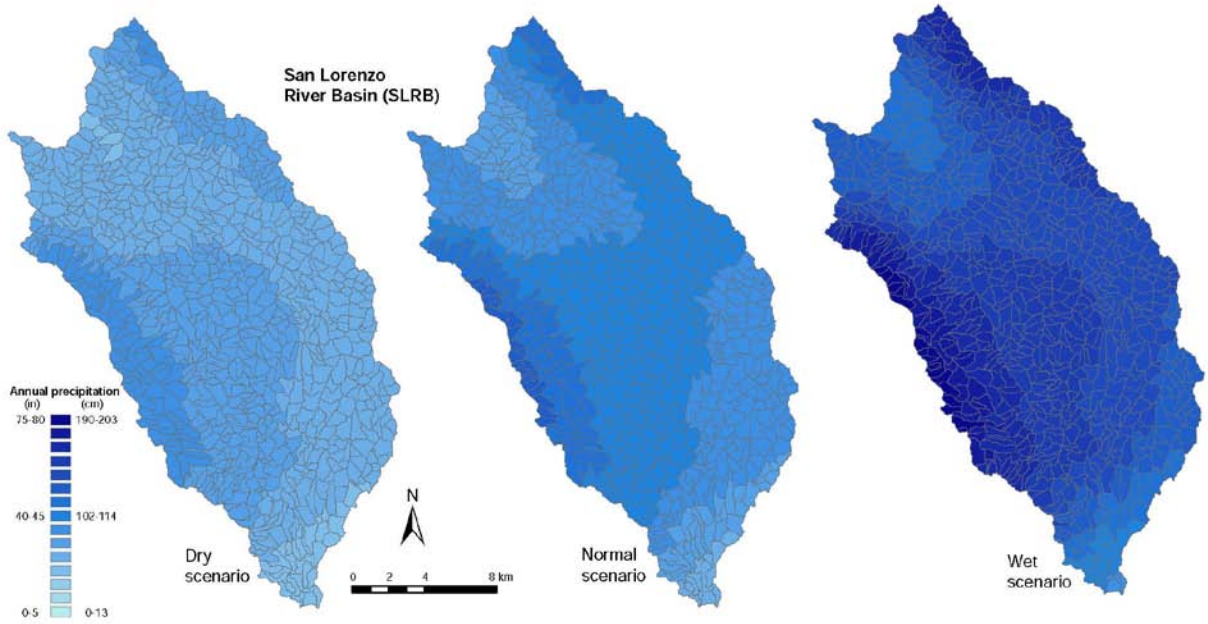

Figure IV-6A

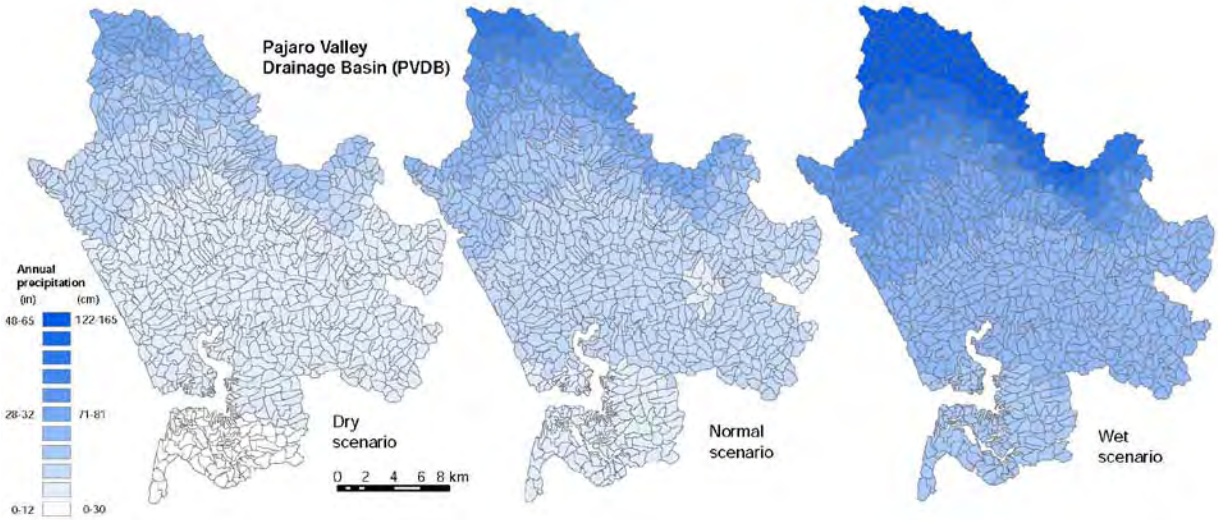

Figure IV-6B

C. Hillslope Runoff: Entire Basins

As described earlier, we restrict assessment of runoff to that generated on hillslopes, categorized by PRMS as Hortonian and Dunnian runoff and interflow (aka, *hillslope runoff*). This includes water that may originate from an upslope HRU and cascade downslope to an adjacent HRU, and water that enters an HRU as precipitation; this categorization neglects streamflow in defined channels. Comparison of precipitation hyetographs and *hillslope runoff* hydrographs show several common characteristics in the SLRB and PVDB (**Fig. IV-7**).

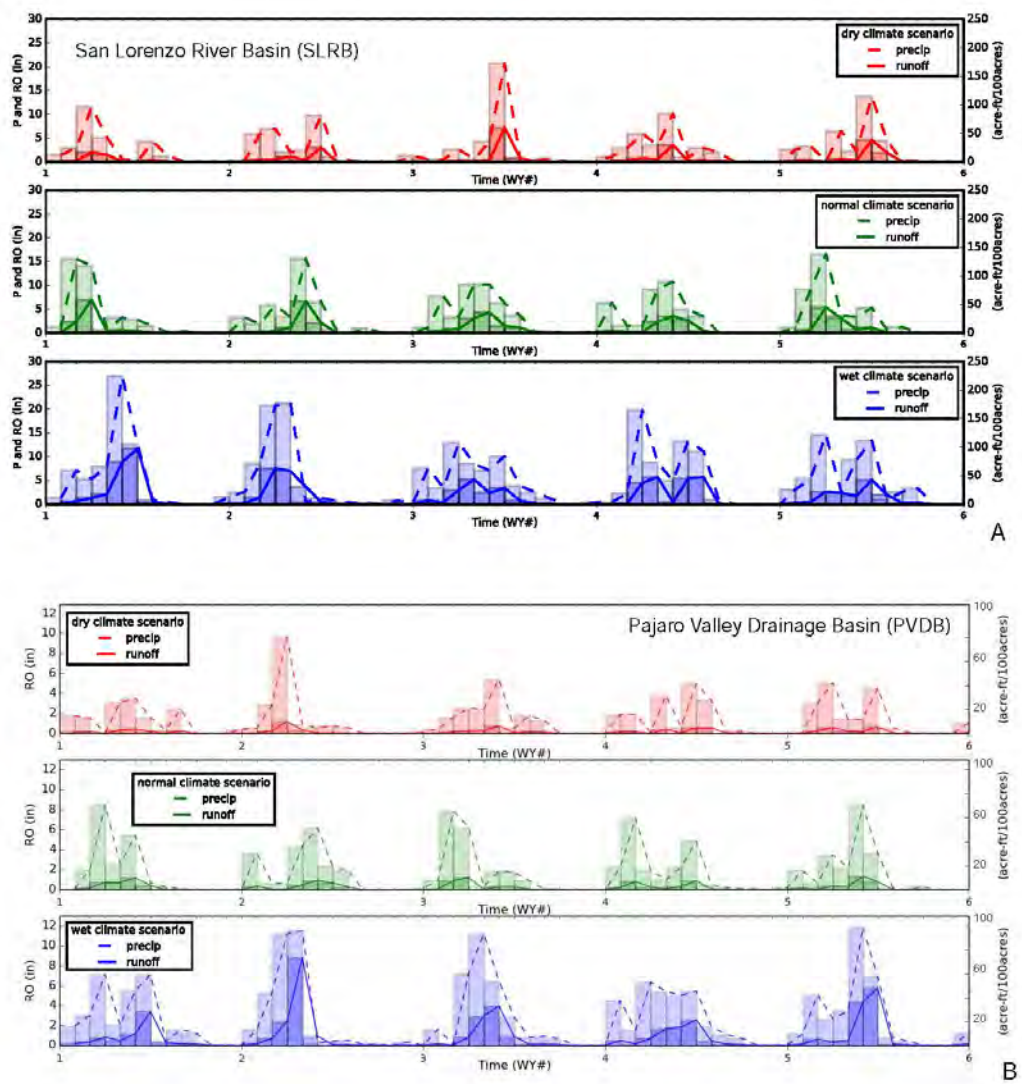

Figure IV-7

In general, the hydrographs are subdued versions of the hyetographs. Not surprisingly, there is little hillslope runoff outside of the rainy season (November to April), but there is also little runoff generated during the rainy season when precipitation during one month follows a dry month, even when monthly precipitation is relatively large. This illustrates how the landscape can hold and store considerable precipitation, potentially losing much of this water to ET, until soil and interception reservoirs have begun to fill. This effect is more strongly pronounced in the PVDB than in the SLRB, mainly because there is less precipitation overall to the south, and the effect is strongest in both basins under the *dry* climate scenario. The lack of precipitation persistence during the dry scenario thus has a major influence on basin-wide runoff generation. The lack of *hillslope runoff* during dry months does not mean that all rivers and streams will be dry, as there are alternative sources of (modest) flow in some channels in both basins: Loch Lomond Reservoir and Pinto Lake in the SLRB and PVDB, respectively, and the upper watershed of the Pajaro River, which plays a dominant role in the stream hydrograph as measured where the river enters the PVDB.

Within each basin, there is considerable variability in *hillslope runoff* across all three climate scenarios (**Fig. IV-8**). Cumulative cascades of water from HRU to HRU can result in considerable runoff being generated some downslope HRUs, particularly during the *normal* and *wet* climate scenarios. Every inch of *hillslope runoff* corresponds to ~8.3 ac-ft of runoff per 100 ac of drainage area. There can be sites where drainage areas of several hundred acres can generate enough runoff during a rainy season to justify development of a MAR project fed by stormwater, with significant benefit generated even under *dry* climate conditions. Thus it is especially important to consider possible sources of water for DSC-MAR based on the spatial distribution of *hillslope runoff*, as discussed in the next section.

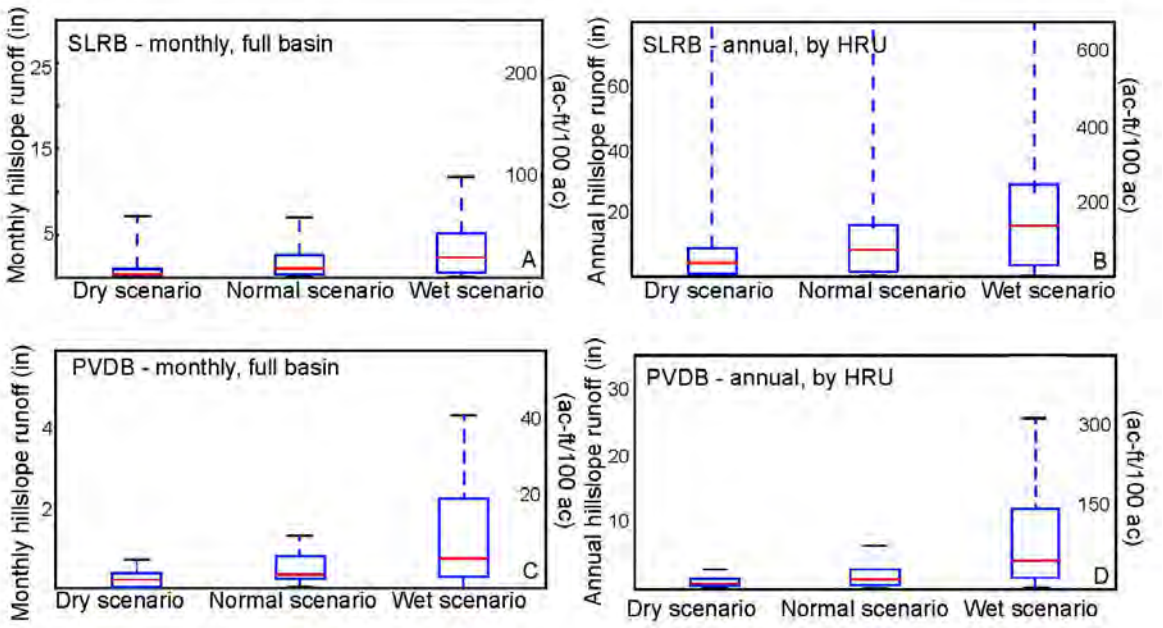

Figure IV-8

In addition to having greater mean *hillslope runoff*, the *wet* climate scenario tends to result in greater temporal and spatial variability in runoff as well (**Fig. IV-8**). This occurs for several reasons. When conditions are relatively dry, under all three climate scenarios, monthly runoff is considerably reduced (**Fig. IV-7**). The lower limit to monthly runoff (none) is the same under all climate scenarios, but the median and extreme values of monthly runoff are considerably greater during persistently wet months. Major precipitation events also tend to be larger under *wet* scenarios, so there is a larger fraction of precipitation that becomes *hillslope runoff* under these conditions (**Fig. IV-9**). The median runoff-precipitation ratio (RPR) varies from <0.1 in both basins during *dry* scenarios, to 0.2 in the PVDB and 0.3 in the SLRB during *wet* scenarios. For this project, we are less interested in full basin conditions than we are in how runoff generation might be distributed within each basin, as discussed in the next section.

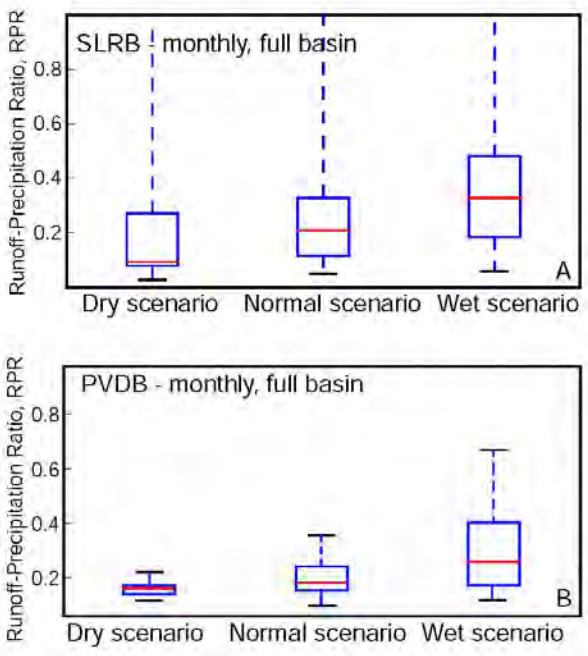

Figure IV-9

D. Hillslope Runoff: Spatial Distribution

Development of DSC-MAR projects requires a spatial assessment of conditions for *hillslope runoff* generation. Runoff generation depends on the rate at which *hillslope runoff* is generated [L/T, normalized by area] and the area across which runoff can be routed into a suitable structure. For purposes of the current analysis, we focus on the first of these topics. Each potential project site must also be assessed for drainage area, and the availability of ditches, culverts, and other water conveyance structures.

For the SLRB, there is significant *hillslope runoff* generated under all climate scenarios, with high variability throughout the basin (**Fig. IV-10**). The areas generating the least runoff are generally on the western and northern side of the basin; in many HRUs in this area, relatively little runoff is generated, even during *wet* climate conditions. In contrast, areas in the central and southern sides of the SLRB generate significant runoff even during *dry* conditions.

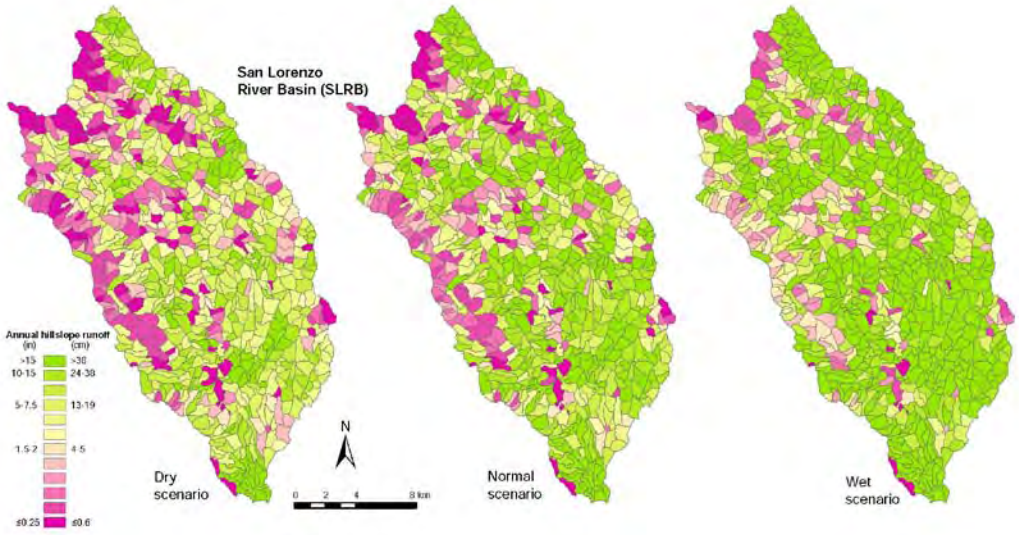

Figure IV-10

There is considerably more variability in runoff generation in the PVDB, both spatially during all climate scenarios, and between different climate scenarios (**Fig. IV-11**). Areas generating the most runoff are in the central part of the basin, within the City of Watsonville, and in the northern and eastern parts of the basin. Even under *dry* conditions, these areas generate significant runoff, often >4 in/yr. Coastal and southern parts of the basin generate much less *hillslope runoff* (**Fig. IV-11**).

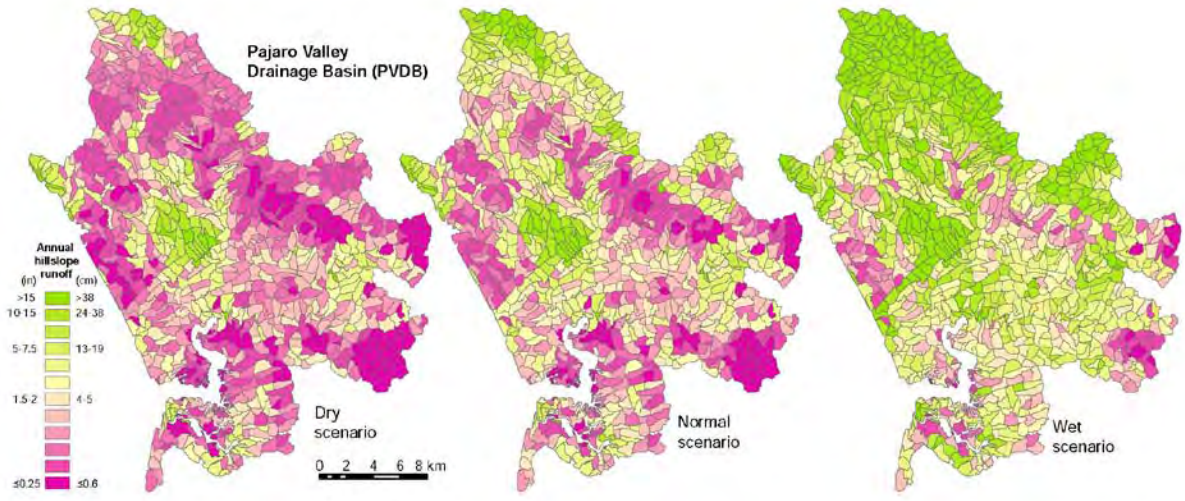

Figure IV-11

The runoff-precipitation ratio (*RPR*) illustrates how water flowing from one HRU to another as *hillslope runoff* can increase the efficiency of runoff collection. Patterns of *RPR* distribution look similar, in many ways, to patterns of *hillslope runoff* generation, but *RPR* corrects (to some degree) for variations in precipitation in different parts of each basin. *RPR* maps for all three climate scenarios are presented in **Figs. IV-12** and **IV-13,** for the SLRB and PVDB, respectively. Elevated *RPR* values are most prominent in areas that are highly urbanized, the City of Santa Cruz and Scotts Valley in the SLRB, and the City of Watsonville in the PVDB. High *RPR* values are also found in steeply sloped areas, particularly those that receive runoff from adjacent hillslopes.

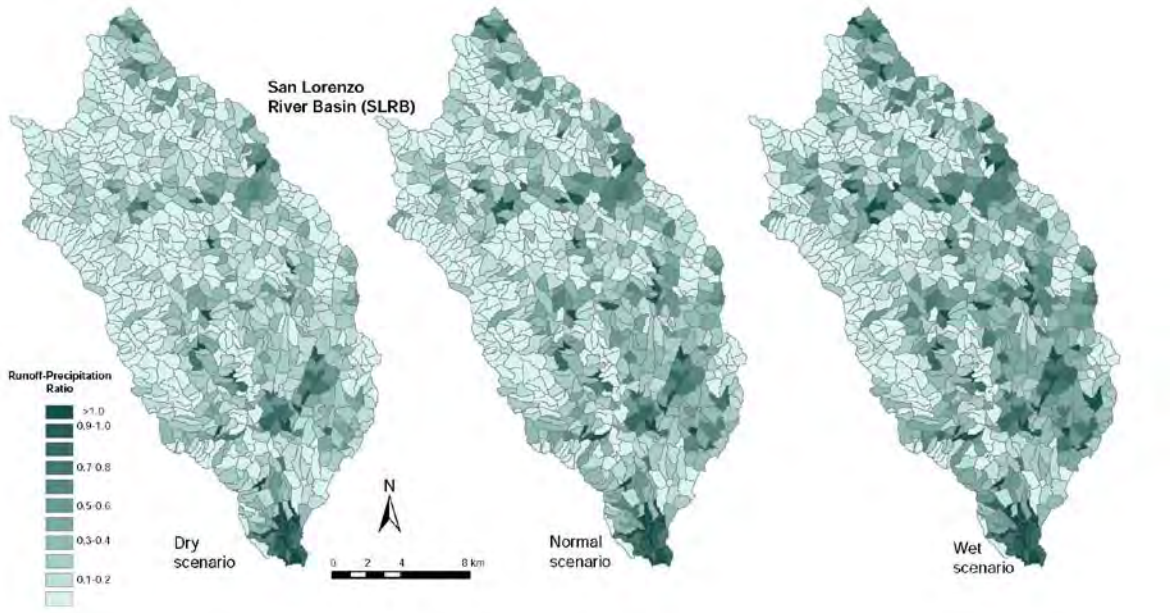

Figure IV-12

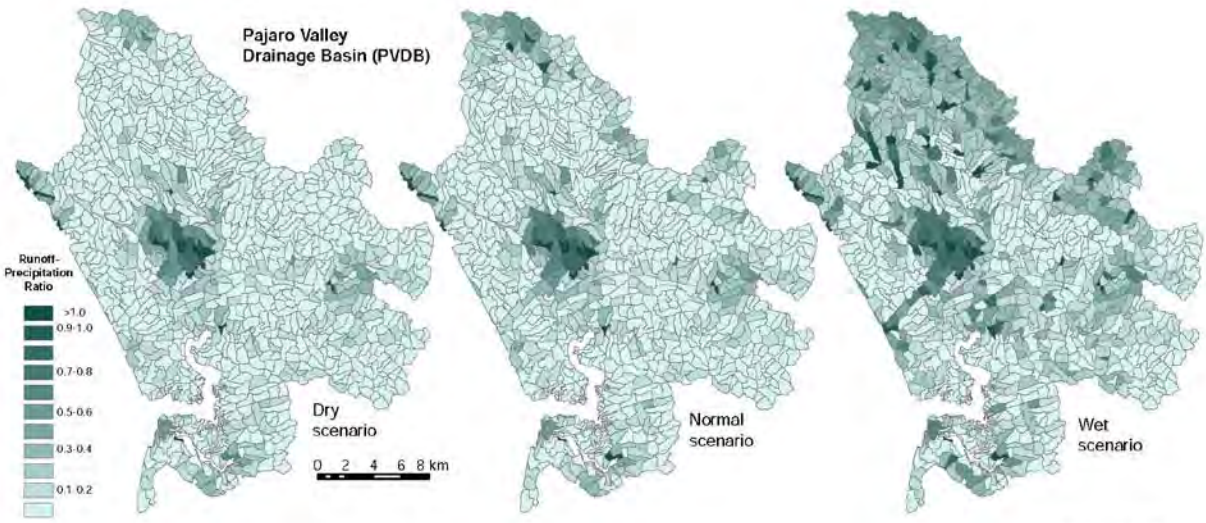

Figure IV-13

The spatial distribution of *hillslope runoff* (**Figs. IV-10** and **IV-11**) and *RPR* (**Figs. IV-12** and **IV-13**) are both impacted by the distribution of precipitation across each basin (**Fig. IV-6**), and also by the distribution of landscape properties that impact how water is subsequently routed. **Figs. IV-14** and **IV-15** illustrate examples of three of these properties for the SLRB and PVDB, respectively. *Hillslope runoff* and the *RPR* are both greater in locations where there is a high fraction of impervious area, soils have a relatively low sand content, and there is a low vegetation density. These characteristics are not necessarily independent; for example, vegetation density tends to be very low where there is a high percentage of impervious area. Still, it is informative to consider these and other parameters for which spatially continuous data are available, to assess where new DSC-MAR projects might be considered, even in the absence of a formal GIS analysis or runoff model.

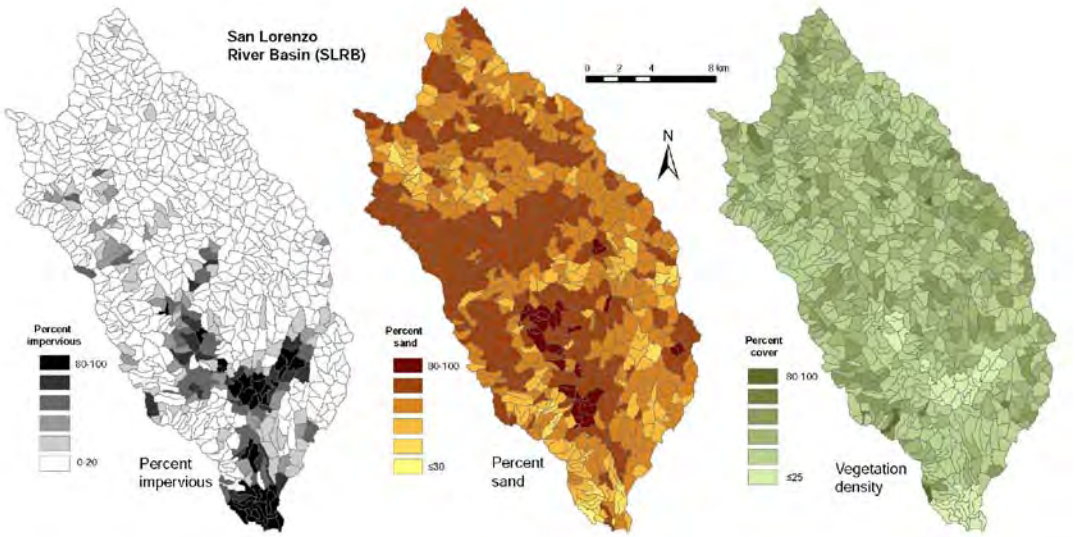

Figure IV-14

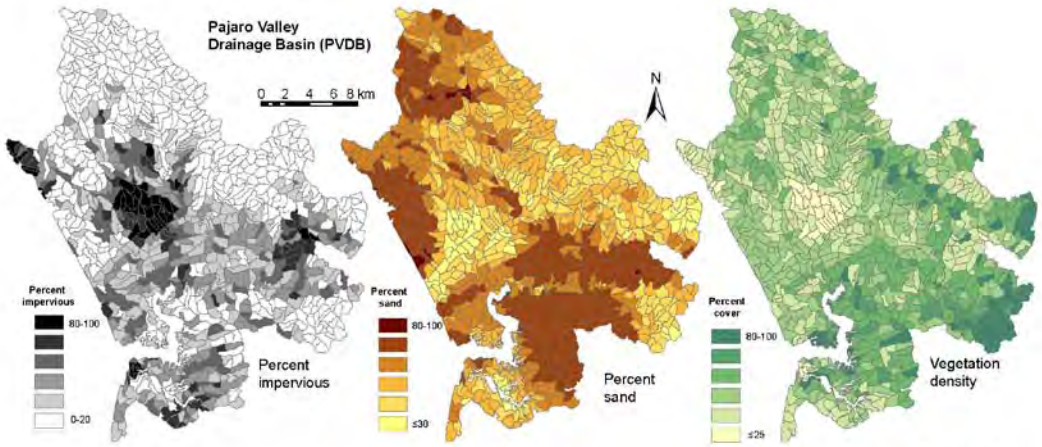

Figure IV-15

It is also helpful to consider the cumulative areas generating significant amounts of *hillslope runoff* in each basin (**Fig. IV-16**), as these areas indicate the maximum benefit that could be derived from DSC-MAR, and help to place individual projects in context. For example, in the SLRB, about 10% of the basin area (~35 km^2, ~8,700 acres) is predicted to generate at ≥12 in/yr of *hillslope runoff*, even under *dry* climate conditions. This amount of runoff is equivalent to 100

ac-ft for each 100 ac of drainage area. The fraction of the SLRB generating ≥12 in/yr of *hillslope runoff* increases to ~35% of the basin area during the *normal* climate scenario, and ~55% of the basin area during the *wet* climate scenario. Conditions in the PVDB are not as favorable, mainly because there is considerably less rainfall than in the SLRB under all climate scenarios, yet there is still considerable opportunity to develop successful DSC-MAR projects. In the PVDB during a *normal* water year, about 5% of the basin area contributes ≥12 in/yr of hillslope runoff. But even an area generating 4 in/yr of hillslope runoff (as was simulated across 20% of the basin during a normal climate scenario, equivalent to ~110 km^2 or ~27,000 acres) could contribute to 100 ac-ft/yr of DSC-MAR benefit, if the water supply were collected from a drainage area of ≥300 ac (**Fig. IV-16**). A smaller fraction of the basin will provide enough runoff during *dry* years to support DSC-MAR projects, but this illustrates how important it is to assess, position, and design these projects based on local conditions (drainage area, soils, runoff patterns, etc.).

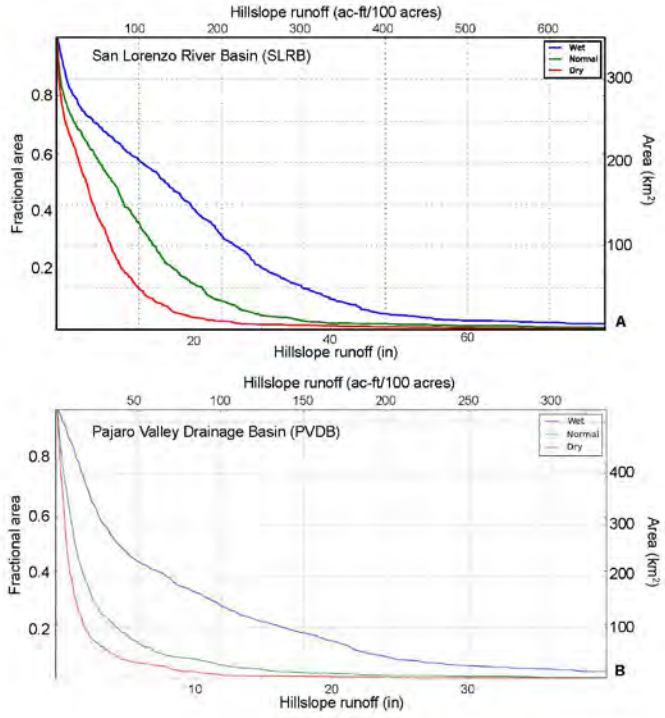

Figure IV-16

V. Discussion of Project Results

A. Limitations of Work to Date

Results from this study are helpful for planning and development of new DSC-MAR projects, but it is important to consider limitations of the data, analytical tools, and how thy were applied. The data coverages and maps produced through this project are tools that are helpful for screening of potential project sites, and for assessing the regional benefits that could result from a series of mitigation strategies.

For MAR suitability analyses, soils and bedrock data were available on a regional scale, but in many cases are assigned values based on limited direct observations. In some cases, parcels or polygons may have been classified based on a small number of observations. It is important to check conditions at individual project sites, updating data sets and maps as new information becomes available. Subsurface data were the most limiting in terms of the spatial coverage of these analyses. Additional work is needed to add new water level data to develop contour maps, unit by unit, and to verify that data from multiple aquifer layers are not inadvertently mixed. This can be challenging, particularly when using data from older groundwater wells, because the nature of subsurface stratigraphy is not always clear from associated well logs. In addition, it used to be common practice to screen water supply wells across multiple aquifer units to meet design and production objectives. Water level data from these wells can provide confounding information.

One approach that could help to extend the availability of limited water level data, particularly for earlier times, would be to incorporate results from groundwater models. Model results are only as good as the data entered to build and run them, but it might be worth adding a little bit of uncertainty into the composite MAR suitability analyses to extend the results spatially

and temporally. Additional benefit can come from applying the details of calibrated groundwater models to assessment of aquifer layer properties (transmission and storage parameters). We took this approach based on recent modeling in the SMGB and PVGB, but modeling in the SAGB is currently in progress. When these models are complete, and calibrated results are available for distribution, MAR suitability analyses for this part of the project region could be updated.

Runoff modeling provides useful information especially on relative differences in water routing, but the accuracy of simulated values is limited by the data available for calibration. In the SLRB, we had gauge data from the lower part of the basin, which was helpful in assessing full-basin runoff characteristics. But in the PVDB, ≤20% of the basin area was subject to calibration/validation based on gauged channel discharge data. It would helped if data from a gauge farther downstream had been available. Of course, stream gauge measurements have their own challenges and errors, especially during high flow conditions. It is also difficult to assess how well PRMS represents water routing between ET and groundwater recharge fluxes - both flows essentially leave the model domain, and there is little independent calibration data that allows assessment of how accurately these flows are represented in the simulations. Calibration might have been improved through adjustment of additional parameters (for example, those assigned to individual HRUs), but it seems likely that this exercise would be subject to "overfitting." The fundamental challenge is that many of the parameters that have a significant influence on PRMS simulations, including those subject to large spatial variations in values, are not independently known.

As discussed earlier, the limitation of using daily rainfall, temperature and PRMS time steps means that models are guaranteed to underrepresent the actual intensity of storm events. In addition, although using small HRUs (0.1 to 1 km^2, 25 to 250 acres) allowed us to represent

considerable variability in soil and land use properties, this might also have contributed to an excess of water routing into soil zone reservoirs. We were also limited in availability of continuous data showing land use over time. Historic land use maps are available for some areas, but given data limitations (even for the most recent datasets) and the scope of this project, we elected to use a single set of land use and vegetation data for runoff modeling. Evaluation of past and future differences in runoff characteristics could be improved by changing land use according to historical and projected changes. We chose to use historical climate data in lieu of results from regional climate models, mainly because regional models are still too coarse to represent the detailed distribution of precipitation, and because there is considerable disagreement as to what changes are likely to occur to the hydrologic cycle in the future. More significantly, whether the future climate is wetter, drier, or about the same on average, there could be more variability and/or persistence in prolonged dry or wet periods. The approach taken in this project allowed an assessment as to how a range of conditions might influence *hillslope runoff* going forward.

B. Implications of Analyses of MAR Suitability and Runoff

This project has resulted in creation of datasets and simulations to help guide placement and design of DSC-MAR projects intended to improve groundwater supplies and quality. GIS analyses were used to create maps illustrating which parts of the landscape may be most amenable to development of new field projects. Models help to assess one potential source for water, *hillslope runoff*, which could be collected before it reaches a stream channel. Datasets and maps show that MAR suitability and runoff generation are highly variable in both space and time, depending on the nature of soil and rock conditions, land use and vegetation, and the distribution and magnitude of rainfall. Datasets generated as part of this project are being made

available for public use at the RCD website (http://www.rcdsantacruz.org/managed-aquifer-recharge), and we are glad to see these results distributed and used for a variety of purposes.

Simulations of water routing across the landscape suggest that in both the SLRB and PVDB, there is considerable opportunity to improve groundwater conditions through DSC-MAR, even under *dry* climate conditions. There is even more opportunity for successful DSC-MAR projects to be run during *normal* to *wet* climate conditions. Only a small fraction of a groundwater basin needs to be developed for DSC-MAR to have a significant, positive influence on groundwater resource conditions. There is considerable leveraging of resources when runoff from hundreds of acres is directed to infiltrate through a small area. Of course, other strategies could be adapted for this purpose, for example the flooding of farm fields or reoccupation of flood plains through diversions or levee setbacks. DSC-MAR could be considered as part of a portfolio of options - no one solution is best in all areas and at all times.

C. Next Steps

This project has generated data products that should be useful for water managers, planners, regulators, and stakeholders who have concerns about the sustainability of water supply and water quality. Results from this project can be used for preliminary screening of potential DSC-MAR sites. These results should not be considered to be absolute, and there are other factors that may need to be taken into account when considering development of new projects, including: access to land, interest of land owners and tenants, possible ancillary benefits (e.g., improvements to streamflow or wetland conditions), and engineering and operations costs. Still, when faced with many potential DSC-MAR project sites, it makes sense to begin with a basic spatial assessment of MAR suitability and *hillslope runoff* generation.

Other kinds of projects could also be considered based on this work. For example, infiltration to be accomplished with dry wells might not depend on the nature of shallow soils, provided there are good aquifer conditions at an accessible depth. In this case, a different MAR suitability calculation might omit soils data, or even prioritize sites where shallow soils will limit infiltration, except where desired through an engineered structure.

Work is underway to develop additional DSC-MAR projects in the PVGB, and similar approaches are being considered in other parts of the project region. We hope that these mapping and modeling results might streamline the process of site assessment, and provide a basis for justifying site selection and securing external funding as needed for more detailed site investigation, testing, and installation. In the same way, as new projects come online, they can be used to assess the accuracy and efficacy of this approach, perhaps leading to improved maps and models. We also hope that this approach might be used as a template around California and beyond. Given the steadily increasing power of computers and the wider availability of spatial data, it makes sense to continue pressing forward with efforts to bring the best information and methods to addressing critical water challenges.

VI. References cited

Bouwer, H. (2002), Artificial recharge of groundwater: hydrogeology and engineering, *Hydrogeol. J.*, *10*(1), 121-142.

Brabb, E. E., S. E. Graham, C. Wentworth, D. Knifong, R. Graymer, and J. Blissenbach (1997), Geologic map of Santa Cruz county, California: A digital database, Open-File Report 97-489, U. S. Geological Survey, Menlo Park, CA.

Brabb, E. E., R. W. Graymer, and D. L. Jones (1998), Geology of the Onshore Part of San Mateo County, California: A Digital Database, Open File Report 98-137, U. S. Geological Survey, Menlo Park, CA.

Canadell, J., R. Jackson, J. Ehleringer, H. Mooney, O. Sala, and E.-D. Schulze (1996), Maximum rooting depth of vegetation types at the global scale, *Oecologia*, *108*(4), 583-595.

Chenini, I., A. B. Mammou, and M. El May (2010), Groundwater recharge zone mapping using GIS-based multi-criteria analysis: a case study in central Tunisia (Maknassy Basin), *Water Resour. Management*, *24*(921-939), doi:10.1007/s11269-009-9479-1.

Clark, J. C., W. R. Dupre, and L. I. Rosenberg (1997), Geologic Map of the Monterey and Seaside 7.5-minute Quadrangles, Monterey County, California: A Digital Database, Open File Report 97-30, U. S. Geological Survey, Menlo Park, CA.

Couturier, D., and E. Ripley (1973), Rainfall interception in mixed grass prairie, *Can. J. Plant. Sci.*, *53*(3), 659-663.

Crouse, R. P., E. S. Corbett, and D. W. Seegrist (1996), Methods of measuring and analyzing rainfall interception by grass, *Hydrol. Sci. J.*, *11*(2), 110-120.

Culkin, S., M. Cloud, and C. Tana (2015), Draft Technical Memorandum, Soquel-Aptos Groundwater Flow Model Construction (Task 3), 43 pp, HydroMetrics, Inc., Oakland, CA.

Digital Mapping Inc. (2011), LIDAR Data Collection and Processing for the Central Coast of California, 2010, 30 pp.

Fathizadeh, O., P. Attarod, T. Pypker, A. Darvishsefat, and G. Zahedi Amiri (2013), Seasonal variability of rainfall interception and canopy storage capacity measured under individual oak (Quercus brantii) trees in Western Iran, *J. Ag. Sci. Tech.*, *15*(1), 175-188.

Fetter, C. W. (2001), *Applied Hydrogeology*, 4th ed., 598 pp., Macmillan College Publishing Company, New York.

Freeze, R. A., and J. A. Cherry (1979), *Groundwater*, 604 pp., Simon & Schuster, Englewood Cliffs, NJ.

Fugro West Inc. (1995), North Monterey County Hydrolgeologic Study, Volume I, Water Resources, 423 pp, Monterey County Water Resources Agency.

Garcia-Estringana, P., N. Alonso-Blázquez, and J. Alegre (2010), Water storage capacity, stemflow and water funneling in Mediterranean shrubs, *J. Hydrol.*, *389*(3), 363-372.

Hamon, W. R. (1961), Estimating potential evapotranspiration, *Proc. Am. Soc. Civil Eng., J. of Hydraul. Div.*, *87*(HY3), 107-120.

Hanson, R. T. (2003), Geohydrologic framework of recharge and seawater intrusion in the Pajaro Valley, Santa Cruz and Monterey Counties, California, Water Resources Investigation 03-4096, U. S. Geological Survey, Sacramento CA.

Hanson, R. T., W. Schmid, C. C. Faunt, J. Lear, and B. Lockwood (2014), Integrated Hydrologic Model of Pajaro Valley, Santa Cruz and Monterey Counties, California, Scientific Investigations Report 2014–5111, U. S. Geological Survey, Menlo Park, CA, 166 pp.

Heitman, J., X. Xiao, R. Horton, and T. Sauer (2008), Sensible heat measurements indicating depth and magnitude of subsurface soil water evaporation. Water Resources Research, 44(4). , *WRR*, *44*(4), doi:10.1029/2008WR006961.

Jasrotia, A. S., R. Kumar, and A. K. Saraf (2007), Delineation of groundwater recharge sites using integrated remote sensing and GIS in Jammu District, India, *Int. J. Remote Sens.*, *28*(22), 5019-5036, doi:10.1080/01431160701264276.

Johnson, N. M., D. Williams, E. B. Yates, and G. Thrupp (2004), Groundwater Assessment of Alternative Conjunctive Use Scenarios, Technical Memorandum 2: Hydrogeologic Conceptual Model, 389 pp, Soquel Creek Water District, Soquel CA.

Kennedy/Jenks Consultants (2015), Santa Margarita Basin Groundwater Modeling Technical Study, 163 pp, Scotts Valley Water District, San Francisco, CA.

Klaassen, W., F. Bosveld, and E. De Water (1998), Water storage and evaporation as constituents of rainfall interception, *J. Hydrol.*, *212*, 36-50.

Leavesley, G. H., R. W. Lichty, B. M. Troutman, and L. G. Saindon (1983), Precipitation-runoff modeling system-User's manual, Resources Investigations Report 83-4238, 207 pp, U. S. Geological Survey.

Markstrom, S., R. Niswonger, S. Regan, D. Prudic, and P. Barlow (2008), GSFLOW: Coupled groundwater and surface-water flow model based on the integration of the precipitation-runoff modeling system (PRMS) and the modular groundwater flow model (MODFLOW-2005), Techniques and Methods 6-D1, 240 pp, U. S. Geological Survey, Reston, VA.

Markstrom, S. L., R. S. Regan, L. E. Hay, R. J. Viger, R. M. T. Webb, R. A. Payn, and J. H. LaFontaine (2015), PRMS-IV, the precipitation-runoff modeling system, version 4, Techniques and Methods, book 6, chap. B7 158 pp, U. S. Geological Survey.

O'Geen, T., M. B. B. Saal, H. Dahlke, D. Doll, R. Elkins, A. Fulton, G. Fogg, T. Harter, J. W. Hopmans, C. Ingels, F. Niederholzer, S. S. Solis, P. Verdegaal, and M. Walkinshaw (2015), Soil suitability index identifies potential areas for groundwater banking on agricultural lands *California Agriculture*, *69*(4), 75-84, doi:10.3733/ca.v069n02p75.

PRISM Climate Group (2016), Daily Climate Values, Parameter-elevation Relationship on Independent Slopes Model (PRISM) project, http://www.prism.oregonstate.edu, Oregon State University, Corvalis, OR.

Reid, L. M., and J. Lewis (2009), Rates, timing, and mechanisms of rainfall interception loss in a coastal redwood forest, *J. Hydrol.*, *375*(5), 459-470.

Russo, T. A., A. T. Fisher, and B. S. Lockwood (2014), Assessment of managed aquifer recharge potential and impacts using a geographical information system and numerical modeling *Groundwater*, doi: 10.1111/gwat.12213.

Schenk, H. J., and R. B. Jackson (2002), Rooting depths, lateral root spreads and below‐ground/above‐ground allometries of plants in water‐limited ecosystems, *J. Ecol.*, *90*(3), 480-494.

Soil Survey Staff (2014), Soil Survey Geographic (SSURGO) Database, https://gdg.sc.egov.usda.gov/GDGOrder.aspx, U. S. Department of Agriculture, Washington, D. C.

U. S. Geological Survey (2014a), National Elevation Dataset (NED), https://lta.cr.usgs.gov/NED, U. S. Geological Survey, Reston, VA.

U. S. Geological Survey (2014b), National Hydrolography Dataset (NHD), http://nhd.usgs.gov/, U. S. Geological Survey, Reston, VA.

U. S. Geological Survey (2014c), Watershed Boundary Dataset (WBD), http://datagateway.nrcs.usda.gov, United States Department of Agriculture-Natural Resources Conservation Service (USDA-NRCS), the United States Geological Survey (USGS), and the Environmental Protection Agency (EPA), Reston, VA

USDA Forest Service (2014), ExistingVegCenCoast1997_2013_v1, http://www.fs.usda.gov/detail/r5/landmanagement/resourcemanagement/?cid=stelprdb5347192, USDA Forest Service - Pacific Southwest Region, McClellan, CA.

USDA-NASS (2015), Cropland Data Layer, https://nassgeodata.gmu.edu/CropScape/, U. S. Department of Agriculture, Washington, D. C.

Viger, R. J., L. E. Hay, J. W. Jones, and G. R. Buell (2010), Effects of including surface depressions in the application of the Precipitation-Runoff Modeling System in the Upper Flint River Basin, Georgia U.S. Geological Survey Scientific Investigations Report 2010–5062, 36 pp, U. S. Geological Survey, Denver, CO.

Wagner, D. L., H. G. Greene, G. J. Saucedo, C. L. Pridmore, S. E. Watkins, J. D. Little, and J. Bizzarro (2002), Geologic Map of the Monterey 30' x 60' Quadrangle and Adjacent Areas, California: A Digital Database, Department of Conservation, California Geological Survey Sacramento CA.

Young, K. S. (2016), A high-resolution, regional-scale analysis of stormwater runoff in the San Lorenzo River Basin for managed aquifer recharge decision making, 119 pp, University of California, Santa Cruz, Santa Cruz, CA.

VII. Figure and Table Captions

Figures

Fig. I-1. Cartoons showing the approach taken to map suitability for managed aquifer recharge using a geographic information system (GIS). A. Spatial datasets are compiled, edited, and combined for the study region. For each property of interest, areas with higher or lower characteristics are delineated. Sets of properties are combined (overlain) to determine where the best combinations of conditions are found. B. Six primary datasets were used to assess suitability for managed aquifer recharge, two for surface suitability (soil properties, bedrock geology), and four for subsurface suitability (transmissivity, available storage, recent change in groundwater level, and thickness of the vadose zone). Datasets were available for surface suitability analysis for the full study region, whereas subsurface data were available for only part of the region.

Fig. I-2. Map of project region, including mainly Santa Cruz County and part of northern Monterey County, plus small parts of San Mateo County, San Benito County, and Santa Clara County. A few small areas in northern Santa Cruz County were also excluded because topographic basins in these areas drain outside the county.

Fig. II-1. Map showing coverage for the digital elevation model (DEM) used in this study, including areas with gaps that were patched using multiple data coverages. Elevation in most of the area was represented with a USGS DEM with 3 m resolution. Rectangles show gaps in the primary DEM that were patched with data developed from a LIDAR survey conducted by the Association of Monterey Bay Area Governments (AMBAG, yellow) or USGS data with a coarser resolution (10 m, green).

Fig. II-2. Work flow for processing of digital elevation data, summarizing steps needed to acquire, reconcile, and combine different data sets. After a complete DEM was created for the full study region, it was into separate study subregions (**Fig. II-3**).

Fig. II-3. Delineation of full project region and subregions. The study region was divided into four topographically-defined drainage basins, as shown. Suitability for managed aquifer recharge was assessed across all four drainage basins using surface data. Subsurface data were available for parts of three drainage basins: SLRB, MSCC, and PVDB. Runoff modeling was completed for the SLRB and PVDB, and is in progress for MSCC. Areas of project subregions are listed in **Table I-1**.

Fig. II-4. Locations and extent of groundwater basins for which subsurface data are available. Groundwater data were available for three primary basins: Santa Margarita Groundwater Basin (SMGB, dark blue outline), Soquel Aptos Groundwater Basin (SAGB, purple and pink outlines) and Pajaro Valley Groundwater Basin (PVGB, gold outline). Complete datasets for analysis of the SAGB were available only for a small region near the coast (pink outline), where all six factors could be considered (**Fig. I-1A**). There was information for a much larger region (purple outline) on transmissivity, allowing a three-factor analysis to be completed for all of the SAGB. For SMGB and PVGB, water level data coverages were a limiting factor on spatial coverage.

Fig. II-5. Diagrams showing the basis for simulation of hydrologic processes using Precipitation-Runoff Modeling System (PRMS). A. Conceptual model showing major reservoirs (colored rectangles) and flows (arrows) in PRMS [modified from *S L Markstrom et al.*, 2015]. PRMS is also capable of representing snow hydrology, but there is little snow in the study region, so we removed those reservoirs and flows from this diagram. B. Cartoon illustrating the three primary soil zone reservoirs (CPR: capillary reservoir, GVR: gravity zone reservoir, PFR: preferential flow reservoir) and how PRMS routes water between them. Bold terms in parentheses are parameters that help to determine how much water is stored and/or routed (as are soil depth, evap depth, and root depth), and numbers indicate the rough order in which the reservoirs and flows are considered.

Fig. II-6. Map data showing land use and vegetation cover. Data were acquired from the USDA Forest Service Classification and Assessment with LANDSAT of Visible Ecological Groupings (CALVEG) project [*USDA Forest Service*, 2014], and augmented by the USDA, National Agricultural Statistics Service's Cropland Data Layer (CDL) [*USDA-NASS*, 2015]. CALVEG data were classified as comprising one of nine land use/vegetation types, CON = coniferous forest, HDW = hardwood forest, MIX = mixed coniferous and hardwood forest, HEB = herbaceous vegetation, SHB = shrubs, AGR = agricultural, URB = urban, BAR = barren, and WAT = water. CALVEG datasets contain secondary information on vegetation and crop classification and, for many vegetation types, information on plant density. The CALVEG dataset contained some areas with data gaps (G=gap), and an abrupt shift in how agricultural areas were classified on two sides of the Pajaro River (M=misclassification) (inset). These areas were patched and reclassified using data from the CDL dataset and by hand, after looking at areal photographs.

Fig. II-7. Vegetation classification scheme for use with PRMS. The runoff model includes five major vegetation/land use classifications: conifer, deciduous, shrub, grass, and bare. Vegetation and land use data were recategorized into these five bins for use with PRMS. For vegetation classified as conifer, hardwood, shrub, herbaceous, urban, water, and barren, this conversion was straightforward. Vegetation units classified as agricultural or mixed forest were examined in greater detail to determine the appropriate PRMS classification. For example, agriculture with fruit trees was assigned a category of deciduous (code = 3) for use with PRMS.

Fig. II-8. Comparison of PRISM and spatially averaged precipitation data, with example for the SLRB. A. PRISM data across the SLRB, showing 800 m spatial discretization. B. PRISM data averaged to fill hydrologic response units (HRUs) for use by PRMS, overlain on raw PRISM data. The weighted averaging scheme accurately represents variability seen in the raw data, e.g., the small region of lower rainfall in the center-right side of the basin. Daily data of this kind were developed for the SLRB and PVDB for WY82 to WY14, as input data for PRMS.

Fig. II-9. Locations of stream gauging stations in the SLRB ad PVDB. A. SLRB. The Santa Cruz station on the San Lorenzo River (11161000, drainage areas in purple and gold) was used for primary calibration and validation, but data were also examined for consistency at the Big Trees station (11160500, drainage area in gold). B. PVDB. There is no stream gauge that represents drainage from most of the PVDB, so calibration was accomplished using data from the Green Valley Road station on Corralitos Creek (11159200, drainage area in teal). The Chittenden station on the Pajaro River (11159000) records water flowing into the lower Pajaro River basin, but was of little use for calibration and validation of PRMS because most of the flow measured here originates in the upper watershed, beyond the project region.

Fig. II-10. The distribution of annual precipitation values for the period of WY82-14 in the San Lorenzo River Basin (SLRB) and Pajaro Valley Drainage Basin (PVDB), showing the catalogs of data used to develop dry, normal, and wet climate scenarios. Years of data used for each climate scenario are listed in **Table II-5**. A. SLRB. B. PVDB

Fig. III-1. Project digital elevation model (DEM). DEM was developed for the full project area with nominal resolution (pixel size) of 3 m, as described in the text. Patched gaps and processing flow are shown in **Figs. II-1** and **II-2**.

Fig. III-2. Soils polygons extracted from the SSURGO database [*Soil Survey Staff*, 2014]. Each polygon represents a separate soil type, with properties calculated as described in the text. Inset

shows a cumulative distribution function of effective infiltration capacity (IC_E) values, plotted on a $\log_2$ scale. Vertical dotted lines indicate boundaries between indices used to classify calculated IC_E values.

Fig. III-3. Classified soils based on effective infiltration capacity (IC_E) values, with classification based on a $\log_2$ scale (CDF shown in **Fig. III-2**). Bar plot shows the relative distribution of classified IC_E values.

Fig. III-4. Map showing bedrock geology (sources cited in text). Individual geological units are shown. Dashed line shows profile for cross section *A*-*A*' shown in **Fig. III-5**.

Fig. III-5. Bedrock geologic cross-section showing three main groundwater basins in in the study region: Santa Margarita, Soquel Aptos, and Pajaro Valley.

Fig. III-6. Bedrock geology reclassified in terms of likelihood that there is a shallow aquifer exposed at the ground or below shallow soils. Rated values for different bedrock units are summarized in **Table II-1**.

Fig. III-7. Effective transmissivity values calculated across the study region, using methods discussed in the text. Map shows values classified using the same color scheme for the full project area, with the highest values for each groundwater basin as marked.

Fig. III-8. Transmissivity values (A) and indices (B) for the SMGB. Rated values are summarized in **Table III-2**.

Fig. III-9. Transmissivity values (A) and indices (B) for the SAGB. Rated values are summarized in **Table III-2**. White patches are locations where mapped aquifer thickness is 0.

Fig. III-10. Transmissivity values (A) and indices (B) for the PVGB. Rated values are summarized in **Table III-2**.

Fig. III-11. Storage values (A) and indices (B) for the SMGB. Rated values are summarized in **Table III-3**.

Fig. III-12. Storage values (A) and indices (B) for the SAGB. Rated values are summarized in **Table III-3**.

Fig. III-13. Storage values (A) and indices (B) for the PVGB. Rated values are summarized in **Table III-3**.

Fig. III-14. Vadose zone thickness values (A) and indices (B) for the SMGB. Rated values are summarized in **Table III-4**.

Tables

Table I-1. Project regions defined by topography and groundwater basins.

	Area (km^2)	Area (acres)	Groundwater basin [a]	MAR suitability (GIS) [b]	Runoff (PRMS) [c]
Full Project	1,386.5	342,602	NA	Surface	-
Northern Santa Cruz County (NSCC)	283.6	70,069	NA	Surface	-
San Lorenzo River Basin (SLRB)	351.4	86,826	Santa Margarita Groundwater Basin (SMGB)	Surface/subsurface	√
Mid-Santa Cruz County (MSCC)	209.2	51,685	Soquel Aptos Groundwater Basin (SAGB)	Surface/subsurface	(√)
Pajaro Valley Drainage Basin (PVDB)	541.1	133,706	Pajaro Valley Groundwater Basin (PVGB)	Surface/subsurface	√

[a] Groundwater basin as designated in this report
[b] Analyses completed using a GIS for suitability for managed aquifer recharge (MAR) using stormwater
[c] Analyses completed using a runoff model, PRMS, to assess potential for using stormwater as a source for MAR. √ = analysis complete and included in this report. (√) = analysis underway, with results to be added to the project website when ready.

Table II-1. Summary of soil reports from the SSURGO database used in this study.

Report name	Data included	Data used for MAR suitability [a]	Data use for runoff modeling [b]
Soil names, polygon sizes, fraction of area	Map unit name, map symbol, area (acres, %)	Unit name, area	Unit name, area
Wind erosion prediction	Fraction of sand/silt/clay (%), soil horizon thickness(es), texture, taxonomic order, albedo, fraction of area (%), slope	Soil horizon thickness	Soil horizon thickness, fraction sand/silt/clay
Physical soil properties	Soil thickness, fraction of sand/silt/clay (incomplete), bulk density, saturated conductivity (range), available water capacity, linear extensibility, organic matter, erosion factors, wind erodability group/index	Saturated conductivity	Soil thickness, saturated conductivity, available water capacity

[a] Data processed for use in calculation of MAR suitability, along with other datasets.
[b] Data processed to generate input for runoff modeling.

Table II-2. Summary water level data availability.

Groundwater basin	Area for which contoured water level data was available (km^2)	Year of most recent water level records	Year of earliest water level records
Santa Margarita Groundwater Basin	75.6	2014	1992
Soquel Aptos Groundwater Basin	4.8	2014	2009
Pajaro Valley Groundwater Basin	238.6	2010	1998

Table II-3. Summary of PRMS parameters and values, organized by module.

PRMS module	Parameter	Units	SLRB	PVDB
basic physical	hru_area	acres (km^2)	5.7 - 245.7 (0.02 - 1.0)	1.0 - 266.9 (0.004 - 1.08)
	hru_aspect	degrees	49 - 262	0.1 - 291
	hru_elev	meters	4.0 - 839	2.3 - 781
	hru_lat	degrees N	37.0 - 37.2	36.8 - 37.1
	hru_slope	dec. frac.	0.03 - 0.72	0.00 - 0.65
	hru_type	-	0, 1, 3	1
strmflow - muskingum	hru_segment	-	0 - 859	0 - 953
	K_coef	hours	0.01	0.01
	obsin_segment	-	0	0
	segment_flow_init	-	0.0	0.0
	segment_type	-	0, 2	0
	tosegment	-	0 - 859	0 – 953
	x_coef	dec. frac.	1.0	1.0
subbasin	hru_subbasin	-	1 - 3	1 - 6
	subbasin_down	-	0, 2, 3	0, 1, 3, 4, 6
cascade	cascade_flg	-	1	1
	cascade_tol	acres	0.0	0.0
	hru_down_id	-	0 - 859	0 - 953
	hru_pct_up	dec. frac.	1.0	1.0
	hru_strmseg_down_id	-	0 - 859	0 - 953
	hru_up_id	-	1 - 867	1 - 1025
cascade gw	gw_down_id	-	0 - 859	0 - 953
	gw_pct_up	dec. frac.	1.0	1.0
	gw_strmseg_down_id	-	0 - 859	0 – 953
	gw_up_id	-	1 - 867	1 – 1025
gwflow	gwflow_coef	fraction/day	0.015	0.001
	gwsink_coef	fraction/day	0.035	0.6
	gwstor_init	inches	10.0	10.0
	gwstor_min	inches	0.0	0.0

	fastcoef_lin	fraction/day	0.001	0.001
	fastcoef_sq	-	0.001	0.001
	slowcoef_lin	fraction/day	0.001	0.001
	slowcoef_sq	-	0.001	0.001
	ssr2gw_rate	fraction/day	0.01 - 0.41	0.04 - 0.156
	ssr2gw_exp	-	2.0	1.8
	soil2gw_max	inches	0.0	0.0
soilzone	soil_rechr_init	inches	0.0	0.0
	soil_rechr_max	inches	0.041 - 0.098	0.072 - 0.286
	soil_moist_init	inches	0.0	0.0
	soil_moist_max	inches	0.11 - 20.95	0.65 - 64.8
	pref_flow_den	dec. frac.	0.0	0.0001 - 0.033
	sat_threshold	inches	0.41 - 33.16	0.116 - 7.64
	ssstor_init	inches	0.0	0.0
	soil_type	-	1 - 3	1 - 3
	transp_beg	cal month	1	1
	transp_end	cal month	13	13
transp-tindex	transp_tmax	°C	0.0	0.0
	potet_sublim	dec. frac.	0.5	0.5
	rad_trncf	dec. frac.	0.5	0.5
	smidx_coef	dec. frac.	0.06	0.02
srunoff-smidx	smidx_exp	1/inch	0.5	0.1
	hru_percent_imperv	dec. frac.	0.0 - 1.0	0.0 - 0.79
	imperv_stor_max	inches	0.05	0.05
	cov_type	-	0 - 4	0 - 4
	covden_sum	dec. frac.	0.0 - 0.90	0.0098 - 1.0
intcp	covden_win	dec. frac.	0.0 - 0.90	0.0098 - 1.0
	srain_intcp	inches	0.0 - 0.067	0.0361-0.067
	wrain_intcp	inches	0.0 - 0.067	0.0361-0.067
et – potet_hamon	hamon_coef	-	0.004 - 0.008	0.0064 - 0.0094

Table II-4. PRMS parameter input as defined by soil and vegetation information

Soils

Soil PRMS input [a]	Sand	Loam	Clay	Source(s) [b]
Porosity, n (-)	0.35	0.45	0.50	1
Field capacity, FC (-)	0.15	0.30	0.40	1
Evap. depth (in)	0.59	0.59	0.59	2
Available water capacity, AWC (-)	0.07-0.15	0.05-0.19	0.10-0.20	3
Infiltration capacity, IC (in/day)	3.6 - 578	0.0 - 61.4	0.0 - 25.6	3

[a] Units listed are those used by PRMS. (-) = fraction, 0 to 1.
[b] 1 = Freeze and Cherry [1979], Fetter [2001], 2 = Heitmann et al. [2008]; 3 = Soil Survey Staff [2014].

Vegetation

Vegetation PRMS input [a]	Bare	Grasses	Shrubs	Deciduous	Confierous	Source(s) [b]
Rooting depth (in)	0	50	79	87	117	1
Coverage density (-)	0	100	55	35	35	2
Impervious fraction	1	0	0	0	0	3
Interception storage (in)	0	0.0672	0.0361	0.0490	0.0573	4

[a] Units listed are those used by PRMS. (-) = fraction, 0 to 1.
[b] 1 = Schenk and Jackson [2002], Canadell et al. [1996]; 2 = USDA Forest Service [2014]; 3 = Viger et al. [2010]; 4 = Crouse et al. [1996], Couturier and Ripley [1973], Garcia-Estringana et al. [2010], Fathizadeh et al., [2013], Klaassen et al. [1998], Reid and Lewis [2009].

Table II-5. PRMS climate scenarios based on daily PRISM data for each basin.

Purpose [a]	Climate scenario	SLRB	PVDB
Model stabilization	Normal	1984	2004
		1992	2001
		1999	1984
		2001	1985
		2002	1992
		2003	2003
		2004	1999
Analysis	Normal	1984	2004
		1992	2001
		1999	1984
		2001	1985
		2002	1992
		2003	2003
		2004	1999
Analysis	Wet	1986	2011
		1997	1997
		2005	1993
		2006	2005
		2011	1986
Model stabilization	Normal	1984	2004
		1992	2001
		1999	1984
		2001	1985
		2002	1992
		2003	2003
		2004	1999
Analysis	Dry	1988	1990
		1989	2013
		1991	1994
		1994	2012
		2012	1989

[a] Model stabilization helps to avoid a major influence from initial conditions, including antecedent moisture.

Table III-1. Bedrock geology index assignments for full project region.

Bedrock Geology Index	Units [a]	Polygons [b]	Area (km^2) [c]
4 = Primary aquifer	MPe, Ppu, Qae, Qar, Qbs, Qce, Qcl, Qcu, Qd, Qds, Qe, Qe?, Qem, Qes, Qf, Qf?, Qfa, Qod, Tbl, Tblc, Tbm, Tbu, Tlo, Tlss, Tmm, Tp [d], Tps, Tsm	462	390
3 = Primary (minor) aquifer	Tp [d]	42	165
2 = May be primary aquifer	af, Ess, Orb, Ovq, Q, Q?, Qaf, Qaf?, Qal, Qb, Qcf. Qfl, Qls, Qms, Qmt, Qmt?, Qo, Qof, QT, Qt, QTc, Qtl, Qtw?, Qwf, Qyfo, Tl, Tmp, Ts, Tvq	615	433
0 = Not an aquifer (confining layer, other)	ch, db, Ebu, Ebu?, EOsj, ga, gd, gs, H2O, hcg, Jhg, Kcg, Kgr, Kgs, KJf, ls, m, Msh, Mv, Puc, Puc?, Pus, Pus?, qd, Qg, Qt?, Qyf, sch, Tbs, Tla, Tm, Tmb, Tms, Tsc, Tsl, Tsr, Tst, Tz, um	500	404

[a] Symbols for geologic units derived from data products used to develop index [*Brabb et al.*, 1997; *Brabb et al.*, 1998; *Clark et al.*, 1997; *Wagner et al.*, 2002].
[b] Number of individual bedrock polygons from geological maps within project area.
[c] Values rounded to nearest 1 km^2.
[d] Purisima Formation assigned bedrock geology index of 3 outside of the SAGB, because it is a minor aquifer in the SMGB and PBGB. Within the SAGB, the index assignment depended on the Purisima subunit preset in the shallow subsurface.

Table III-2. Transmissivity index assignments for the three main groundwater basins in the study region.

Transmissivity Index [a]	Santa Margarita Groundwater Basin		Soquel Aptos Groundwater Basin		Pajaro Valley Groundwater Basin	
	Range (m^2/day)	Area (km^2)	Range (m^2/day)	Area (km^2)	Range (m^2/day)	Area (km^2)
0	0 to <25	38.79	0 to <75	83.00	0 to <75	1.42
1	25 to <70	14.32	75 to <100	9.33	75 to <250	16.06
2	70 to <100	6.63	100 to <250	51.55	250 to <450	76.06
3	100 to <150	4.66	250 to <450	28.30	450 to <3300	216.65
4	≥150	11.88	≥450	146.80	≥3300	54.62

[a] Indices were assigned based on consideration of the range of values found in each groundwater basin. Although the SAGB and PVGB share some of the same general stratigraphy (Fig. III-5), the Purisima aquifer is more important in the SAGB, whereas the Aromas aquifer is more important in the PVGB.

Table III-3. Available storage index assignments for the three main groundwater basins in the study region.

Available storage, S_a [a]		Santa Margarita Groundwater Basin	Soquel Aptos Groundwater Basin	Pajaro Valley Groundwater Basin
Index	Range (m)	Area (km^2)	Area (km^2)	Area (km^2)
0	< 1	45.29	16.59	115.20
2	1 to < 5	23.19	22.12	86.80
4	≥ 5	5.59	27.05	33.13

[a] Indices were assigned based on consideration of the range of values found across the study region, with a single scale used for all groundwater basins. Because there was a relatively narrow range of available storage values, 0 to 17 m, we use three indices extending across the same range as indices used for other MAR suitability metrics (0 to 4).

Table III-4. Vadose zone thickness index assignments for the three main groundwater basins in the study region.

Vadoze zone thickness, T_{vz} [a]		Santa Margarita Groundwater Basin	Soquel Aptos Groundwater Basin	Pajaro Valley Groundwater Basin
Index	Range (m)	Area (km^2)	Area (km^2)	Area (km^2)
0	$T_{vz} \leq 0$, $T_{vz} \geq 80$	32.24	24.62	65.41
1	$60 \leq T_{vz} < 80$	8.98	13.02	31.32
2	$0 < T_{vz} < 5$, $40 \leq T_{vz} < 60$	13.19	15.28	62.05
3	$20 \leq T_{vz} < 40$	11.44	9.33	69.22
4	$5 \leq T_{vz} < 20$	9.49	3.51	65.45

[a] Indices were assigned based on consideration of the range of values found in each groundwater basin and across the full project region. The most favorable ratings were assigned to vadose zone thicknesses that are low enough to allow relatively rapid infiltration into underlying aquifers, but high enough to allow some water-soil interaction (including processing of potential contaminants) during transport.

Table III-5. Recent water level change index assignments for the three main groundwater basins in the study region.

Rate of change of water level, ΔW[a]		Santa Margarita Groundwater Basin	Soquel Aptos Groundwater Basin	Pajaro Valley Groundwater Basin
Index	Range (m/yr)	Area (km^2)	Area (km^2)	Area (km^2)
0	$\Delta W \geq 0$	55.62	27.11	109.37
2	$-0.5 < \Delta W < 0$	12.03	6.01	61.01
4	$\Delta W \leq -0.5$	7.70	3.45	66.12

[a] Indices were assigned based on consideration of the range of values found across the study region, with a single scale used for all groundwater basins. Because time periods for which data were available differed by basin (**Table II-2**), the annual rate of change in water level was used as the primary metric.

Table III-6. Summary of MAR suitability analyses using surface data (soils, bedrock geology).

MAR suitability [a]	Northern Santa Cruz County (NSCC)		San Lorenzo River Basin (SLRB)		Mid-Santa Cruz County (MSCC)		Pajaro Valley Drainage Basin (PVDB)	
	(km^2)	(% of area)	(km^2)	(% of area)	(km^2)	(% of area)	(km^2)	(% of area)
Q1	55.1	19.4	45.1	12.8	17.1	8.2	35.3	6.5
Q2	61.4	21.6	81.3	23.1	28.6	13.7	226.6	41.9
Q3	110.6	39.0	112.8	32.1	82.7	39.6	158.2	29.2
Q4	56.5	19.9	112.3	32.0	80.8	38.6	120.9	22.3

[a] MAR suitability calculated from soils and bedrock geology data on a relative scale, converted to equivalent index quartiles: $0 \leq Q1 < 25\%$, $25 \leq Q2 < 50\%$, $50 \leq Q3 < 75\%$, $75 \leq Q4 \leq 100\%$.

Table III-7. Summary of MAR suitability analyses using surface data (soils, bedrock geology), screening for areas with surface slopes <10%.

MAR suitability [a]	Northern Santa Cruz County (NSCC)		San Lorenzo River Basin (SLRB)		Mid-Santa Cruz County (MSCC)		Pajaro Valley Drainage Basin (PVDB)	
	(km^2)	(% of area)	(km^2)	(% of area)	(km^2)	(% of area)	(km^2)	(% of area)
Q1	24.8	27.3	11.3	14.9	3.8	6.2	14.4	4.6
Q2	14.6	16.1	20.4	27.0	8.6	14.0	157.8	50.6
Q3	37.5	41.3	22.5	29.7	34.9	56.8	86.5	27.8
Q4	13.9	15.3	21.5	28.4	14.1	23.0	52.9	17.0

[a] MAR suitability calculated from soils and bedrock geology data on a relative scale, after screening out all areas having steep surface slopes, converted to equivalent index quartiles: $0 \leq Q1 < 25\%$, $25 \leq Q2 < 50\%$, $50 \leq Q3 < 75\%$, $75 \leq Q4 \leq 100\%$. For these calculations, % of area applies to areas having surface slopes <10%.

Table III-8. Summary of MAR suitability analyses using a combination of surface and subsurface data.

MAR suitability [a]	Santa Margarita Groundwater Basin (SMGB)		Soquel Aptos Groundwater Basin (SAGB), three factors [b]		Soquel Aptos Groundwater Basin (SAGB), six factors [b]		Pajaro Valley Groundwater Basin (PVGB)	
	(km^2)	(% of area)	(km^2)	(% of area)	(km^2)	(% of area)	(km^2)	(% of area)
Q1	17.85	24.1	25.27	8.0	2.44	6.7	5.43	2.3
Q2	26.44	35.7	55.47	17.5	15.99	43.8	128.02	55.0
Q3	24.76	33.5	144.48	45.5	13.56	37.1	83.97	36.1
Q4	4.95	6.7	92.34	29.1	4.52	12.4	15.29	6.6

[a] MAR suitability calculated on a relative scale, converted to equivalent index quartiles:
$0 \leq Q1 < 25\%$, $25 \leq Q2 < 50\%$, $50 \leq Q3 < 75\%$, $75 \leq Q4 \leq 100\%$.

[b] For the "three factor" analysis in the SAGB, only transmissivity was used to represent subsurface properties, being available for the full basin (**Fig. III-7**). A complete "six factor" analysis was completed for a smaller SAGB area (**Fig. III-9**), using the standard two surface factors (soils and bedrock geology) and four subsurface factors (transmissivity, storage, vadose zone thickness, and recent changes in water levels).

Table IV-1. PRMS calibration parameters, ranges and final values.

Parameter	PRMS units [a]	Description	Calibration range [b]	Final value(s) [c]	
				SLRB	PVDB
K_coef	hr	Muskingum coefficient (travel time)	0.01 - 1.0	0.01	0.01
x_coef	(-)	Muskingum coefficient (attenuation)	0.2 - 1.0	1.0	1.0
gwflow_coef	(-)/day	Baseflow linear routing coefficient	0 - 0.5	0.015	0.001
gwsink_coef	(-)/day	GW extraction linear routing coefficient	0 - 0.8	0.035	0.6
fastcoef_lin	(-)/day	Preferential flow linear routing coefficient	0.001 - 1.0	0.001	0.001
slowcoef_lin	(-)/day	Gravity soilzone linear routing coefficient	0.001 - 0.5	0.001	0.001
slowcoef_sq	-	Gravity soilzone non-linear routing coefficient	0.001 - 0.35	0.001	0.001
ssr2gw_rate	(-)/day	Gravity soilzone drainage coefficient (to GW)	0.01 - 1.2	0.01 - 0.41	0.004-0.156
ssr2gw_exp	-	Gravity soilzone drainage exponent (to GW)	0.0 - 3.0	2.0	1.8
soil_moist_max	in	Max normalized water volume of capillary soilzone (AWC x rooting depth)	0.05 - 100	0.11 - 20.95	0.65-64.8
pref_flow_den	(-)	Fraction of the total soil depth in which preferential flow occurs	0.0 - 0.5	0.0	0.0001 – 0.033
sat_threshold	inn	Max normalized water volume of gravity + preferential soil zones: (*n-FC*) x *soil depth*	0.3 - 179	0.41 - 33.16	0.116 – 7.64
smidx_coef	(-)	Hortonian runoff contributing area coefficient	0.001 - 0.06	0.06	0.002
smidx_exp	in^{-1}	Hortonian runoff contributing area exponent	0.3 - 1.0	0.5	0.1

[a] Units used by PRMS

[b] Range of values that was explored to improve calibration fit

[c] Single values are uniform across drainage basin. Range of values indicates scaling for each HRU, based on available soils data, as described in the text.

Table IV-2. PRMS calibration and validation time periods and results summaries, SLRB and PVDB.

SLRB

Time period [a]	Purpose	Wet months [b]		Annual	
		N months	NRMSD	N years	NRMSD
WY88-01	Calibration - initial	84	0.158	14	0.109
WY88-01 [c]	Calibration - final	82	0.137	12	0.106
WY02-14	Validation - initial	78	0.246	13	0.100
WY02-14 [c]	Validation - final	76	0.212	11	0.100

[a] WY = water year, calibration/validation follows model stabilization period of WY82-87
[b] Data compiled on a monthly basis for November - April of each water year
[c] Data neglected for two months of relatively extreme rainfall, as described in text

PVDB

Time period [a]	Purpose	Wet months [b]		Annual	
		N months	NRMSD	N years	NRMSD
WY01-14	Calibration	84	0.064	14	0.102
WY88-00	Validation	78	0.098	13	0.168

[a] WY = water year, calibration/validation follows model stabilization period of WY82-87
[b] Data compiled on a monthly basis for November - April of each water year